

República Federativa do Brasil
Ministério de Minas e Energia
Companhia de Pesquisa de Recursos Minerais
Diretoria de Geologia e Recursos Minerais
Departamento de Recursos Minerais

PROJETO PLATINA E ASSOCIADOS

GEOLOGICAL, GEOCHEMICAL AND POTENTIALITY ASPECTS OF Ni-Cu-PGE DEPOSITS OF THE PARANÁ BASIN MAGMATISM

Organization

Sérgio José Romanini and Luiz Fernando Fontes de Albuquerque

Superintendência Regional de Porto Alegre
Abril 2001

TECHNICAL TEAM

Luiz Fernando Fontes de Albuquerque
Geology and Mineral Resources Manager

Sérgio José Romanini
Mineral Resources Supervisor

Luiz Antonio Chieregati
Andrea Sander
Adalberto Dias
Project Chiefs

Luís Edmundo Giffoni
Editing

PROJETO PLATINA E ASSOCIADOS

Geól. Adalberto de Abreu Dias
Geól. Andrea Sander
Geól. Claudemir Severiano de Vasconcelos*
Geól. Idio Lopes Jr.*
Geól. Luiz Antonio Chieregati*
Geól. Luiz Fernando Fontes de Albuquerque
Geól. Sérgio José Romanini
Geól. Valdomiro Alegri*

* Superintendência Regional de São Paulo

Geochemical Prospection

Geól. Larry Hulbert*
Geól. D. Conrod Grégorie*

* Geological Survey of Canadá

Typing

Suzana Santos da Silva

Digitizing/Illustration

Giovani Milani Deiques

English Version

Arthur Schulz Junior

Informe de Recursos Minerais
Série Metais do Grupo da Platina e Associados, 29

Ficha Catalográfica

R758 Romanini, Sérgio J.; org.

Geological, geochemical and potentiality aspects of Ni-Cu-PGE deposits of the Paraná Basin magmatism / Sérgio J. Romanini; Luiz Fernando F. Albuquerque; orgs. - Porto Alegre : CPRM, 2001.

1 v. ; il - (Informe de Recursos Minerais - Série Metais do Grupo da Platina e Associados, n.º 29)

1. Projeto Platina e Associados
- I. Albuquerque, Luiz Fernando F.; org.
- II. Título
- III. Série

CDU 553.491 (811.1)

Presentation

The Informe de Recursos Minerais is a publication that aims to ordem and divulge the results of the technical activities that CPRM carries out in the fields of economic geology, prospection, exploration and mineral economics. These data are issued as maps, papers and reports.

According to the subject there are eight series of publications, named below.

- 1) Série Metais do Grupo da Platina e Associados;
(Metals of the Platinum Group and Related Metals Series)
- 2) Série Mapas Temáticos do Ouro, Escala 1:250.000;
(Thematic Maps for Gold – Scale 1:250.000 Series)
- 3) Série Ouro – Informes Gerais;
(Gold – General Information Series)
- 4) Série Insumos Minerais para Agricultura;
(Mineral Inputs for Agriculture Series)
- 5) Série Pedras Preciosas;
(Precious Stones Series)
- 6) Série Economia Mineral;
(Mineral Economy Series)
- 7) Série Oportunidades Minerais – Exame Atualizado de Projetos;
(Mineral Opportunities – Up-Dated Review of Project Series)
- 8) Série Diversos
(Sundry Series)

Please contact directly the Superintendência Regional de Porto Alegre – SUREG-PA or the Divisão de Documentação Técnica – DIDOTE, in Rio de Janeiro to ask for copies of this issue, using the addresses listed in the back cover.

1 - Foreword

CPRM National PGE project start-up and its activities were grounded on the Brazilian territory high potential regarding platinum group metals and Ni-Cu sulphides ore deposits. M. Farina, 1988, through quantitative gitology principles enlightened the geological environments favorable to mineralization, among them the Paraná Basin magmatism.

This magmatism was considered similar to the Siberian Platform mineral fields of Noril'sk and Talnakh and those of the Karoo Province, South Africa. The first ones are Ni-Cu producers - 6% and 46% of world production, respectively – and their total reserves are 8% of known ones (US Geol. Survey, Min. Comm. Summaries, Jan. 1999). USGS also inform that mineral consumption between the years 1994 and 1998 was increasing and the cumulative growth was 46% regarding Pt and 57% to Pd. Prices show the same trend with an important growth in the 1999/2000 years (Gazeta Mercantil).

Aiming to a preliminary evaluation of PGE metal potential of Paraná Basin magmatism and taking into account the favorable economic world consumption, a number of intrusions – dykes, sills and complexes – were listed and investigated. Geological and geochemical aspects of

these bodies were studied by Dias (1992-93), Chieregati (1995) and Sander (1993 – 94a, 94b and 95), Romanini and Albuquerque (1996), Alegri and Vasconcelos (1997) and Hulbert and Gregory (1999). The present report is based on these studies and is, in part, a compilation. So, this is an integration document of a part of significance of the present knowledge, encompassing regional geological context and detailed intrusions investigations in regard to their geochemical aspects, also including the volcanic rocks and some Paleozoic sediments. Analytical results of all samples made by the Geological Survey of Canada are also included.

Annex, there are tables showing geographic location of analyzed intrusive and sedimentary samples, due to the fact that it is unpractical to put this situation into a single map.

Among the results of geochemical prospecting of stream sediments and heavy minerals presented by Chieregati (1995), only the Franca's sill chromite and chalcopyrite grains are considered. As it seems, other results of this exploration are unimportant because of a general depletion of chalcophyles of these sill rocks. Negative results were achieved in other services done afterwards.

2 - Methodology

The following methodology was adapted: target areas selection using traditional literature models for similar geological environments, field reconnaissance, drill profiles studies, rock sampling and chemical and petrographycal analysis. Field teams were updated regarding new technologies and Drs. R. Eckstrand and L. Hulbert (GSC) worked as technical advisors.

Surface rock sampling focused into sills, dykes and hypabyssal mafic bodies as well as core samples of previous exploration services of sills intercalated into sedimentary sequence. Biggest and the most textural/compositional variegated mafic bodies were selected to be sampled.

Paleozoic country rock sediments were also sampled for comparison purposes.

Sill samplings were done accordingly to textural and compositions changes. Dykes were sampled at their border, intermediate and central positions.

Samples Selection and Analytical Procedures

Geochemical investigations were conducted for 302 samples, among them 225 of intrusive rocks, 63 of basaltic flows and 14 of country sedimentary rocks.

Major elements, trace elements and REE analyses were done at GSC labs in Ottawa. SiO_2 , TiO_2 , Al_2O_3 , $\text{Fe}_2\text{O}_3\text{t}$, MnO , MgO , CaO , Na_2O , K_2O and P_2O_5 are determined by means of X-ray fluorescence with an 1% error regarding concentration. H_2O , FeO , CO_2 , C and fire assay were done by means of traditional chemical methods. S, F and Cl were analyzed by

pyrohydrolysis with a detection limit of 50 ppm.

ICP-MS was used for REE with a detection limit of 0.1 ppm for Ce, La and Nd, 0.05 ppm for Yb and 0.02 for the others. IGP-MS limits are: for Cs, Ti, U and Th : 0.02 ppm; Hf, In, Nb and Rb: 0.05 ppm; Ag and Ga: 0.1 ppm; Cd, Mo and Ta: 0.2 ppm; Bi, Sn and Zn: 0.5 ppm and Pb: 2 ppm. ICP-ES determinations included: Co, V and Zn with a limit of 5ppm; Cr, Cu and Ni with 10 ppm and Ba, 20 ppm.

Intrusive rock elements Pt, Pd and Au were analyzed by means of ICP ultrasonic nebulizer after a tablet fire assay concentration of 30 g of samples, in Pb tablets in the ACME Analytical Labs, Vancouver. This method has a 0.5 ppb limit for Pb and Pt and 1ppb for Au. For 0.1 and 0.01 ppb for Pt and Pd respectively, ICP-MS was also used.

Drs. L.S. Marques (Instituto Agromônico e Geofísico – USP) and D.W. Peate (Dept. of Earth Sciences, The Open University, England) provided samples of volcanic suites for analyses at GSC for additional elements. References on these samples and regarding geochemical background are in Peate and Hawkesworth (1986), Piccirillo et al (1988), Bellieni et al (1984) and Mantovani et al (1985).

All analytical data were recalculated in an anhydric base and $\text{Fe}_2\text{O}_3/\text{FeO}$ ratio was turned equal to 0.15 before Mg#⁽¹⁾ and other parameter calculations.

Table A, following, shows groups of samples and their specimen numbers (quantity):

INTRUSIVE BODIES,VOLCANIC SUITES AND SED. ROCKS	SAMPL.	QTY
Porto Alegre Metropolitan Region and Irui-Leão Area		
Intrusive Bodies	(PA)	29
Lomba Grande Basic Complex	(LG)	03
Maracajá-Barro Branco Basic Body- core samples	(MB)	26
Maracajá-Barro Branco Basic Body – surface samples	(MBB)	32
Rio Urussanga Basic Body	(RU)	16
Pouso Redondo-Rio do Campo Basic Body	(PRR)	40
Ponta Grossa Arch Dykes	(PGA-D)	25
Ponta Grossa Arch Sills	(PGA)	54
High Ti Basic Volcanic Suite	(HTV-B)	19
High Ti Intermediate Volcanic Suite	(HTV-I)	04
Low Ti Basic Volcanic Suite	(LTV-B)	23
Low Ti Intermediate Volcanic Suite	(LTV-I)	11
Low Ti Acidic Volcanic Suite	(LTV-A)	06
Sedimentary Rocks	(SD)	14

Table A – List of sampled rocks and their number of specimens⁽¹⁾ Mg# = Mg/Mg + Fe

3 - Stratigraphy and Magmatism

3.1 Generalities

Paraná Basin is an intracratonic basin, located at South-American Platform, covering an area of 1,200,000 km², about 1,000,000 km² in the Brazilian territory. Some authors consider Chaco-Paraná Basin, located at Argentinean territory, as an integrating part of Paraná Basin, increasing its area to more than 1,600,000 km² (**Figure 01**).

Paraná Basin development came since Medium-Low Palaeozoic until the end of Mesozoic, building more than 4,000 meters of sediments, plus 1,700 meters of lava flows (Almeida, 1981; Zalan et al, 1986). More than 1,000,000 km² are covered by lava (750,000 km² in the Brazilian territory) and its volume reaches circa 790,000 km³ (Bellieni et al, 1986).

In association with this volcanic episode, there was a very intense sub-volcanic activity as sills and dykes located above all in the sedimentary country rock area. This belt comes from São Paulo State to the South-Center of Rio Grande do Sul, with an area of about 160,000 km².

3.2 Stratigraphy and Tectonic Evolution

There is, nowadays, a good knowledge of the Paraná Basin stratigraphy thanks to hydrocarbon exploration surveys through deep drilling works. PETROBRAS (Schneider et al, 1974) and PAULIPETRO (Gama Jr. et al, 1982) reports illustrate the level of knowledge and data integration of the basin (**Figures 02 and 03**).

Stratigraphic columns show that basin development was not uniform e.g. the lack of Devonian sediments in Rio Grande do Sul. Those differences are credited to transversal N-S tectonic movements above all in the Ponta Grossa region (Ferreira, 1982).

Sedimentary rocks are predominantly siliclastics, covered by the most important lava flow event in the world. Limestone levels, thin and isolated, lie in the Upper Permian, only, and are well repre-

sented in Irati Formation, basin's North third portion. There are also evaporites and bituminous mudstone horizons into this formation. Another must into this basin are coal deposits of Rio Bonito Formation, in the states of Santa Catarina and Rio Grande do Sul.

In the tectonic and stratigraphic evolution of the Paraná Basin four stages were identified (Melfi et al, 1988). The first one corresponds to the deposition of the marine sediments of the Paraná Group (Devonian – Lower Carboniferous) that was preceded by the imposition of the Ponta Grossa Arch which played an important role to this sedimentation (Fulfaro et al, 1982). This stage ended with epigenetic movements and faultings responsible for the surficial erosion that produced one of the main stratigraphic unconformities in the basin.

The second stage, Lower Carboniferous-Middle/Upper Permian in age, started by tectonic movements that gave birth to local depressions and uplifts. Most of the major tectonic structures were already active during the sedimentation, favoring its quick accumulation. These deposits are represented by marine and continental sediments (Itararé Group). The Itararé cycle and subsequent glaciation were followed by a relative tectonic stability characterized by a slow subsidence. The sedimentation resumed with fluvial, deltaic and marine shelf deposits of the Rio Bonito and Palermo formations, Passa Dois Group.

In the third stage (Upper Paleozoic to Jurassic) it was a general uplifting, that led to a remarkable erosional process and to the final development of the NW "in arch" structural trend – Ponta Grossa is an example. A Mesozoic Continental Sedimentation took place, represented by fluvial sandstones and siltstones of the Piramboia and Rosario do Sul formations in a rather tectonically stable basin. Desertic conditions prevailed in the beginning of the Jurassic period when a wide deposition of eolian sandstones covered the whole Paraná Basin.

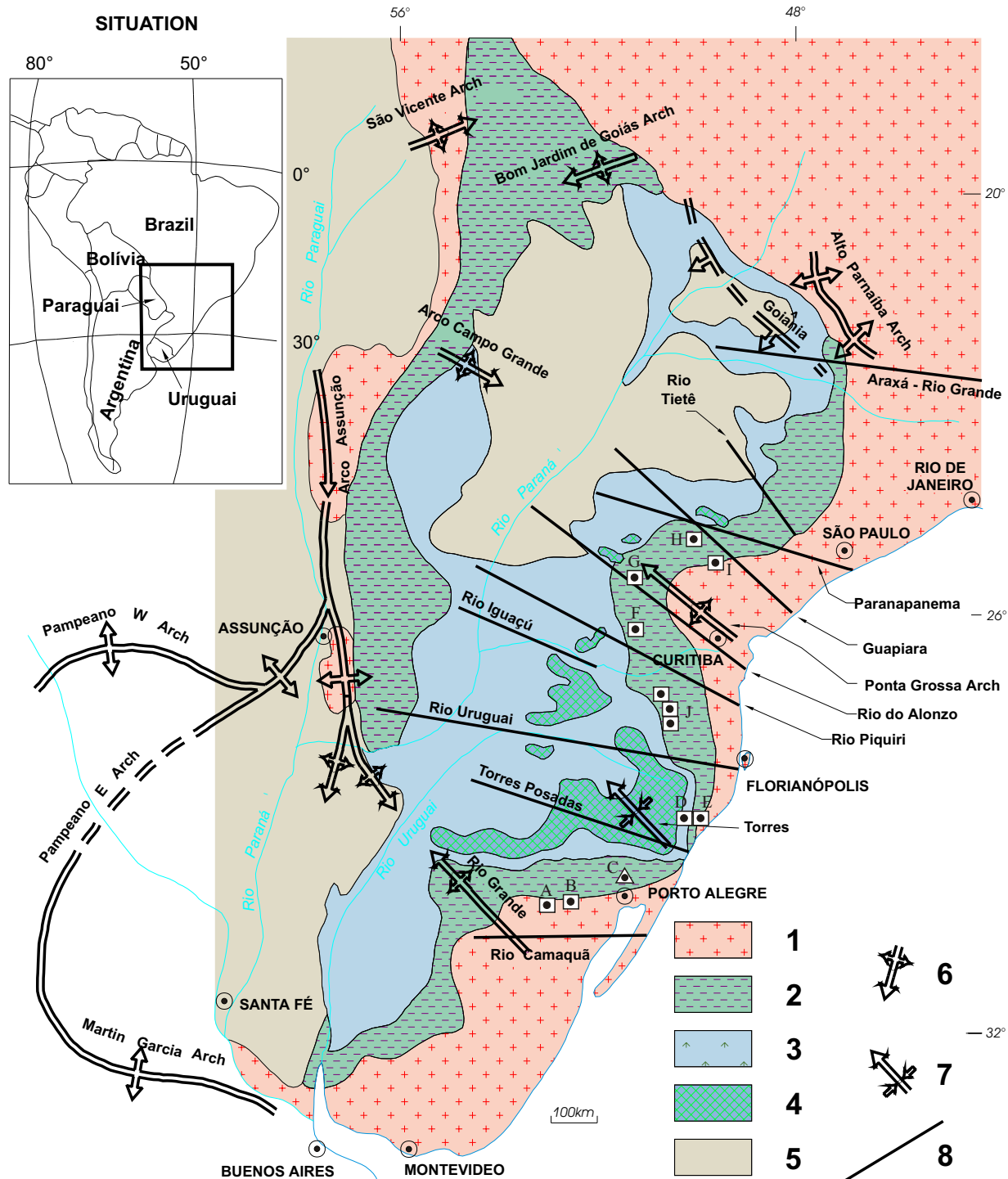


Figure 01 - Paraná Basin Geological Sketch (Melfi et al., 1988, mod.): 1 Pre-Devonian crystalline basement; 2 Dominantly paleozoic pre-volcanic sediments; 3 Intermediate to basic volcanic lavas; 4 Acidic stratified lava flows; 5 Pos-volcanic sediments (mainly Upper Cretaceous); 6 Arch-type structure; 7 Syncline-type structure; 8 Tectonic and/or magmatic lineation. Sills ◻; hypabyssal intrusion ▲; A: Iruí-Leão-PA region; B: Rio Pardo-PA region; C: Lomba Grande-LG; D: Maracajá/Barro Branco Sill; E: Rio Urussanga Basic Body-RU; F: Irati-PGA Sill; G: Reserva-PGA Sill; H: Siqueira Campos-PGA Sills; I: Fartura-PGA Sill; J: Pouso Redondo - Rio do Campo Basic Body-PRR.

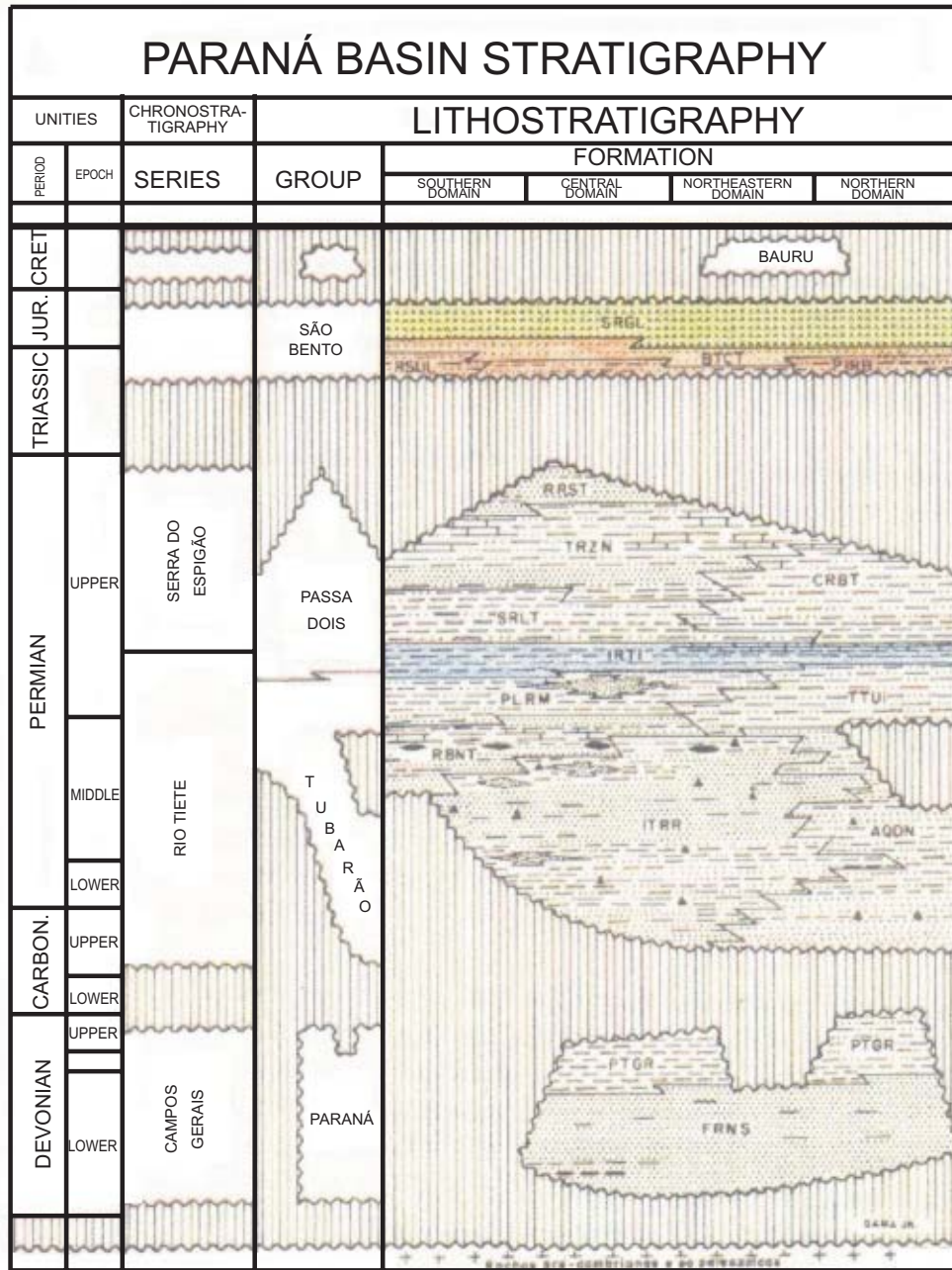


Figure 02 - Correlation among Paraná Basin stratigraphic units (Schneider et al., 1974)

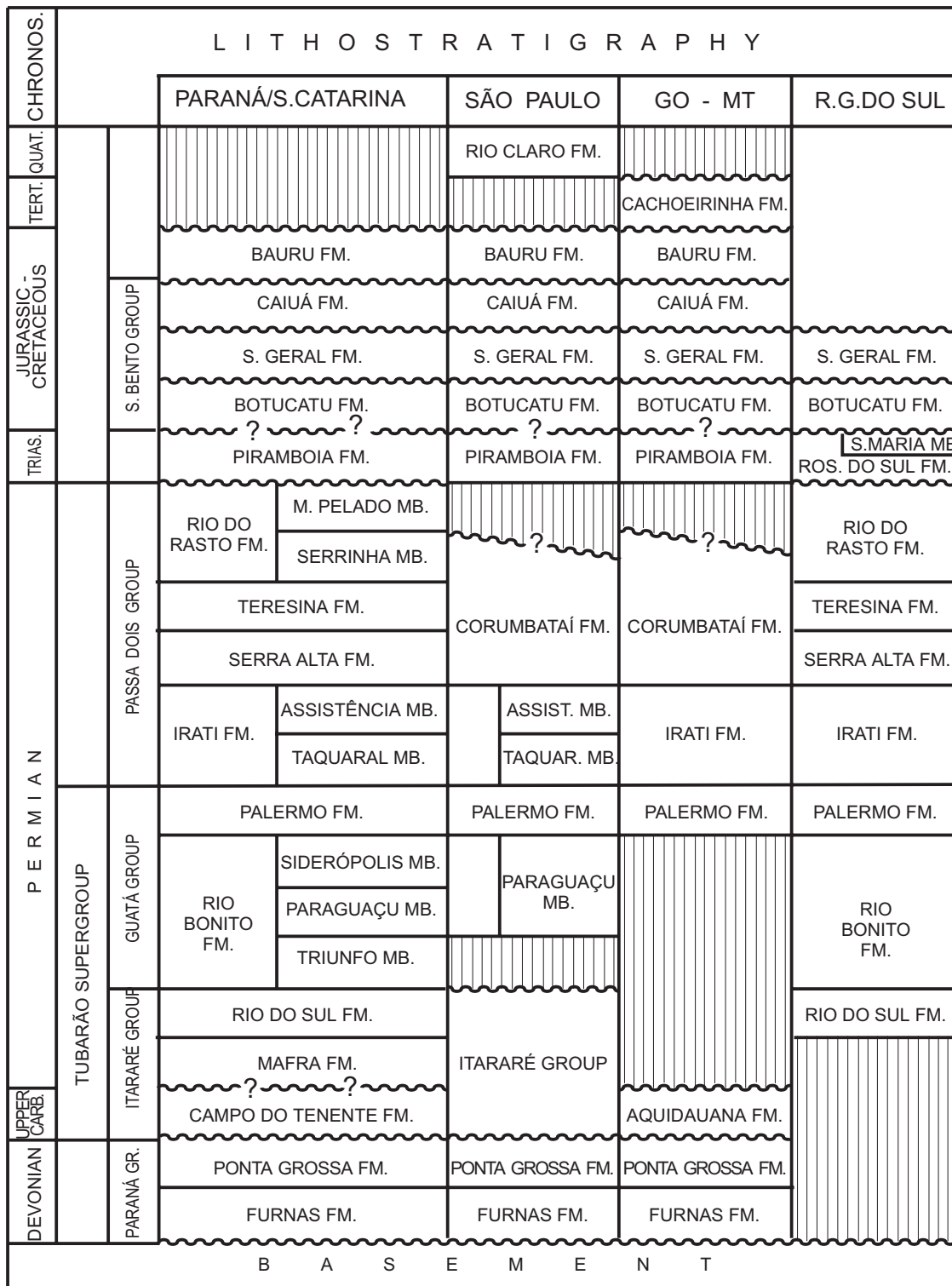


Figure 03 - Correlation among Paraná Basin stratigraphic units (Gama Jr. et al., 1982)

The last stage – Upper Jurassic to Lower Cretaceous – started with important tectonic events that produced an antiformal structure in the Paraná Basin (Almeida, 1981). The extensional tectonics caused an intense rifting that favoured the extrusion of huge amounts of tholeiitic basalts and subordinately acid and intermediate volcanic rocks – Serra Geral Formation. This volcanism, according to several authors in Melfi et al (1988), occurred between 140 and 120 Ma.

3.3 Volcanic Activity

The lava flows of the Serra Geral Formation lie unconformably on the Botucatu sandstones and locally on sedimentary rocks of the Passa Dois Group. There are places near the borders of the Paraná Basin where they lie directly on pre-Devonian crystalline rocks (Petry and Fulfaro, 1983).

These volcanic suites lie essentially in a sub-horizontal position, gently dipping (<5%) to the basin center. Nevertheless, lower lava flows can show strong dips, more than 15%, in regard to the basement topographic irregularities.

Volcanic pile total thickness varies from 350 to more than 1,000 meters. A single flow thickness is often about 50 meters, but can be of a few meters up to about 1,000 meters. Geologic paleomagnetic and geochemical studies (Bellieni et al, 1986), suggest an average thickness of 10 to 20 meters for a single lava flow.

Paraná Basin volcanic rocks are represented by different kinds of rocks such as: tholeiitic basalts (90%), tholeiitic andesites (7%) and rhyodacites-rhyolites (3%). The former ones covers an area of 150,000 km².

Basaltic and andesitic lava flows are represented by dominantly aphyric to subaphyric rocks and their separation is very difficult, in the field work. On the other hand, acidic lavas are very easy to distinguished into two main kinds, called Palmas and Chapecó. Palmas (PAV) are usually aphyric or subaphyric, black colour and coidal fractures and are covered by

Chapecó (CAV). CAV are porphyritic with plagioclase crystals of 20mm and are easy to separate of PAV type. PAV are concentrated in the state of Rio Grande do Sul and are rare in Santa Catarina and Paraná states. CAV ones predominate in the Northeast border of Paraná Basin.

Concerning their petrography, Paraná Basin volcanic rocks are divided into three main regions: Southeast – South of Rio Uruguay lineament; Central – a region between Rio Uruguay lineament and Rio Piquiri; and Northeast – a region North of Rio Piquiri (Piccirilo et al, 1988).

Southwestern region is represented mainly by basic volcanics and subordinately by acidic and intermediate rocks. As a rule, accordingly to Melfi et al (1988), the lower portion is composed by tholeiitic basalts and andesite-basalts and the upper portions are essentially rhyodacites and rhyolites Palmas type. In this region, according to W. Wildner, A. Caldasso and A. Dias (pers. Comm.), the lowest part of the volcanic building shows tholeiitic basalts, the medium part consists of rhyodacites and rhyolites, both of them covered by a tholeiitic basalt recurrence.

In the Northeastern region the tholeiitic basalt dominates, sometimes covered by acidic volcanics of Chapecó Formation at South and East portions. Locally, the volcanic suite ends, at its top, with a thin basaltic flow, covering acidic volcanic rocks. In this case, intermediate volcanic rocks are absent.

Central region shows volcanic suites similar to the other ones. Basic volcanics predominate. They are tholeiitic and andesite-basalts covered by rhyodacites and rhyolites. Locally, acidic rocks Chapecó type are covered by basalt. Intermediate rocks are rare and they are solely linked to extrusive suites, encompassing acidic volcanics Palmas type.

Bellieni et al (1984/86) and Mantovani et al (1985) proved that Paraná Basin basalts shall be considered as homogeneous rocks regarding their composition only in a broad sense as far as they are, in fact, two main types of rocks.

fact, two main types of rocks. Those two basalt types show very important chemical composition differences and can be recognized by their high TiO_2 or low TiO_2 content and by their incompatible trace elements and are nominated as LTB and HTB, respectively.

It should be emphasized that LTB predominate in the Southeastern region, and the HTB in the Northeast, whereas there is a mixture in Paraná Basin central region.

Acidic volcanics Palmas type are almost poor regarding TiO_2 and incompatible trace elements and, as a rule, they are associated to LTB in the basin southeast. On the other hand, Chapecó acidic volcanics are, in comparison, rich regarding TiO_2 and incompatible trace elements and they are associated to the HTB in the northeast of Paraná Basin.

3.4 Intrusive Rocks

Intrusive magmatism related to Paraná Basin lava flows is also characterized by its basaltic chemical composition and is predominantly represented by dikes and sills and subordinately by the intrusive complexes. Geochronology data of their samples show large variation: sills are between 106 to 161 Ma and dykes 119 to 142 Ma. Both cases confirm that intrusive activity happened at the same time as volcanics activities.

Dykes

Dyke intrusions show two main directions: NW – SE and NE – SW. The first ones are concentrated at Ponta Grossa Arch region, although there are also some NE – SW directions.

The former one are more frequently hosted by basement rocks, reflecting the strongest structural directions of these.

According to a number of authors, dykes show thicknesses varying between 20 to 50 meters, reaching, in some points, until 600 meters (Marini et al ,1967). Along the strike they have 1 to 5 kilometers long, and they can reach up to 20 km, as reported by Ferreira (1982). Most of them

consist of plagioclase (labradorite), clinopyroxens, magnetite, ilmenite, pyrite, apatite and some quartz. Diorite and quartz-diorite differentiated rocks also are present and generally lie in the central portions of the thickest dykes.

The majority of reports focusing Ponta Grossa Arch dykes inform that intrusives are the result of the way followed by Low Cretaceous Paraná Basin lava flows to reach the surface. Meanwhile, Piccirillo et al (1988) put that, to the geochemistry point of view, dykes are similar to the northeast basin region volcanic rocks. This statement discards the possibility of Ponta Grossa Arch dykes being the feeders of southern and center basaltic Paraná Basin lava flows.

Sills

Sill intrusions are also Low Cretaceous and they are of the same age of the principal volcanic activity (120 to 130 Ma). They lie at the interior of Paraná Basin, in the Palaeozoic sediments at different stratigraphic and tectonic levels.

Sills often show a thickness between 2 and 200 meters and the same body shows a great variety of them (Cordani and Vandoros, 1967). Due to the lack of outcroppings, it is very difficult to evaluate the extension of the sills. The biggest one was estimated in 900 km^2 at Piracicaba-Limeira sill, State of São Paulo (Cordani and Vandoros, op. Cit.).

Stratigraphic position of sills are known because of the existence of preferred intrusion levels, due to lithological discontinuities or to the presence of fragile lithologies, like mudstones levels.

Zalán et al (1986), introduced Aquidauana Formation of Itararé Group as the stratigraphic unit to show the most frequent intrusions (22%), followed by Irati Formation (18.1%) and Teresina and Ponta Grossa Formations, among others. Taking into account the relation between cumulative sill thickness and the stratigraphic unit thickness, Irati Formation is the one that shows the best favorable index to intrusions.

As the best tectonic environment, dykes become present in the areas that horizontal stress reaches the maximum force; above a given level, they develop another environment favoring sill intrusions.

Regional differences due to the most important force component, tension compression or gravity (magmas column

weight) shall have existed in the Paraná Basin, taking into account basement arc uprising and subsidences, accordingly to the Dallmus theory (in Soares, 1981).

There are some regions where dykes predominate and in others, sills do. This is an evidence of tectonic environment in relation to intrusive bodies emplacement.

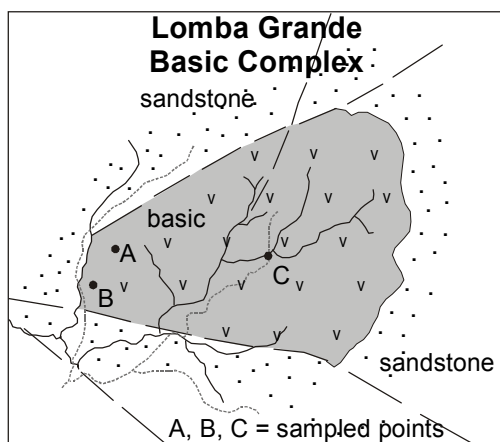
4 - Geological Synthesis of the Investigated Intrusive Bodies

Outcropping and non-outcropping intrusive bodies in Rio Grande do Sul, Santa Catarina, Paraná and São Paulo States were studied regarding geological, geochemical and economic potential. Concerning the two last states, Chieregatti (1995) already evaluated other intrusive bodies; nevertheless, into the present paper, only the chemical analyses done by the Canadian Geological Survey were taken into account. They are shown in **Figure 01**.

4.1 Intrusions in the Rio Grande do Sul State

Lomba Grande Basic Complex and Porto Alegre Metropolitan Region sills and Irui-Leão and Rio Pardo areas were studied in Rio Grande do Sul State.

Lomba Grande Basic Complex is located in the north-eastern area of Porto Alegre Metropolitan Region, at the Pedreira Lomba Grande place (**Figure 04**). It is a hypabyssal body of a lopolith shape with 440 m in thickness and a minimum volume of 0.47 cubic kilometers (Viero's geophysical data, 1991). In a map it has ellipsoidal aspect covering an area of 6 square kilometers. Most of it is a rock mass of olivine gabbro, dark-grey, medium equigranular texture grading to microphaneritic diabase without olivine. Mineralogy consists of olivine (0 to 35%), labradorite, clino and orthopyroxen and metallic minerals grading from 0.5 to 2% (magnetite, ilmenite, chalcopyrite, pyrite, chalcocite and maucherite). Sandstones of the Jurassic-Cretaceous Serra Geral Formation constitute the country rock, with markedly faults in the northern and southern borders of the intrusive body, such as sketched below.



Outcropping sills at Irui-Leão and Rio Pardo regions (Sander, 1993), at west-north-west from Porto Alegre (**Figure 01**), show various thicknesses and the biggest one is 80m thick. Generally these rocks are very homogeneous, texturally varying from phaneritic to thin equigranular up to microporphyritic and porphyritic (microphenocrystals with a diameter of 0.5 to 1 mm).

Mineralogical composition is simple, including plagioclase (more or less 70%), andesine-labradorite type and pyroxen (+/- 25%) is pygeonite and/or augite. Metallic minerals (ilmenite and magnetite) in an interstitial fulfilment reach +/- 5% of the rock. There are no olivine nor sulphides.

In the Porto Alegre Metropolitan Region (**Figure 04**), as in the Irui-Leão and Rio Pardo areas, 485 sills drill profiles were studied from which the twelve thicker ones were selected for chemical and petrographic analyses purposes. In the two latter regions sills showed 30m of thickness as a medium and their rocks varies from aphanitic to microaphanitic textures on the upper part of the profiles, to fine-to-medium porphyritic ones, with augite and subordinate plagioclase phenocrysts as predominant lithologies. Olivine is rare and, as a rule, occurs as traces.

Among selected profiles of the Porto Alegre Metropolitan Region, sill thicknesses vary from 55 to 84 meters (Sander, 1994 a), and normally their structure is: first type on the top and on the lowest part of the sill, aphanitic to fine porphyritic, plagioclase and pyroxen predominates; a second predominant type, medium equigranular, occurring in the center of the sill, intergranular texture where olivine varies in the mineralogy from 10 up to 50% and is normally euhedral showing corrosion borders giving a picritic characteristic to the rock; a third type, with pegmatitic texture occurs as layers or amas, has the medium intergranular type as its wall and olivine is present or absent. There are no sulphides in this region.

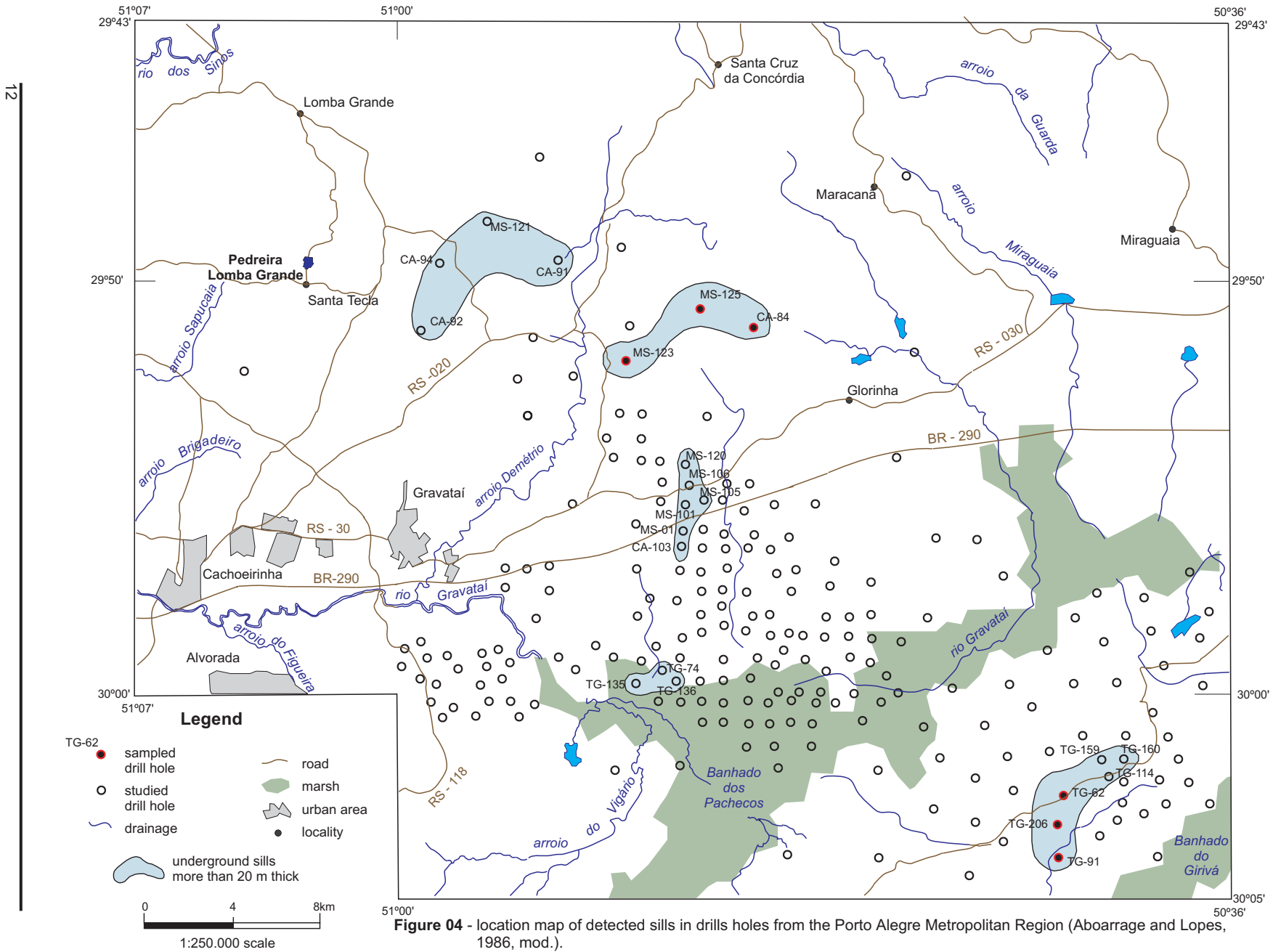


Figure 04 - location map of detected sills in drills holes from the Porto Alegre Metropolitan Region (Aboarrage and Lopes, 1986, mod.).

4.2 Intrusions in the Santa Catarina State

Maracajá-Barro Branco sill, Rio Urussanga body and Pouso Redondo-Rio do Campo sill, all in Santa Catarina State, were studied. Maracajá-Barro Branco sill, located at a south-western area of Florianópolis (**Figure 05**), has almost 100 square kilometers of outcropping area, is elongated in the N-S direction, has a 49 kilometers major axis (Dias, 1993). Medium width varies from 5 kilometers in the northern portion to 10 to 15 kilometers at the center and 0.5 kilometers in the southern portion. This sill is an intrusion located between Iriti and Serra Alta formations, has a wedge shape with a maximum known thickness of 136.8 m (hole CR-17) in the septentrional area and a minimum of 27.4 m in the meridian portion (hole MB-25).

Rio Urussanga body (**Figure 06**) has an area of about 33 square kilometers and a thickness between 60 up to 140 m, is placed on Rio Bonito Formation without any remaining covering of the other Palaeozoic sedimentary package.

From the petrographic point of view rocks of both sills are very similar. Predominant lithotype has a fine equigranular to microphaneritic texture with very local variation, sharp and without lateral continuity to the porphyritic or medium granulation facies. Regarding their composition, they show very little variation, are located between basalts and granophyric basalt fields; they show plagioclase (40 to 60% with a Na 30-50 tendency), plus clinopyroxen-augite and pygeonite. Disseminated, or as a fracture fulfilment pyrite can have very high proportions (5 to 15%), mainly at sills bottom.

Pouso Redondo-Rio do Campo sill widespread over an area of about 500 square kilometers, at locations of the same names, highest part of Itajai-Açu river, in the north of Santa Catarina State. Considering, however, that it can stand intercalated in different levels of the sedimentary sequence of the Paraná Basin – between Mafra and Serra Alta/Teresina formations – it is understood as a little sill association. Medium thickness, of about 8 to 15 m, lead

to this interpretation. Basic rocks textural varieties at these sills, as well as composition and granulation, follow homogeneous standards that are regionally persistent. Aphanitic and fine-granulated to aphanitic textures predominate; they are fast cooling typical ones, where plagioclase ripple-arrays are a must. Gradations into medium textures are rare and they lack any area expression.

4.3 Intrusions in Paraná and São Paulo States

Dykes and sills of the Ponta Grossa Arch at Siqueira Campos and Salto do Itararé in the Paraná State and Taguai and Fartura in São Paulo State were investigated (**Figure 07**). Sills are almost totally confined to Iriti and Serra Alta formations, in the Paraná State; they are hosted by Palermo, Rio do Rasto, Teresina and Botucatu/Piramboia formations as well as Iriti Formation, in São Paulo State.

In Siqueira Campos region there is a number of sills covering a total area of 180 square kilometers. The main body is located between Siqueira Campos and Catingua towns and has an area of almost 80 square kilometers and a maximum thickness of 100 m, being composed of diabase of medium to coarse granulometry, is very homogeneous, without olivine and with a very rare sulphide punctuation. Other minor intrusions in this region, like Patrimônio, Boa Esperança, Santana do Itararé and Salto do Itararé are formed by similar lithotypes as the above cited and they can show olivine in grades up to 5%.

Salto do Itararé sill, located at the village of the same name, shows a restricted outcropping area but also shows a wide textural variety in the vertical direction. Basal rocks are gabbros with pegmatoidic and coarse granulometry showing prismatic augites very well developed, grading of fine to medium granulometry gabbros in the way to the top of the intrusion. Presence of olivine is very common. Thickness of this sill is of about 30 m, as a preliminary evaluation.

Reserva sill lies in the southern flank of the Ponta Grossa Arch. It has an area of about 100 square kilometers, me-

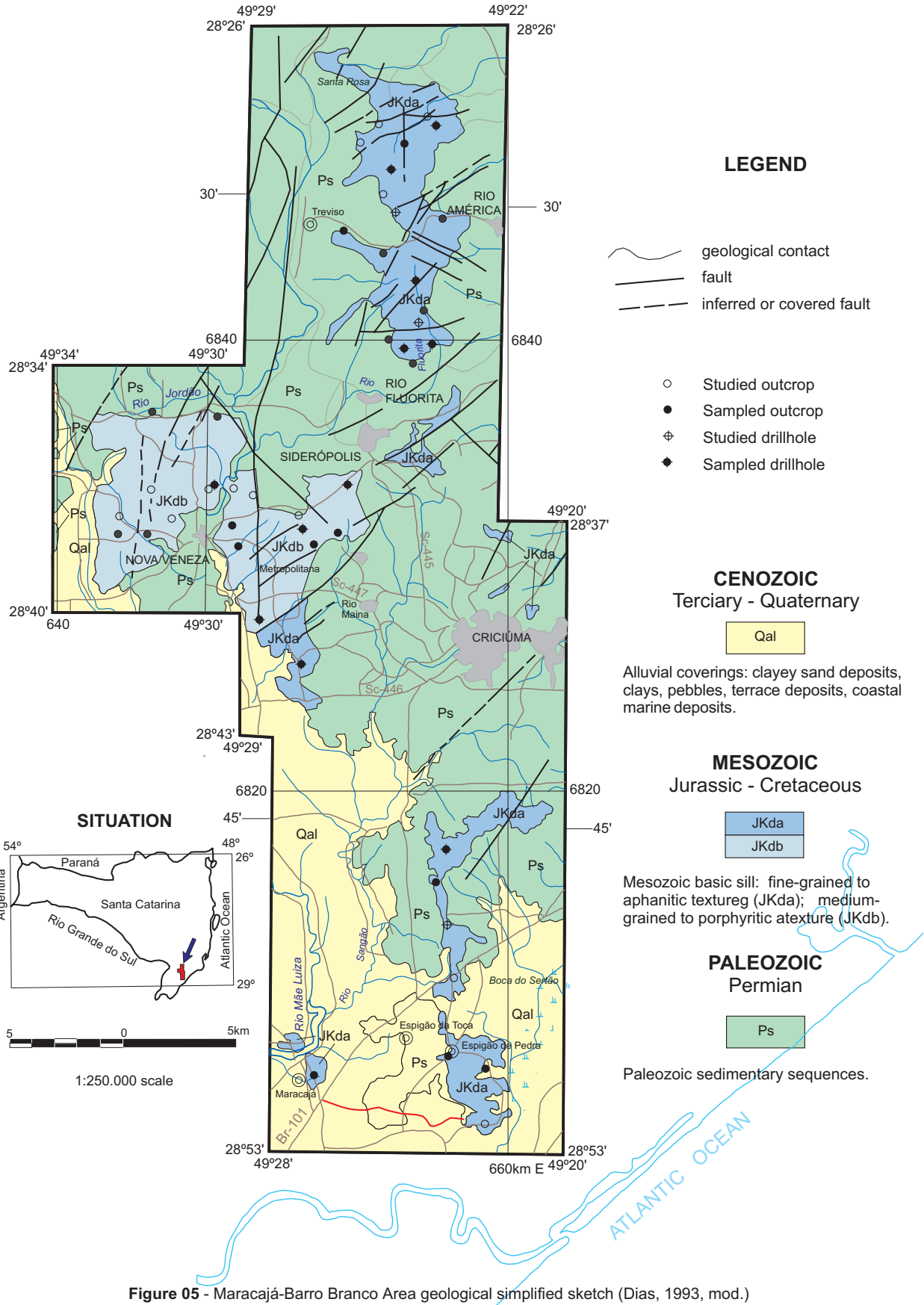


Figure 05 - Maracajá-Barro Branco Area geological simplified sketch (Dias, 1993, mod.)

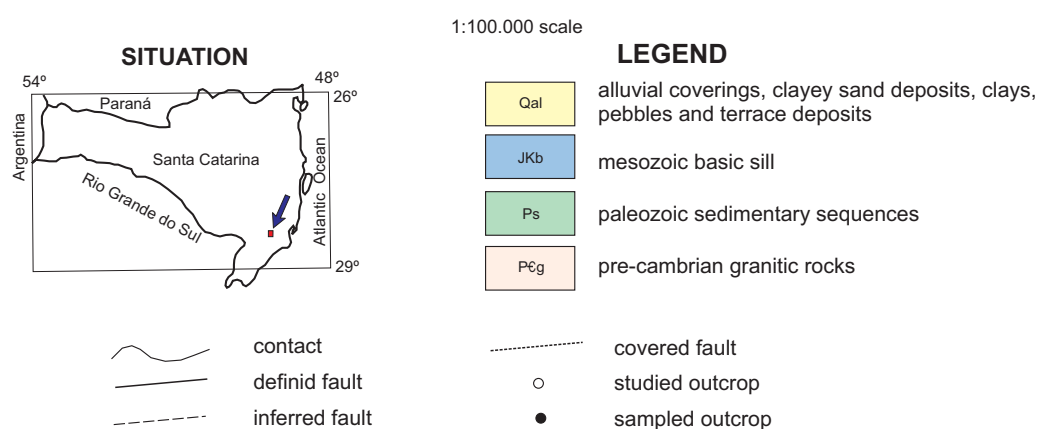
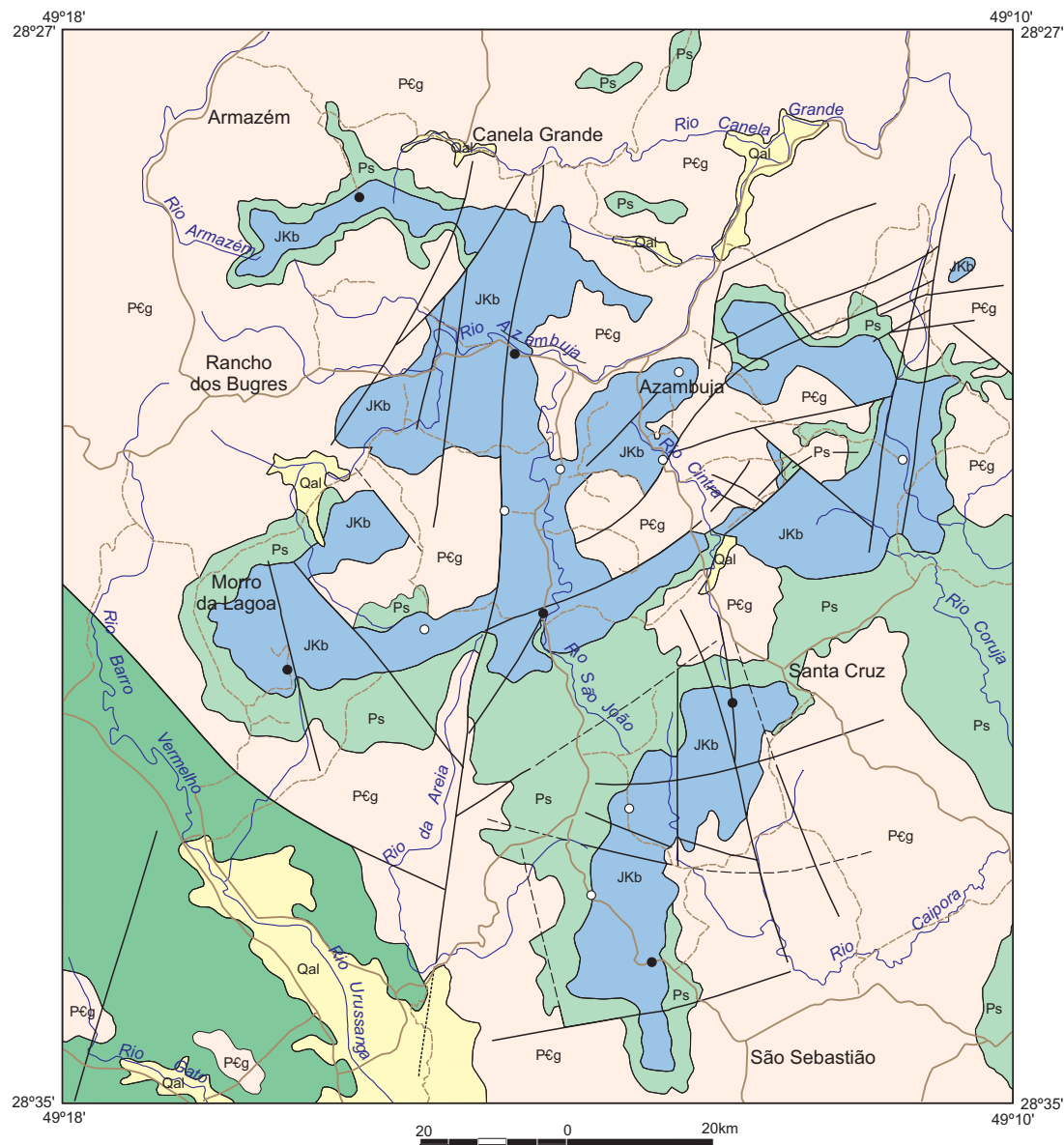


Figura 06 - Rio Urussanga Basic Body geological simplified sketch (Dias, 1993, mod.).

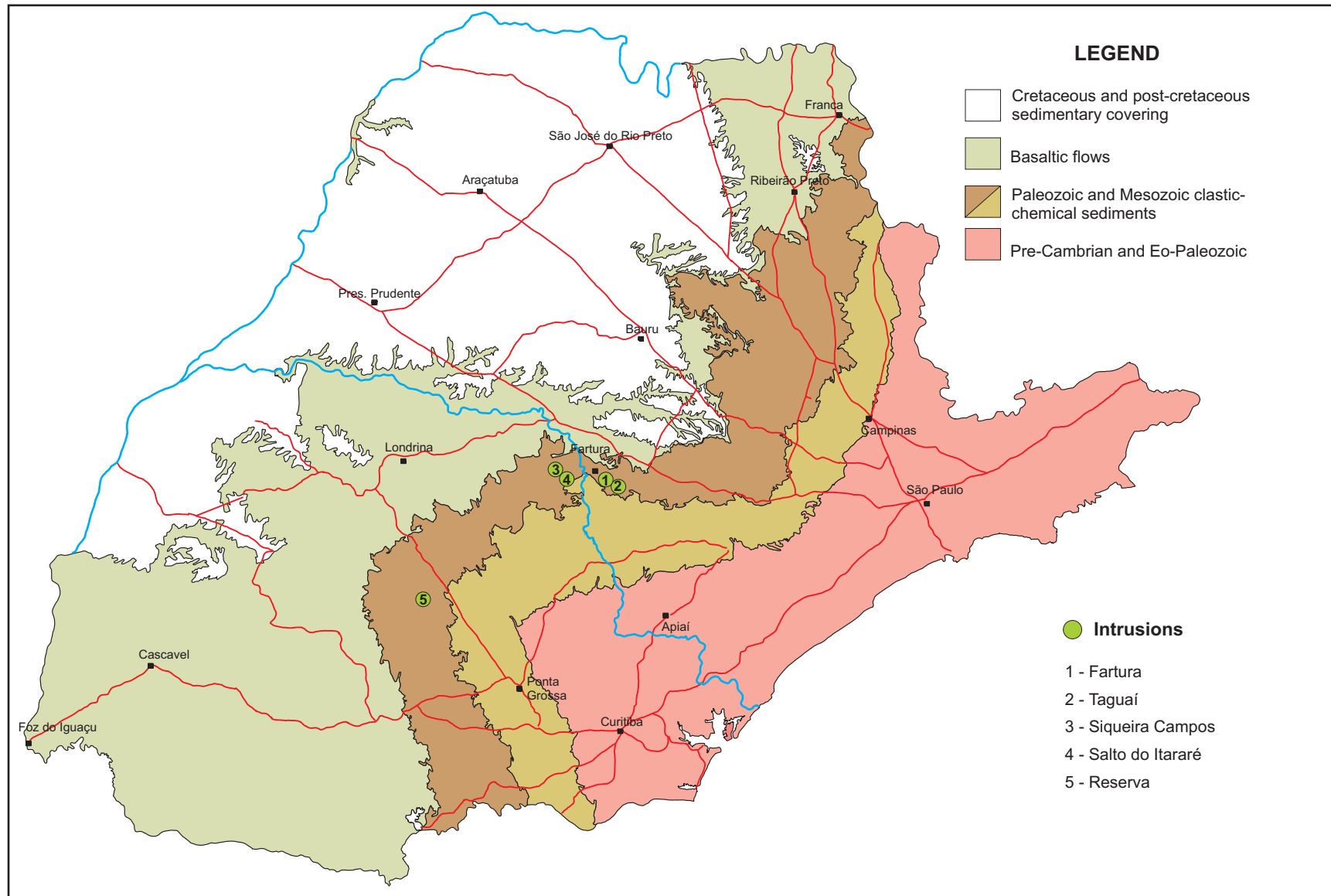


Figura 07 - Paraná and São Paulo (part) states geological simplified sketch with its investigated intrusions location (Chieregati, 1995, mod.).

dium thickness between 90 to 110m with a maximum of 150m in the Anta Gorda region. Lithotypes are diabases, microgabbros and gabbros. Maniese (1991) presented a study of its vertical profiles, surveyed at different sectors of this sill. Among 28 samples analyzed by this author, 10 had olivine presence in grades between 5 and 9%, being at basal or intermediate portions of the sill those of olivine contents of more than 7%.

In the author samples, olivine occurrences were in the form of traces or they were absent. Sulphides are rare and they are restricted to pyrite fulfilling fractures of the main rock.

In the Fartura region there is a sill of an area of about 130 square kilometers and a medium thickness of 100 m, dominantly composed by diabase, microgabbro and gabbro with or without olivine. In some places there are disseminated sulphides, identified as pyrite and chalcopyrite. Many other sills studied by Chieregati (1995) and Romanini and Albuquerque (1996), outcropping in the states of Paraná – Irati re-

gion – and São Paulo – Campinas/Jaguaruna/Limeira/Piracicaba/Leme-Araras/Pirassununga/Cruz das Palmeiras – among other, are not included into this paper because of their lack of rock sampling.

Investigated dykes, dominantly spread in the Fartura region, inserted into Guapiara Structural Trend, which corresponds to the northern limit of Ponta Grossa Arch, where they occur in a great number, as for the dipolar anomalies (high frequency), observed in the airbornemagnetic survey of the area.

Among sampled dykes is the Taquari, east of Fartura, with a thickness of 500 m, disseminated olivine and sulphides, medium to gross granulometry diabases and a lamprophyric dyke in Fartura/Sarutai road showing a thickness of 150 m, with a high olivine content porphyritic rock, juxtaposed to which there is a diabase dyke with 20m of thickness. Another investigated dyke lies on the Reserva region, with a thickness of 60 m, consisting in a coarse granulated diabase with fracture fulfilling sulphides.

5 - Results and Geochemical Variations

Geochemical investigations conducted on basic dykes, sills and intrusions during this study revealed that the most MgO – rich (18.26 wt. Per cent) and primitive (Mg#’s up to 0.74) bodies are found in the *southern Paraná basin*, more specifically with intrusions from the Porto Alegre metropolitan region to Iruí – Leão areas (PA), and in the Lomba Grande Complex (LG), **Figure 08A** and **Tables 01 and 02 (Appendix)**. The most fractionated and MgO – poor differentiates (**Figure 08A**) are associated with diabase sills from the Pont Grossa Arch (PGA), *northern Paraná basin*. Here material with MgO contents as low as 0.75 wt. Per cent and Mg#’s of 0.11 was encountered (**Table 07, Appendix**) However, material from these same bodies can have MgO contents as high as 6.42 wt. Per cent and Mg# up to 0.47. Between these two diverse data sets (PA and PGA) a wide range of compositions and chemical overlaps was observed with respect to the various investigated bodies.

A plot of MgO x Mg# (**Figure 08A**) demonstrates that the slope of the linear portion of the intrusive suites fractionation curve is noticeably flatter than that associated with the Paraná volcanic suite (HTV-, LTV).

MgO and Mg# compositional data for the intruded sedimentary rocks are also shown in **Figure 08A**.

Bellieni et al., (1984) demonstrated that the members of the Paraná high – titanium and low – titanium volcanic suites can be characterized on a silica – alkali plot similar to that in **Figure 08B**. Established high – titanium (HTV – B, basic; HTV-I, intermediate) and low – titanium volcanics (LTV – B, basic; LTV – I, intermediate; LTV – A, acid) samples analyzed parts of this study have also been plotted to confirm the use of this geochemical discriminator and its potential application with respect to the intrusive suites. In **Figure 08B** the solid line separates the high – titanium (HIT) field from the low – titanium field (LOT). Intrusive bodies from the *southern Paraná basin* (Porto Alegre metropolitan region and Iruí –

Leão areas (PA), Lomba Grande Complex (LG), Maracajá – Barro Branco basic body (MB, MBB) and Rio Urussanga basic body (RU) should belong to the low – titanium Paraná suite based on their geographic location. This geochemical association is corroborated by samples from the respective intrusive (as well as extrusive) suites in **Figure 08B**.

The Pouso Redondo – Rio do Campo basic body (PRR), with only a few exceptions, falls well within the high – titanium field. Samples from the Pont Grossa Arch are more equivocal since they can be found in the high – titanium and low – titanium fields. With the exception of some siliceous late differentiates, sill material from the Pont Grossa Arch (PGA) generally falls in the high – titanium field; however dyke (PGA – D) samples are well represented in both the high – and low – titanium fields.

Due to the large number of samples and elements analyzed during this study, and the extensive computations related to diagnostic elemental ratios, the analytical data have been statistically summarized and presented in **Tables 01 to 14 (Appendix)**.

5.1 Major Element Variations with Differentiation

Since the Mg# of a rock monitors the $Mg/(Mg+Fe^{2+})$ of an associated magma plots of this variable with other chemical parameters should depict the chemical evolution of the Paraná magma(s) that gave rise to the investigated intrusions and their extrusive analogues.

Variations in the major element oxides SiO_2 , Al_2O_3 , CaO , TiO_2 , P_2O_5 with respect to the associated Mg# are illustrated in **Figure 09A-E**. The most primitive bodies (Porto Alegre metropolitan region and Iruí – Leão areas (PA).Lomba Grande Complex (LG) have the highest Mg#’s (0.74) and lowest SiO_2 contents (44.34 per cent). However, **Figure 09A** and **Tables 01 and 02, Appendix** reveal that Mg#’s as low

as 0.25 and SiO_2 concentrations as high as 68.13 per cent are also associated with these intrusions (PA). Sills from the Ponta Grossa Arch appear to be the most fractionated Mg# (0.11) and as a group (PGA) contain the highest silica contents. The evolving magmas associated with this group, as well as Paraná magmatism in

general, demonstrate silica – enriched fractionation trends. Sedimentary rocks are generally siliceous in nature (>68 per cent SiO_2) and fall well above the Mg# - SiO_2 fractionation curve shown in **Figure 09A**. A plot of $\text{Al}_2\text{O}_3 \times \text{Mg}\#$ (**Figure 09B**) demonstrates two evolutionary paths. The most primitive group of intrusions (PA, LG) gen-

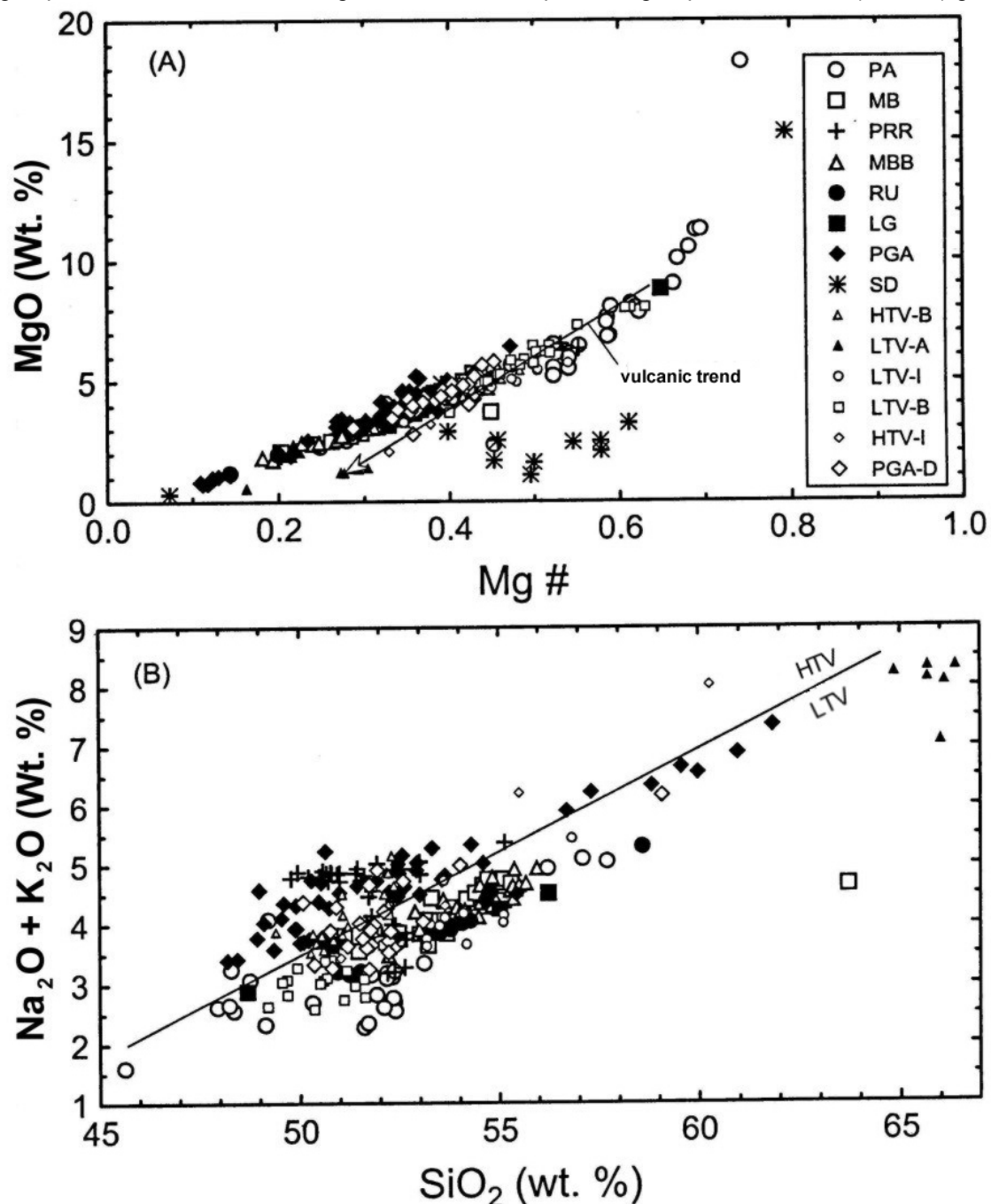


Figure 08 - $\text{MgO} \times \text{Mg}\#$ (A) and silica - alkali (B) diagrams for mafic bodies and sills, dykes (PGA - D), volcanic suites (HTV, LTV), and sedimentary rock (SD), Paraná basin and surrounds.

erally displays an Al_2O_3 – enrichment trend (11.57 to 17.72 wt. Per cent) as the intrusions evolved ($\text{Mg}^{\#}$'s 0.74 – 0.52). This trend is clearly orthogonal to that of the main Al_2O_3 – depletionary trend depicted by the remaining intrusions and volcanics with $\text{Mg}^{\#}$'s in the 0.52 – 0.11 range. A similar trend can also be seen with respect to CaO variations with differentiation.

TiO_2 concentrations of the basic intrusive groups and extrusive suites generally increase with fractionation. However, although the lowest TiO_2 concentrations increase from a low of 0.73 wt. Per cent in the primitive group (PA) to 4.4 wt. Per cent in the fractionated PGA – D group of intrusions, the intrusive groups like their extrusive analogues, can be divided into a high – titanium and low – titanium suites (**Figure 09D**). The solid line in **Figure 09D** separates the low – titanium from the high – titanium suites and was arbitrarily drawn based on the position of established samples from the high – titanium (HTV) and low – titanium (LTV) volcanic suites. With the exception of some of the most primitive samples from the PA group, intrusions belonging to the high – titanium and low – titanium suites are similar to those established on the silica – alkali diagram (**Figure 08B**); however, sill material from the Ponta Grossa Arch (PGA) overlaps both fields particularly in the late differentiates. As was the case for the silica – alkali plot in **Figure 08B**, a plot of $\text{P}_2\text{O}_5 \times \text{Mg}^{\#}$ (**Figure 09E**) appears to more clearly demarcate the high – titanium intrusive and extrusive suites from their low – titanium analogues than the $\text{TiO}_2 \times \text{Mg}^{\#}$ plot in **Figure 09D**. The Pouso Redondo – Rio Campos samples (PRR) are noteable by their markedly discordant P_2O_5 – enrichment trend (0.13 to 2.76 wt. Per cent).

5.2 Trace Element Variations with Differentiation

Rubidium and Ba (**Figures 09F** and **09H**) appear to evolve similarly with fractionation, the lowest concentrations occurring in the earliest differentiates and the highest in the latter. No distinct division is obvious with respect to high – or low – titanium suites.

Concentrations associated with intruded sedimentary hostrocks are generally rather restricted, and their distribution relative to the established trends constrains the role of these elements in crustal contamination of the magma. Strontium (**Figure 09G**) displays a bifurcating trend with fractionation; samples with $\text{Mg}^{\#}$'s in the 0.4 to 0.5 range have relatively flat profiles with concentrations generally < 200 ppm whereas other samples or groups evolve to concentrations in the 200 to 500 ppm range.

The incompatible elements Zr, La, Hf, Nb, Ce and Y tend to behave in a similar manner with differentiation (**Figures 10A** to **10F**). Once again, the lowest concentrations are associated with the PA and LG intrusive groups; whereas, the highest are found in sills from the Ponta Grossa Arch (PGA). It would appear that lower concentrations are associated with the low – titanium intrusive suites: PA, LG, MB, MBB and possibly RU; whereas, higher concentrations are found in their high – titanium counterparts: PGA, PRR, and PGA-D. Examination of volcanic equivalents with similar $\text{Mg}^{\#}$'s suggests that relatively lower values are present in the extrusive counterparts. A notable deviation from the general trend associated with samples from the Pouso Redondo – Rio do Campo basic complex (PRR). As was the case for P_2O_5 , the elements La, Nb, Ce and Y define a steep enrichment trend oblique to the main trend established in the other investigated suites. The close similarity in concentration of these elements in the sedimentary hostrocks (SD) with magmatic rocks with comparable $\text{Mg}^{\#}$'s is shown for comparison. **Tables 01** to **14**, **Appendix** statistically summarizes the concentration of these elements with respect to each group.

Uranium and Th (**Figures 10G** and **10H**) display much better constrained differentiation trends than Zr, La, Hf, Nb, Ce and Y. The host sedimentary rocks also contain significantly higher concentrations of U and Th than the contained intrusions. Samples from the PA group display an array or trend with higher concentration of U and Th than one would expect when analyzing the same group trends with respect to Zr, La, Hf, Nb, Ce and Y.

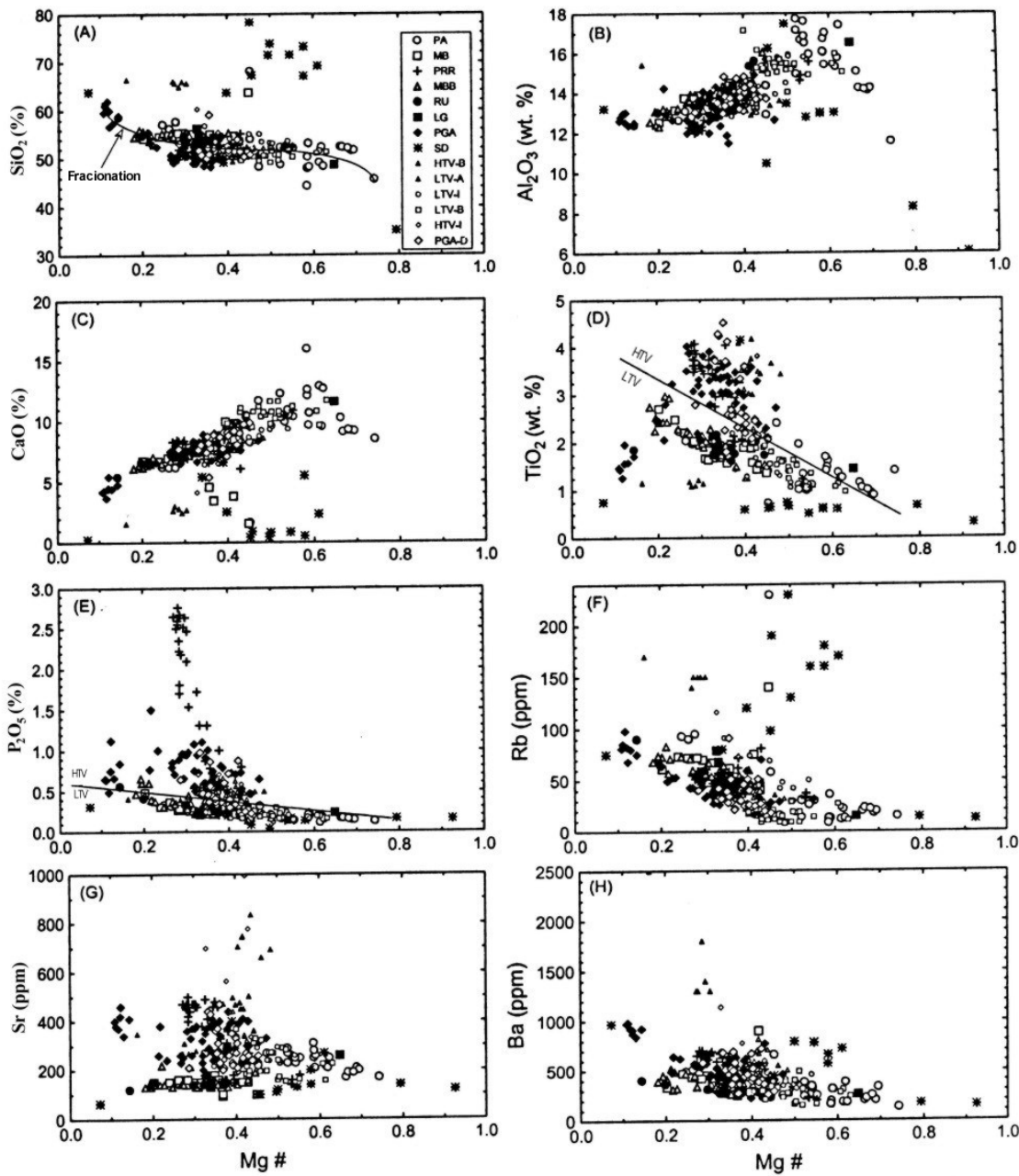


Figure 09 – Mg# x Major (anhydrous) and trace element diagrams for mafic bodies and sills, dykes (PGA – D), volcanic suites (HTV, LTV), and sedimentary rock (SD), Paraná basin and surrounds.

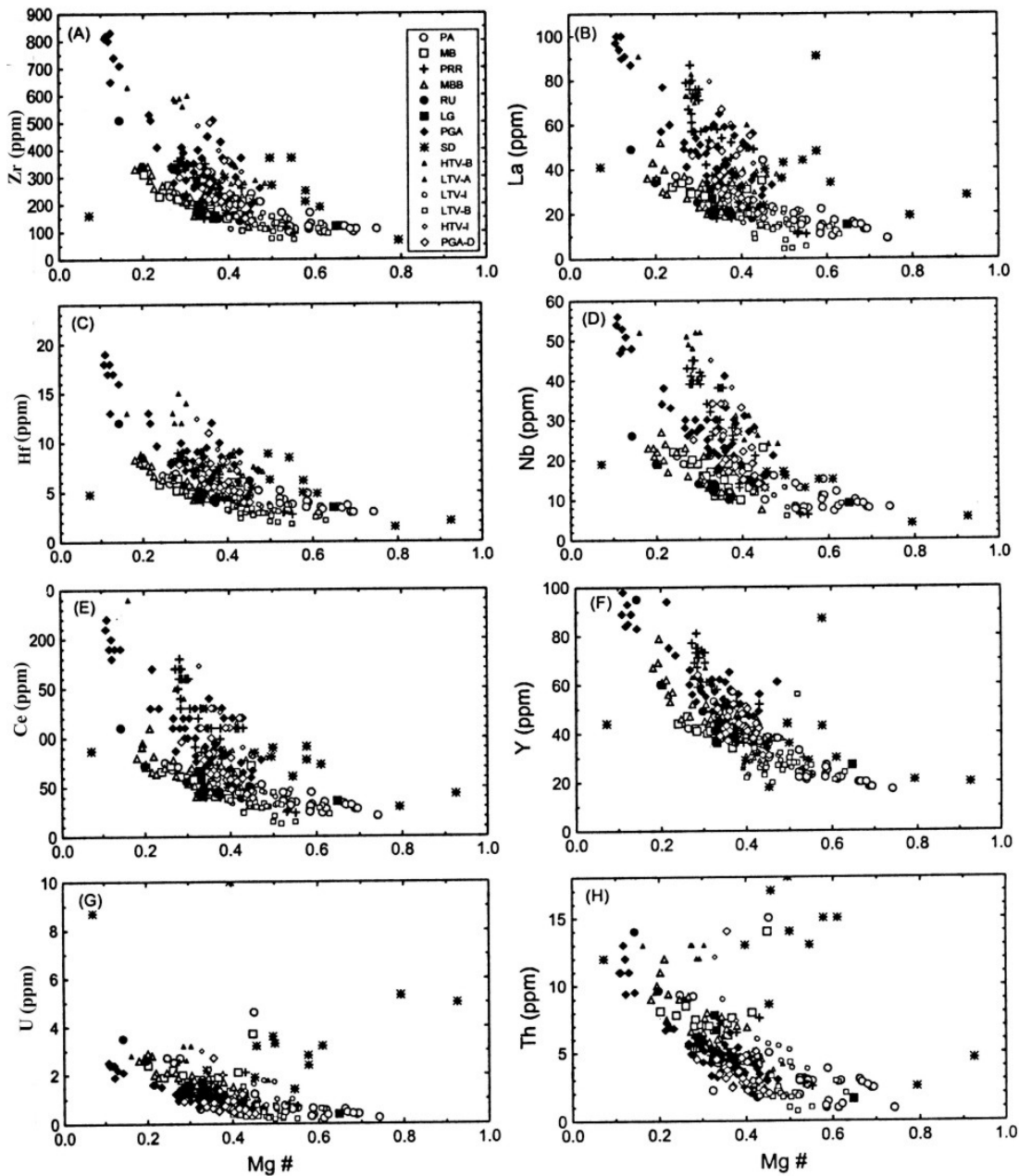


Figure 10 – Mg# x lithophile element diagrams for mafic bodies and sills, dykes (PGA – D), volcanic suites (HTV, LTV), and sedimentary rock (SD), Paraná basin and surrounds.

5.3 Chalcophile Element Variations with Differentiation

In order to monitor the behavior of the chalcophile elements during differentiation it is also important to establish a reference lithophile trend since some elements like nickel are chalcophile in sulphide – rich environments, but can also be lithophile in nature when in the presence of low concentrations of sulphide. During differentiation Cr partitions exclusively into oxide and mafic silicate phases and thus also defines a reference trend for elements like nickel that partitions exclusively into these phases in the absence of sulphide.

The highest Cr concentrations (200 ppm) occur in MgO – rich (up to 50 per cent olivine) rocks from the PA group of intrusions (**Figure 11A**). An exponential decrease in Cr during differentiation is culminated in the Ponta Grossa Arch sill samples where values as low as < 5 ppm were detected. An identical differentiation trend with respect to nickel is demonstrated in **Figure 11E** where concentrations range from 630 ppm (of the scale) to < 5 ppm in the same groupings as described for Cr. These two plots also demonstrate that the confining host sediments have low abundances of Cr and Ni (69 and 42 ppm, respectively).

Sulphur contents in the intrusive, extrusive and host sediments are highly variable and scattered. It is apparent from **Figure 11B** that no fractionation trend exists with respect to S x Mg#. The highest sulphur contents encountered during this study occur in the sedimentary rocks (SD), up to 5.33 wt. Per cent. The highest magmatic S contents (3.22 per cent) are associated with the Maracajá – Barro Branco (MB) intrusion, in particular borehole material from this intrusion. Twenty – six samples of borehole material from this body were found to have a median value of 0.23 per cent, and greater than 25 and less than 75 per cent of the samples have S concentrations than 0.08 and less than 1.39 per cent, respectively (**Table 03, Appendix**).

Surface material (32 samples) collected elsewhere from this body (MBB) was found to have considerably lower S com-

tents (median of 0.03, **Table 4, Appendix**). Most other intrusions have low S contents that range from approximately 150 to 2500 ppm (0.15 to 0.25 per cent) with an median value of about 350 ppm (0.035 per cent).

One of the most striking relationships depicted in **Figure 11B** is the sulphur depletion associated with all members of the low – titanium volcanic suite (LTV – A, LTV – B, LTV – I) compared to the high – titanium suite (HTV – B, HTV – I) which generally has about twice the concentrations. Also, it is clear from **Figure 11B** that the field depicting the volcanic suite sulphur concentrations falls below the lowest values associated with the sulphur – poor intrusive groups.

The copper content of the Paraná intrusive groups depicts a Cu – enrichment trend accompanying fractionation (**Figure 11D**). The lowest concentrations are associated with the most primitive intrusive groups (PA, LG) whereas the highest values tend to be associated with sills from the Ponta Grossa Arch (PGA). However, it is also apparent that some of the sill material from the Ponta Grossa Arch is very depleted in Cu. Depleted samples generally have less than 75 ppm Cu whereas undepleted counterparts with similar Mg#s have Cu contents ranging from 150 to 400 ppm. A fairly distinct compositional gap appears to separate the Cu – depleted field from their non – depleted counterparts.

Platinum – group element variation with respect to the various intrusive and extrusive suites and differentiation is illustrated in **Figures 11E to 11G**. There is a considerable scatter in Pt concentrations from <0.5 ppb to to 33 ppb in samples with Mg#s that range from 0.74 to 0.11. As a group the highest values are associated with the volcanic suites; whereas the highest concentrations in intrusive rocks (14 to 25 ppb) are generally associated with the RU and MBB intrusive groups. There also appears to be a compositional break or gap at about the 4 ppb level. This break is better defined when one observes the fields and trends depicted by Pd (**Figure 11F**) and Pt+Pd (**Figure 11G**). Palladium (**Figure 11F**), as well as Pt+Pd (**Figure 11G**) com

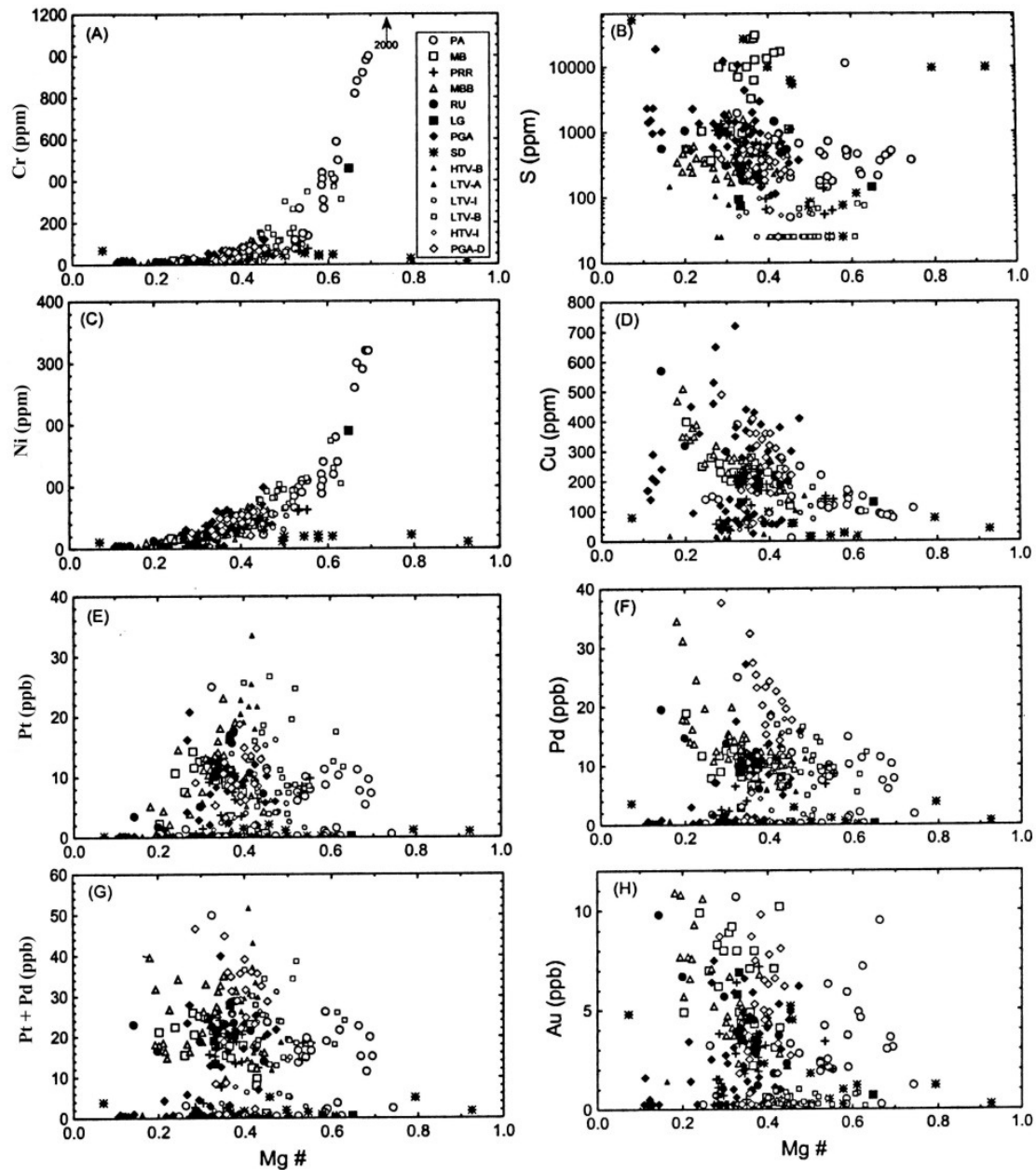


Figure 11 – Mg# x Cr, chalcophile element and noble metal diagrams for mafic bodies and sills, dykes (PGA – D), volcanic suites (HTV, LTV), and sedimentary rock SD), Paraná basin and surrounds.

Centrations tend to increase with fractionation; the lowest values being associated with the relatively primitive PA and LG groups and the highest values with the MBB sill material and dykes from the Ponta Grossa Arch PGA – D). In many respects the Pd, and to a lesser extent Pd+Pt x Mg# distribution patterns and trends are similar to those depicted by Cu in **Figure 11D**. A compositional break between Pd – depleted fields is well defined in **Figure 11F**, and even better constrained with respect to Pt+Pd in **Figure 11G**. Although there are Pd – depleted (<2 ppb) and non – depleted Ponta Grossa Arch dyke (PGA – D) samples nearly all of the Ponta Grossa Arch (PGA) sill material is Pd – depleted. This relationship also holds in **Figure 11G** (Pt+Pd) but not to the degree it does for Pd alone (**Figure 11F**). Gold concentrations relative to the associated Mg# are highly scattered and demonstrate no correlation with differentiation. The highest values are associated with both surface sill material (MB) and borehole samples (MBB) from the Maracajá – Barro Branco intrusion (11 ppb).

5.4 Discussion on Element Variations

The discordant nature of the Mg# x MgO trend of the fractionating magmas that gave rise to the volcanic intrusive trends (**Figure 08A**) may be the result of either variable intensive parameters within and/or the contribution of cumulus components. Since $T - F_{O_2}$ investigations (Bellieni et al., 1986) conducted on flows, dykes and sills define similar trends ranging from magnetite – wustite to nickel – nickel oxide buffers during the emplacement and post – emplacement crystallization history of these magmas one can infer that cumulus processes and not variations in the intensive parameters gave rise to the MgO – enriched differentiation array of the intrusive trend.

The high – and low – titanium volcanic associations outlined on the silica – alkali plot (**Figure 08B**) established by Bellieni et al. (1984) is corroborated in this study with respect to both volcanic and intrusive suites. The geographic location of the various intrusive bodies within the Paraná basin are generally in agreement

with their designation based on silica – alkali contents. The transitional chemical nature of the volcanic suites from the Ponta Grossa Arch region. (i.e. high – and low – titanium associations from the same geographic area) is also present in some of the intrusive bodies. Interpretations of this relationship in the volcanics is also be applicable in the intrusive analogues. It is generally believed that rocks from this area represent a “transition” zone (Bellieni et al., 1986) between their high – and low – titanium members from the northern and southern Paraná basin, respectively. The low – titanium volcanic suite ranges in composition from basalt to rhyodacites (and its intrusive analogues) and are interpreted as magmas that have fractionated in high level crustal magma chambers and may be derived from a different mantle source than their high – titanium counterparts (Mantovani et al., 1985); however, this interpretation is open to debate.

The $SiO_2 \times Mg\#$ trend in **Figure 09A** illustrates a fractionation trend common in many studies of basaltic rocks. It demonstrates that SiO_2 remains almost unchanged during the early and intermediate stages of crystallization and does not begin to increase until the later stages of crystallization. Crystallization during the early stages is dominated by calcic plagioclase and pyroxene, both of which have SiO_2 – contents similar to that of the basaltic liquid. It is usually the onset of crystallization of a SiO_2 free phase such as magnetite or ulvöspinel that eventually causes SiO_2 to become enriched in the residual liquids. The increasing TiO_2 concentrations (**Figure 09D**) in the latter differentiates of both the high and low – titanium associations corroborate the existence of magnetite (ulvöspinel) crystallization in the late differentiates. The actual SiO_2 enrichment in the Mg# interval from 0.55 to 0.33 in **Figure 09A** is very similar to that of the “gabbro fractionation trend” computed by Peate and Hawkesworth (1996) for low – titanium magmas from southern Paraná.

Fractionation trends for CaO and Al_2O_3 vs. Mg# displayed in **Figures 09B** and **09C** are clearly controlled the crystallization and removal of olivine and then pla-

gioclase and pyroxene. Early differentiates with Mg#’s in the 0.74 to 0.60 range demonstrate increasing CaO and Al₂O₃ contents with decreasing Mg#. This trend is best explained as a result of magmas that are crystallizing olivine as a major liquidus phase. Its progressive crystallization and removal from the parental magma leaves the residual magma enriched in CaO and Al₂O₃ since neither of these components are present to any significant degree in olivine. The inflection in the chemical trends towards CaO and Al₂O₃ – depletion marks the cessation of olivine crystallization and the onset of plagioclase – pyroxene crystallization which continued throughout the rest of the magmas evolution even after the onset of magnetite (ulvöspinel) and apatite crystallization during the latter stages of crystallization. The presence of apatite as a crystallization product is apparent in differentiates of the high – titanium suite. P₂O₅ contents up to 2.76 wt. Per cent indicate that anomalous concentrations of apatite have precipitated in these samples relative to counterparts with similar Mg#’s. Increasing Rb, Ba (**Figures 09F and 09H**) and to a lesser extent Sr (**Figure 09G**) concentrations with differentiation reflect the increasing orthoclase component of the plagioclase with differentiation. This is also reflected in the rock K₂O contents (Bellieni, 1988).

Incompatible trace elements like Zr, La, Hf, Nb, Ce, Y, U and Th clearly increase with differentiation; the highest concentrations being associated with members of the high – titanium suite. Anomalous Ce and Y (**Figures 10E and 10F**) trends compatible with that of P₂O₅ (**Figure 09E**) also imply the presence of anomalous apatite differentiates; whereas, the corresponding Nb – La arrays could indicate that allanite also exists as a late differentiate. Increasing concentrations of U and Th (**Figures 10G and 10H**) with differentiation are similar to Zr and Hf and thus are a reflection of changing zircon contents in the rocks as the magmas evolve.

Chrome and Ni (**Figures 11A and 11C**) behave as compatible elements with differentiation in the evolving Paraná magmas. The high Cr (2000 ppm) and Ni (630

ppm) concentrations coupled with the decreasing MgO content of successive differentiated magmas, and the exponential fractionation curves associated with Ni and Cr leaves little doubt that the distribution of these elements relative to the Mg# is governed by the crystallization of mafic silicates and oxides (olivine, piroxene and spinels) almost exclusively.

The distribution of chalcophile elements, which behave incompletely in sulphide – free magmas, is more difficult to interpret (**Figures 11A, B, C, D, E, F, G and H**). The sulphur content of the magmatic rocks, and to a lesser extent the sedimentary rocks, is mainly controlled by the distribution of pyrite within these samples. Since pyrite in the magmatic rocks can be the product of sulphidation of magmatic sulphide assemblages or introduced during the post – crystallization cooling of these bodies its geochemical signature is difficult to interpret. In general, there is an increase in S content with differentiation. An anomalous increase in the S content is associated with the sills of the Ponta Grossa Arch and the Maracajá – Barro Branco body. Ponta Grossa Arch sill samples represent the most differentiated in the study population and thus likely represent sulphides (pyrite and chalcopyrite) crystallizing in the late residual melts. The anomalous, yet discordant, concentrations associated with the Maracajá – Barro Branco body are probably the product of localized crustal contamination. The extremely low values of S (25 ppm) associated with some of the low – titanium volcanics (compared to their high – titanium counterparts) suggest that S – loss due to degassing has affected some of these magmas. Copper (**Figure 11D**) correlates poorly with S; however, it does demonstrate distinct sample population arrays that increase with differentiation and are separated by a compositional gap. This gap separates the main sample population from an array of samples (PA and PGA intrusive groups) that are depleted in Cu when compared to counterparts above the gap. This Cu – depletion is best explained as an artifact of magmas that have segregated sulphides rich in Cu. Platinum (**Figure 11E**) displays no obvious trend differentiation; however, Pd concentrations (**Figure 11F**)

clearly increase with differentiation and correlate well with the corresponding Cu contents and trends (**Figure 11D**). The Pt+Pd concentrations obviously demonstrate trends intermediate between that established in **Figures 11E** and **11F**. Gold (**Figure 11H**) demonstrates considerable scatter with differentiation. The most distinctive geochemical feature in **Figures 11E – 11H**, apart from the high background concentrations in the noble metals, is the compositional gap that separates the PGE – depleted sample population from that of their non – depleted counterparts. This noble metal – and the corresponding Cu – depletion suggests that some members of the PA, PGA and PPR sills/intrusions have been derived from magmas that have experienced enhanced levels of sulphide immiscibility relative to other members from the same or other groups.

5.5 Crustal Contamination

Evaluating the role of crustal contamination of Paraná magmatism which gave rise to the intrusive, and to a lesser degree the extrusive suites, is an important factor to consider when assessing the potential of these intrusive bodies to host Noril'sk – type Cu – Ni – PGE orebodies. Although major, trace and chalcophile element concentrations and variations provide valuable insights into magmas geochemical evolution, trace element ratios are better geochemical discriminators of trends related to differing mantle melting processes and fractional crystallization, and the influence of crustal contamination upon these trends.

A plot of Ti/Zr x La/Sm (**Figure 12A**) for intrusive and extrusive suites from the Paraná basin define a cluster of data points suggestive of a decreasing Ti/Zr and increasing La/Sm trends for the evolving magma compositions. The most primitive magmas are represented by basalts (three) from the low – titanium volcanic suite and have ratios not unlike that of primitive mantle (PM). Some additional three samples from the same volcanic suite occur close to the most primitive intrusive samples (PA, LG). These low – titanium basaltic compositions are probably differentiation products of

magmas that evolved from melts with compositions similar to that derived from primitive mantle (PM) of magmas similar in composition to N – MORB. These three basaltic samples are likely to be close in composition to the parental magma that rise to the early olivine cumulates and associated later differentiates in the PA and LG group intrusions. Material from the Ponta Grossa Arch (PGA) and Maracajá – Barro Bronco (MB, MBB) sills can also be quite evolved with respect to these ratios to the point of having extreme ratios similar to that of some of the siliceous sedimentary rocks. Rocks with these extreme ratios are probably the product of advanced fractional crystallization of magmas that have experienced relatively greater degrees of contamination within the intrusion or locally by the intruded sedimentary rocks.

Bulk partition coefficients for Zr, Ti and Y during partial melting in the upper mantle are in the order $D_{Zr} < D_{Ti} < D_Y$ and are particularly marked if garnet is a residual phase; therefore, variations in the degree of partial melting will generate positive arrays on $Ti/Y \times Zr/Y$ plots like that in **Figure 12B** (Lighfoot et al., 1990, 1993 , 1994). As with other continental flood basalt terranes (i.e. Siberian Trap, Deccan Trap) the high – titanium ($Ti/Y > 500$) and the low – titanium Paraná basalt suites ($Ti/Y < 350$) are consistent with variable degrees of partial melting of source regions with similar Ti/Y and Zr/Y with the high – titanium suite being derived from the smallest degrees of partial melting. Low – titanium basalts examined during this study have the lowest Ti/Y and Zr/Y ratios and fall in the box generally defining primitive mantle (PM) compositions. The wide variation in ratios associated with dykes from the Ponta Grossa Arch (PGA – D) could also be explained as the products of differing degrees of partial melting and fractional crystallization. With the exception of sills from the Ponta Grossa Arch (PGA) most intrusive groups demonstrate a limited range with respect to positive array trends, and where present is probably the result of fractional crystallization and/or mixing of magmas derived from varying degrees of partial melting. **Figure 12B** demonstrates that members of some intrusive groups (PGA) have ratios that

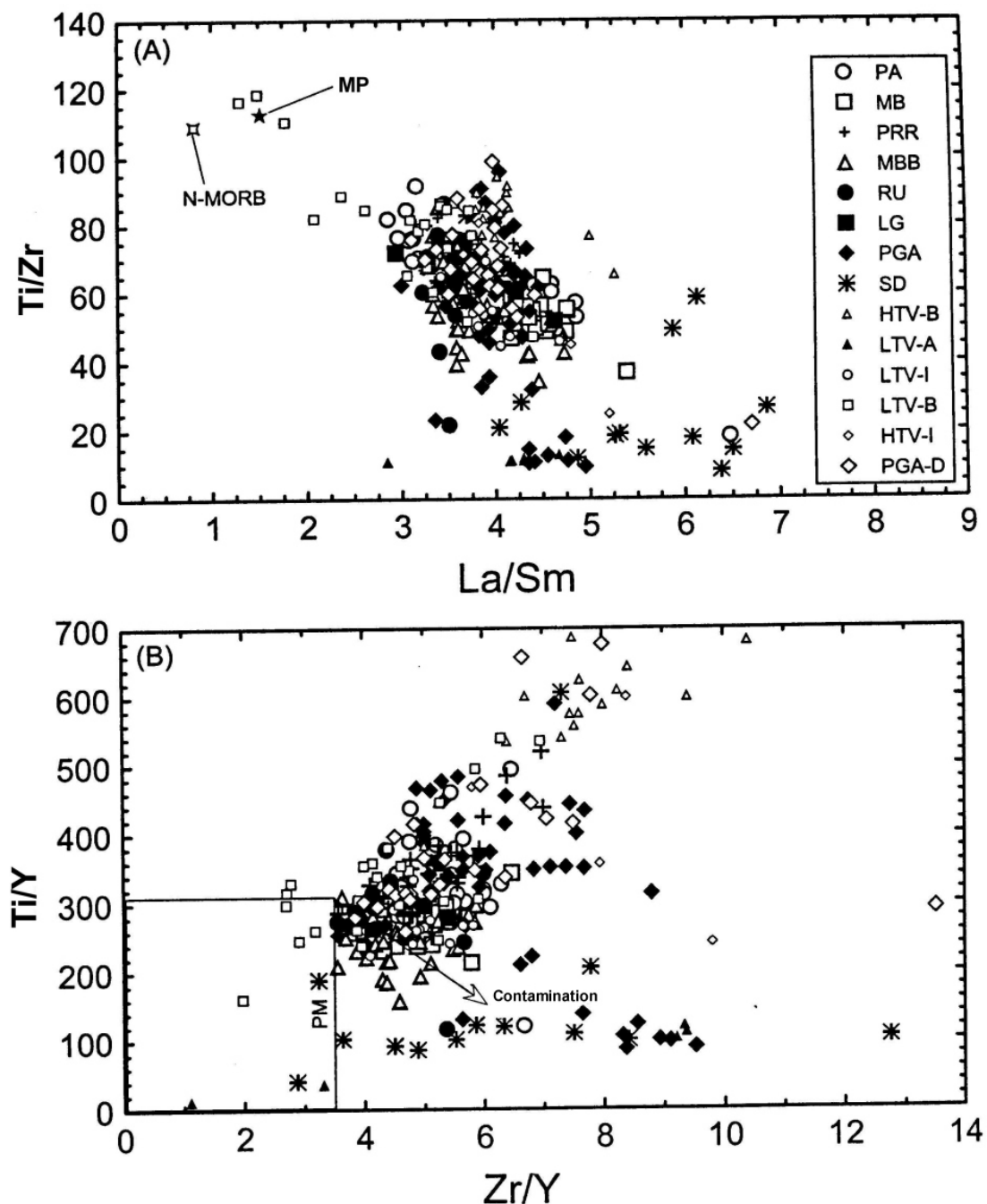


Figure 12 – Ti/Zr x La/Sm (A) and Ti/Y x Zr/Y (B) diagrams for mafic bodies and sills, dykes (PGA – D), volcanic suites (HTV , LTV), and sedimentary rock (SD), Paraná basin.

Overlap those of the sedimentary rocks (SD) or define negative arrays (MBB, RU) towards the sedimentary field.

Variations in La/Sm in continental flood basalt suites are inferred to reflect contributions from lithosphere mantle or crust with variable REE (Lightfoot et al., 1990, 1993, 1994). Although variations in La/Sm – SiO₂ (Naldrett, 1989) have been used to reflect contributions from the continental lithosphere the major difficulty in assessing such plots is: do the variations observed reflect the introduction of sediments to their upper mantle source regions during an ancient episode of subduction, or is it mainly due to crustal contamination accompanying emplacement of the intrusive bodies and their extrusive analogues? A plot of such variables for intrusive and extrusive Paraná magmatic suites, as well as the sedimentary countryrock, is illustrated in **Figure 13A**. Statistical analyses of the Paraná basalts conducted during this study demonstrate that greater than $\geq 25\%$ but $>75\%$ of the high – titanium basalts ($n=19$) have La/Sm values between 3.80 and 4.14 (**Table 09**) whereas their low – titanium analogues ($n=23$) have values of 2.62 to 3.57 (**Table 11**) thus each basalt suite has a rather characteristic range with respect to this ratio. Four samples from the low – titanium basalt suite have lower ratios of 1.2 to 2.0 and probably represent the most primitive magma compositions that would be parental magmas to the more primitive PA, LG, and RU intrusive groups. Samples from dykes (PGA – D) and volcanics of intermediate composition appear to be transitional between the high and low – titanium suites. The composition of N – MORB with respect to these variables is shown for comparison. It would appear that the different La/Sm ratios for basaltic rocks with similar SiO₂ contents are more of a primary magmatic characteristic of the volcanic suites as well as many of the intrusive group samples. Nevertheless, there are specific samples from some intrusions that deviate away from the inferred magmatic array towards the field defined by the sedimentary rocks (SD). There is a population of Ponta Grossa Arch sill samples that define an array of compositions vectoring towards that of the sediments. Individual

samples from the PA, MB, MBB intrusive groups also appear to have been contaminated by local assimilation.

The role of partial melting, fractional crystallization and crustal contamination on the geochemical evolution of mafic intrusive suites can be constrained with the aid of Gd/Yb – La/Sm plots (**Figure 13B**). Fields for other compositionally similar intrusive rocks from comparable geological environments elsewhere are also presented. The N – MORB and PM compositions are given and present the starting point compositions from which the magmas could have evolved. The most striking feature associated with this plot is the near vertical array of Gd/Yb enrichment trends associated with the PRR intrusive groups well as the dykes (PGA – D) and some of the sills (PGA) from the Ponta Grossa Arch. As indicated by the inset this trend is generally believed to be the product of decreasing degrees of partial melting in the presence of garnet. The increased P₂O₅, Ce, and Y concentrations and trends accompanying differentiation (**Figures 09E, 10E and 10F**) of these intrusions may also suggest that in addition on the above interpretation the enhanced Gd/Yb ratios could be the product of increasing phosphate (\pm allanite) component with differentiation. The remaining samples of sill material from the Ponta Grossa Arch, as well as many of the other intrusive bodies, display arrays suggestive of fractional crystallization with or without crustal contamination vectoring towards the sedimentary compositions (SD). Many of the samples from the RU and MBB intrusive groups fall within the field represented by the Lower Taldakh and Lower Noril'sk intrusions with respect to Gd/Yb and La/Sm ratios. Compositional fields for other Taldakh – type intrusions and sill material represented by the Late Proterozoic Mackenzie diabase and Franklin magmatic events in Canada are shown for reference.

A plot of Nb/La x La/Sm (**Figure 14A**) yields compositional arrays and thus petrogenetic interpretations similar to that of the Ti/Zr x La/Sm plot (**Figure 12A**). The wide range in Nb/La and correspondingly narrow extent of La/Sm in the Ponta Grossa Arch dike samples (PGA – D) suggests a

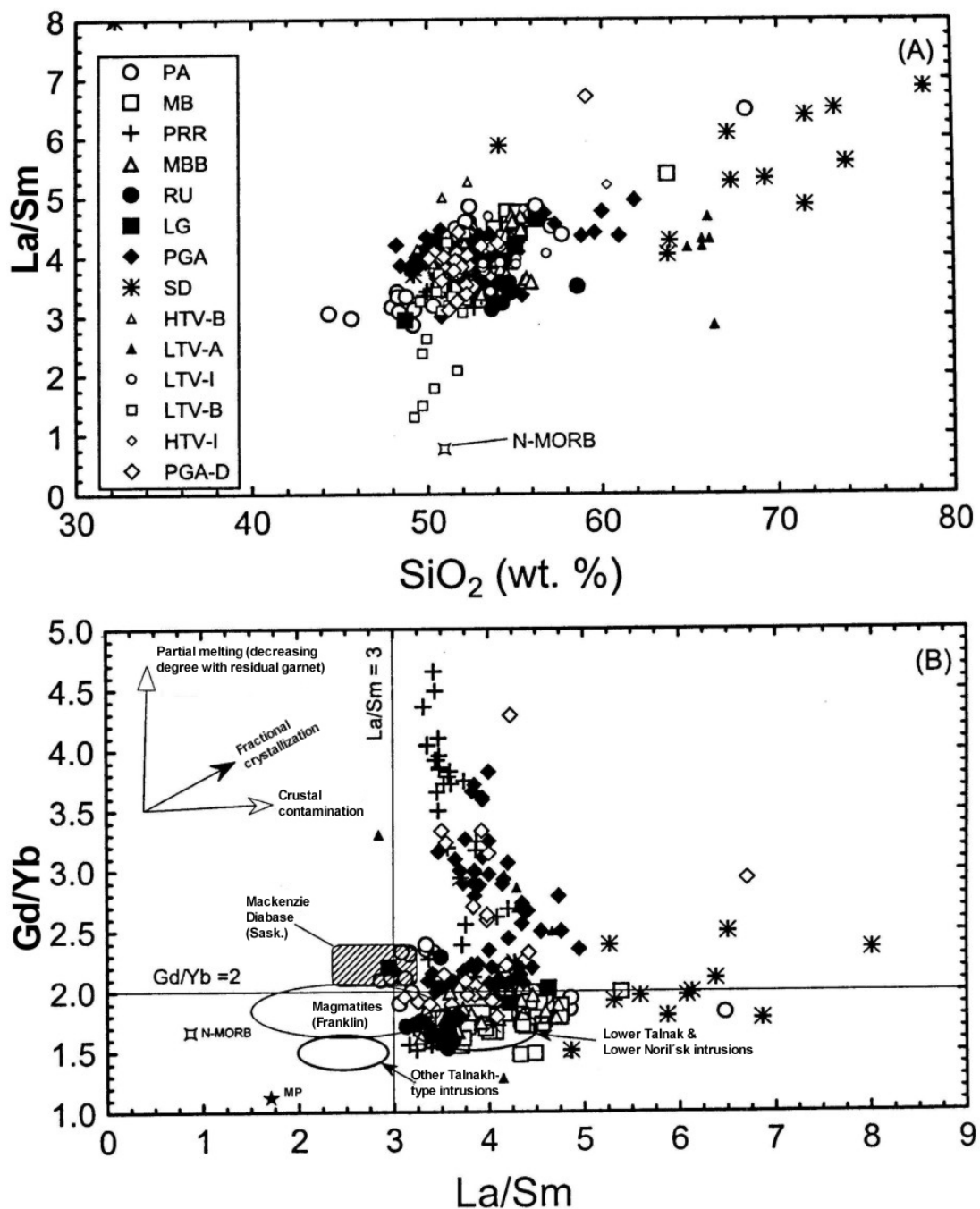


Figure 13 – La/Sm x SiO₂ (A) and Gd/Yb x La/Sm (B) diagrams for mafic bodies and sills, dykes (PAG – D), volcanic suites (HTV, LTV), and sedimentary rock (SD), Paraná basin and surrounds.

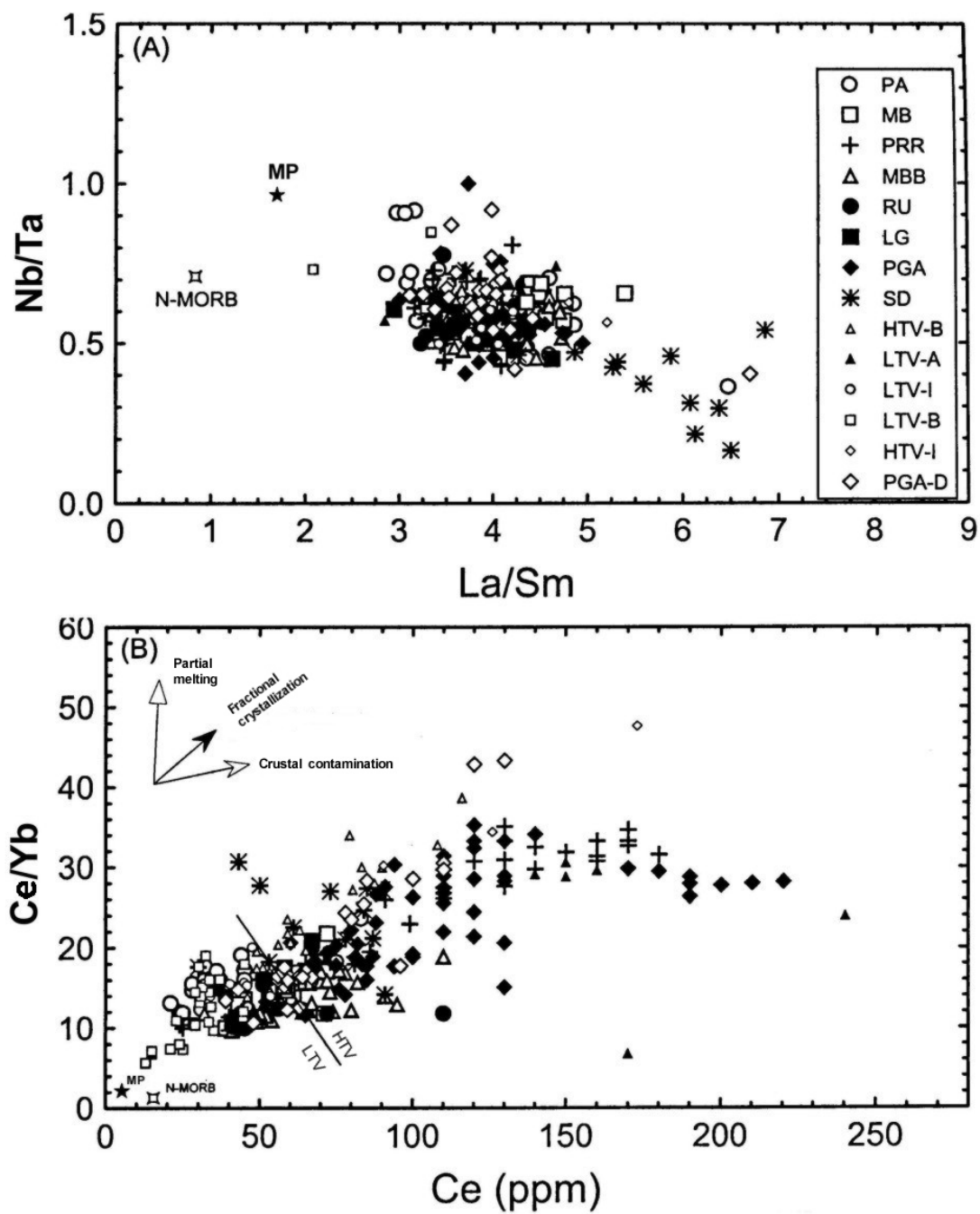


Figure 14 – Nb/La x La/Sm (A) and Ce/Yb x Ce (B) diagrams for mafic bodies and sills, dykes (PGA – D), volcanic suites (HTV, LTV), and sedimentary rock (SD), Paraná basin and surrounds.

Continental lithospheric mantle source with variable Nb/La. Some of the PGA and MBB samples, and their proximity to the sedimentary rock (SD) field, indicate that these rocks have experienced crustal contamination accompanying emplacement. Disparate samples from the PA and MB groups suggest localized contamination of some samples from these bodies.

Ce/Yb x Ce (**Figure 14B**) is another very informative means by which to access the role of partial melting, fractional crystallization and crustal contamination on the geochemical evolution of Paraná intrusive suites and their extrusive counterparts. In addition, this plot also clearly demarcates the high – titanium from low – titanium Paraná suites.

Low – titanium basalts (LTV – B) have the lowest Ce/Yb and Ce concentrations of all the samples investigated during this study. Their compositional evolution away from the primitive mantle composition (PM) along a path defined by the fractional crystallization vector in the inset leaves little doubt as to their origin. Proximity of the LTV – B to the most primitive magmatic differentiates (PA, LG) also suggests that these basaltic compositions are compatible candidates for the parental magmas to the latter. The Ce/Yb – Ce values for the sedimentary (SD) rocks demonstrates that countryrock assimilation had little influence on the composition and evolution of the high – titanium volcanic and intrusive suites. However, The high Ce/Yb – Ce associated with the PRR intrusive group and many of the Ponta Grossa Arch sills, and their correspondingly high phosphorous concentrations, suggest that crystallization of apatite in increasing concentrations with differentiation has occurred in these highly evolved magmas.

This plot also suggests that variable partial melting processes had little influence on the chemical trends.

A plot of Th/U x Ce/Yb (**Figure 15A**) once again demonstrates a clear distinction between the high – and low – titanium suites and the influence of the phosphorous content on the Ce/Yb ratios. Th/U ratios are

approximately twice as variable in the low – titanium suites as in their high – titanium counterparts. With the exception of one sample it would appear that assimilation of sedimentary rocks would not significantly elevate the Th/U. Two HTV – B samples have compositions close to that of PM and N – MORB whereas the remaining HTV – B samples and many of the more primitive intrusive group (PA, LG) samples have compositions that evolve away from the inferred initial magma composition. The variable Th/U and Ce/Yb cannot be explained by assimilation of sedimentary rocks from the Paraná basin or surrounds, but may be a product of varying degrees of assimilation of lower crustal granodioritic material.

Th/Ta x La/Yb (**Figure 15B**) appears to discriminate the high – and low – titanium volcanic suites, but this cannot be said for the intrusive counterparts. End – member magmatic compositions (PM, low Th/Ta members of the LTV – B) mixing with high Th/Ta – La/Yb sediments (SD) could give rise compositional fields along this array. However, samples that fall below and near the LOT – HIT boundary line would appear to be unaffected by assimilation of sediments from the Paraná basin, and thus have compositions more defined by fractional crystallization and to a lesser extent mantle melting processes.

5.6 Chalcophile Element and Noble Metal Abundances as Indicators of Sulphur Saturation

Although the above mentioned trace element ratios provide valuable insights into a magmas origin and evolution via partial melting, fractional crystallization and crustal contamination, it is not indicative of whether sulphide saturation was attained and if so the degree of segregation.

Plots of various chalcophile element ratios are illustrated in **Figures 16A – G**. Variations in Ni/Co and Ni/Cu with Mg# (**Figures 16A and 16B**, respectively) display rather well defined exponential depletion in Ni relative to Co and Cu. This variation is nearly identical to that of Ni and Cr in

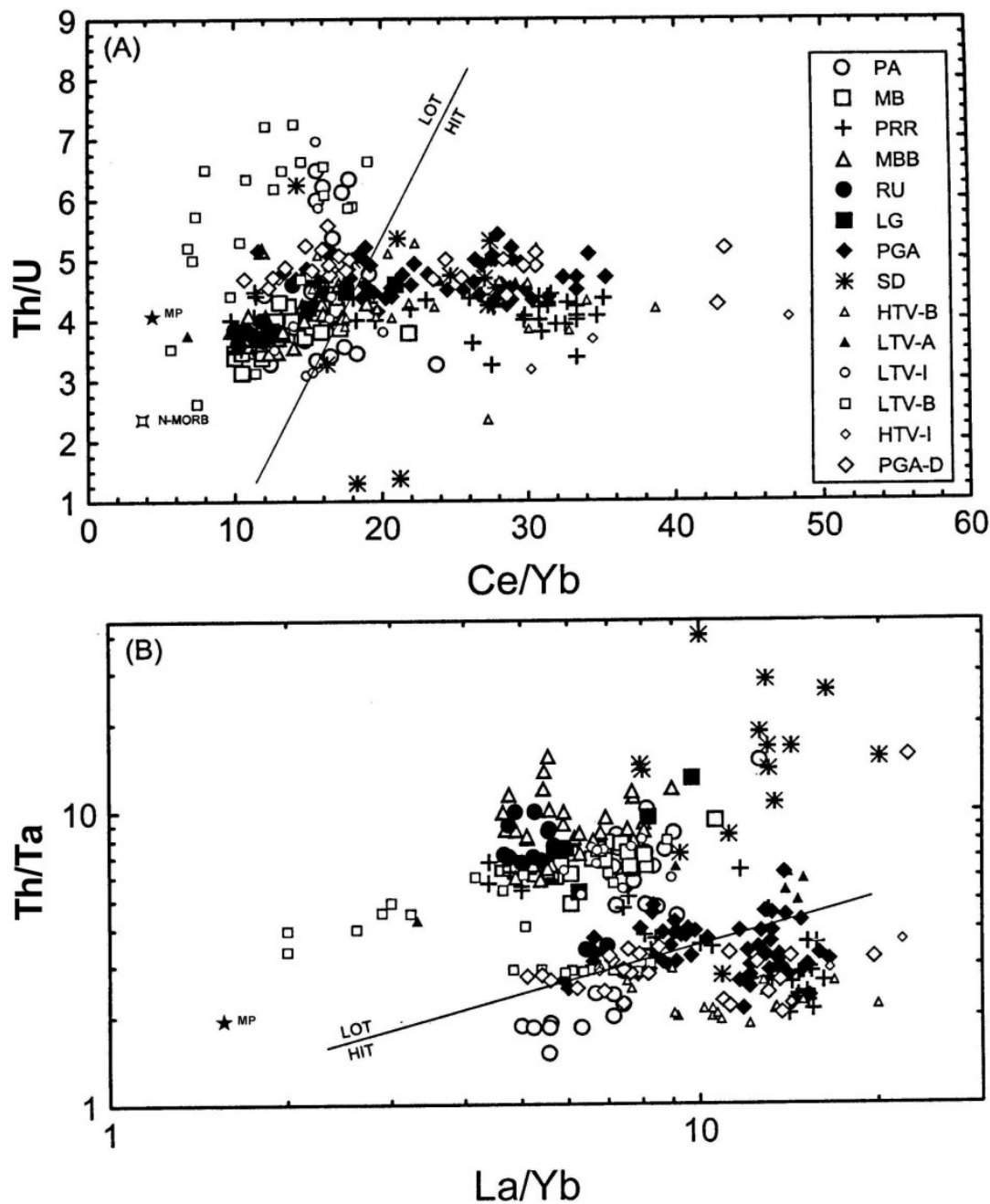


Figure 15 – Th/U x Ce/Yb (A) and Th/Ta x La/Yb (B) diagrams for mafic bodies and sills, dykes (PGA – D), volcanic suites (HTV, LTV), and sedimentary rock (SD), Paraná basin and surrounds.

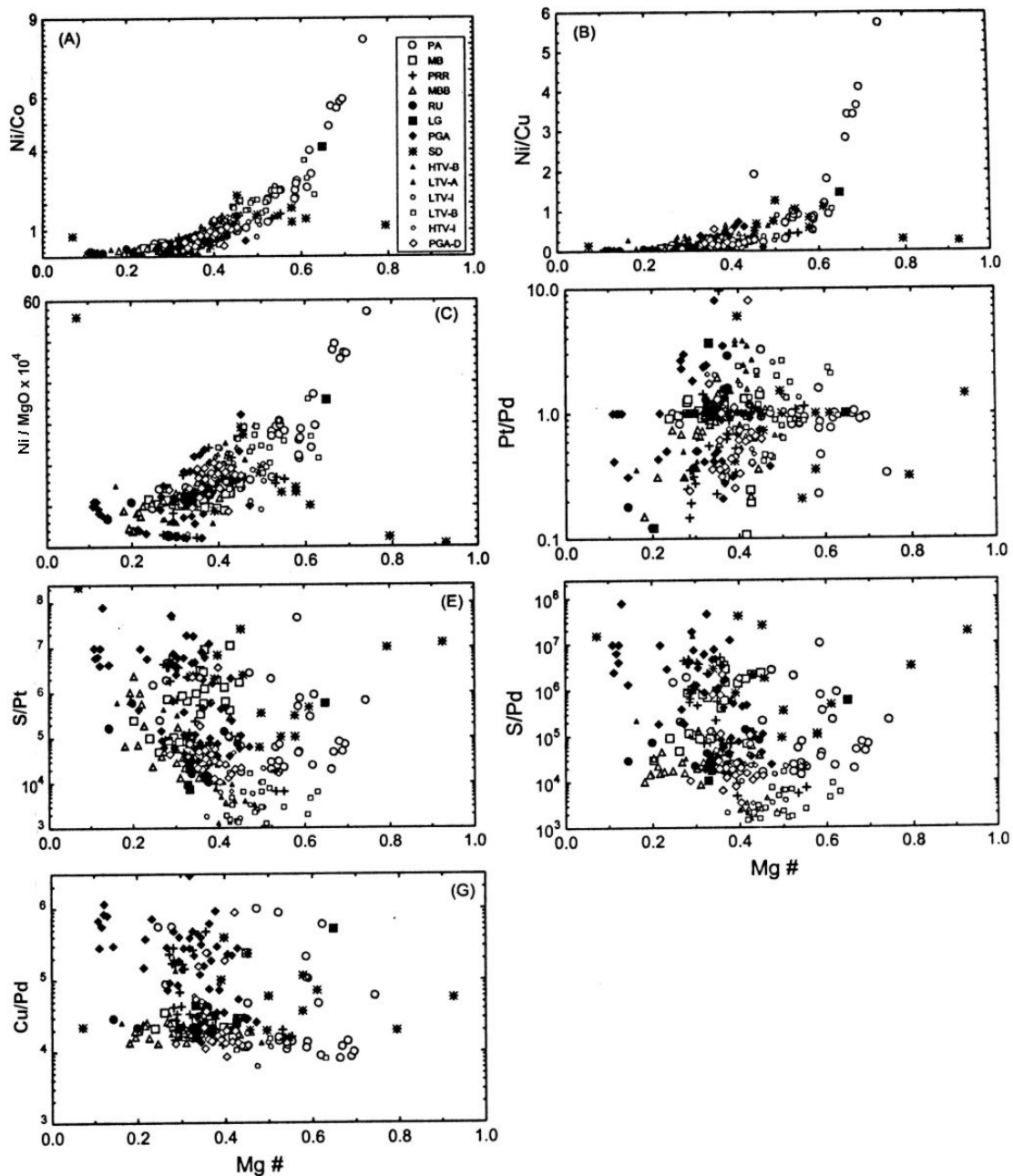


Figure 16 – Mg# x Selected element ratios for mafic bodies and sills, dykes (PGA – D), volcanic suites (HTV, LTV), and sedimentary rock (SD), Paraná basin and surrounds.

Figures 11A and 11C, and is thus interpreted to be controlled by the fractional crystallization of mafic silicate phases olivine, pyroxenes and oxides. Had significant sulphide segregation taken place during the evolution of these magmas the ratio of Ni/Cu should demonstrate some variation from the normal fractionation trends observed. Variations in the Ni contents also have to be interpreted with a knowledge of the associated MgO content of the rock since elevated concentrations of mafic phases will give rise to elevated nickel and MgO, but not necessarily accompanied by increases in the Mg#. A plot of the $\text{Ni}/(\text{MgO} \times 10^4) \times \text{Mg\#}$ (**Figure 16C**) is believed to normalize the influence of increases in the MgO content of the rock on the associated increasing Ni contents and thus detect the addition or subtraction of Ni sulphides from the system. Although no obvious Ni depletion is manifest in **Figure 16C**, a Ni – bearing sulphide – enrichment trend associated with the late differentiates (Mg# 0.37 to 0.11) from the Ponta Grossa Arch sills (PGA) is apparent. Sulphide – enrichment within this fractionation interval is also apparent from the S x Mg# plot (**Figure 11B**). Ratios of Pt/Pd (**Figure 16D**) are highly variable and not a function of their high – or low – titanium association. The fractionation array with a dense concentration of samples with a Pt/Pd of approximately 1.0 is probably reflective of the parental magma composition, and not the initial magma since the chondritic ratio is 1.9 (Naldrett and Duke, 1980). The wide variation in Pt/Pd (two orders of magnitude) has to be the product of both PGE fractionation within the sulphides as well as due to fractionation within the evolving magmas.

Variations in the ratio of S/Pt and S/Pd with fractionation (**Figures 16E** and **16F**) define an array that indicates both Pt and Pd concentrations within the sulphide phase decrease with fractionation. A S/Pd gap or break within the sample population appears to take place at a ratio of approximately 10^5 . A similar but better defined break can also be seen with respect to Cu/Pd in **Figure 16G**. Indications that sulphide segregation took place in the Ponta Grossa Arch sills (PGA) is suggested by the generally high values ($>10^5$) in these bodies

relative to the generally low values associated with the dykes that fed these bodies (PGA – D). A number of samples from the PA and PRR groups also demonstrate the association with both high and low ratios suggesting the presence of a sulphide immiscibility event associated with some members from these intrusive groups.

A plot of the Pt + Pd x S (**Figure 17A**) illustrates a general compositional gap in which most of the samples either fall in a field with concentrations $> 11 \text{ ppb}$ or $< 4 \text{ ppb}$. Samples representative of the two different populations are similar to that for Cu/Pd vs. Mg#. This relationship could suggest that samples from the Pt + Pd depleted population may have been derived from magmas that have experienced a significant sulphide immiscibility event. Analyses of the volcanic suites illustrate that the PGE concentration is not governed entirely by the sulphide present in the sample. Samples with very low S content (25 ppm) have comparable Pt + Pd values to those with higher S contents (200 to 1200 ppm) and thus oxide phases have to also be considered as important carriers of PGE. Although there is no obvious correlation between the S content of rocks derived from Paraná magmas and their PGE concentrations an obvious bi – modal relationship exists between the Cu content and the Pt + Pd concentrations (**Figure 17B**). Samples with $> 11 \text{ ppb}$ Pt + Pd define an array with a positive slope; whereas, samples with $< 4 \text{ ppb}$ demonstrate no correlation with the copper content.

Palladium x Pt (**Figure 17C**) illustrates that a large number of samples define an array with a positive slope of approximately 1.0 which corresponds to general Pt/Pd ratio of most samples. This ratio is probably characteristic of its mantle source. Deviations towards higher Pd values in the investigated samples could imply prior fractionation of sulphides enriched in Pt relative to Pd. The Pt + Pd compositional gap is also present when plotted with respect Rb/Ce (**Figure 17D**) which is supposed to discriminate high – and low – titanium associations, but this is clearly not a reliable discriminator in this study.

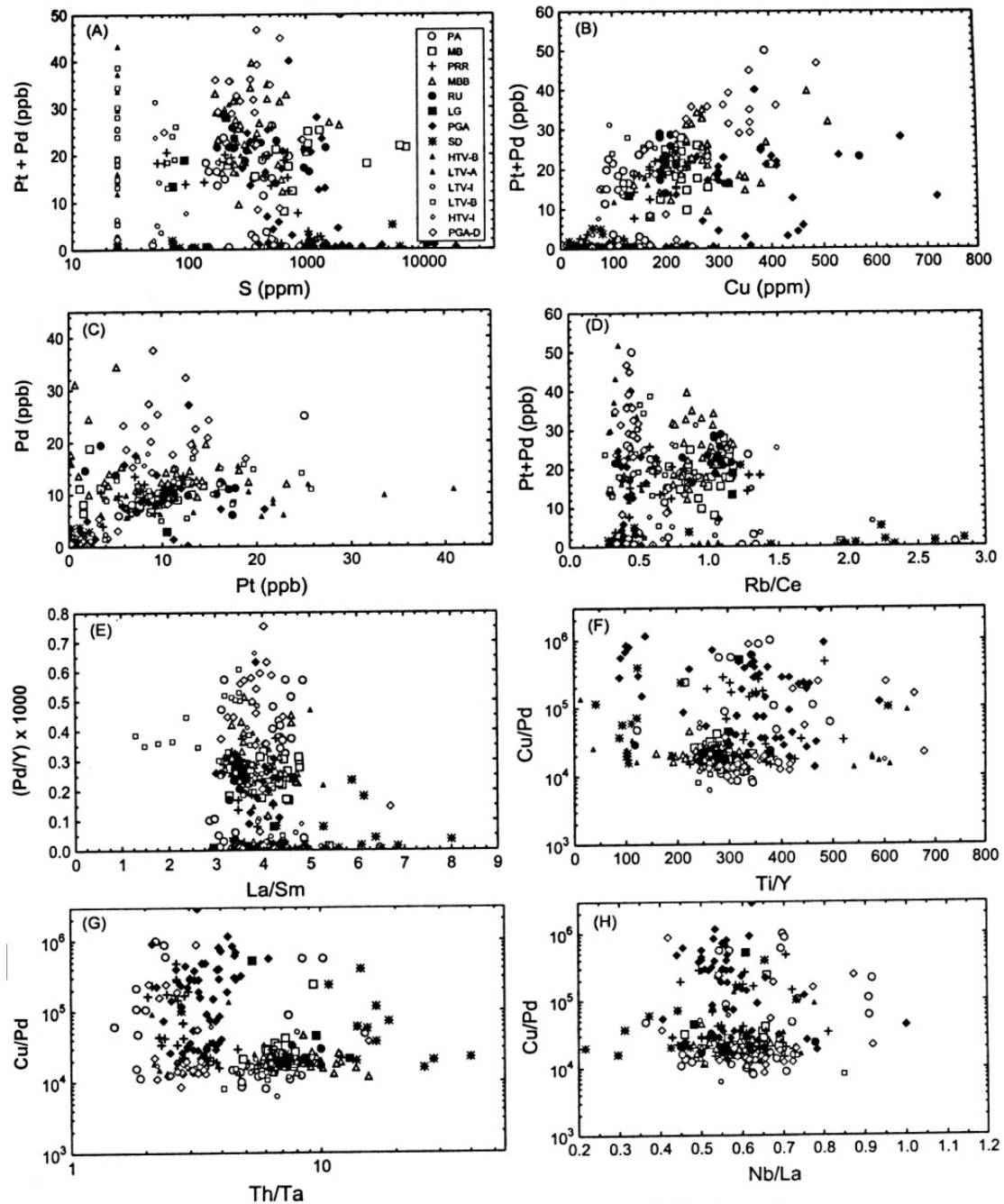


Figure 17 – Selected element ratios plots for mafic bodies and sills, dykes (PGA – D), volcanic suites (HTV, LTV), and sedimentary rock (SD), Paraná basin and surrounds.

Comparison of the abundances of chalcophile and lithophile elements identifies magmas which have experienced even small amounts of segregation of sulphide liquid. The element Y is immobile during alteration and behaves moderately incompatibly in sulphur – undersaturated magmas, like Pt, Pd and Cu (Brügmann et al., 1993). Therefore given a primitive mantle source composition, and similar degree of incompatibility in sulphide – free systems, metals like Pd, Pt and Cu and Y are expected to behave in a similar manner. A plot of $(\text{Pd}/\text{Y})^*1000 \times \text{Lm}/\text{Sm}$ (**Figure 17E**) should identify Paraná magmas which have experienced different degrees of sulphide segregation as well as those that have variable La/Sm ratios resulting from different mantle source regions and/or crustal contamination. An array defined by six samples representative of the LTV – B has relatively primitive La/Sm values (1.2 to 2.8) and is not far removed from primitive mantle ratios of 1.59. Higher La/Sm ratios (3 to 5) for LTV – B samples, as well as other members of the LTV and HTV volcanic suites, demonstrate that variations in this ratio are not due to variable mantle source but are the products of crustal contamination. Since the majority of the intrusive and extrusive samples fall in this range $(\text{Pd}/\text{Y})^*1000$ ratios demonstrate a bi – modal population with a compositional scarcity of samples in the 0.05 to 0.20 $(\text{Pd}/\text{Y})^*1000$ range. Samples with lower ratios are believed to represent magmas that have experienced greater degrees of sulphide segregation and will be discussed later with the aid **Figure 19A**.

The Cu/Pd ratio is also believed to be a reliable indicator of magmas that have suffered varying degrees of sulphide liquid segregation. Although this geochemical discriminator has mainly been used in layered intrusions in search of “Reef” – type PGE mineralization (Maier et al., 1996); it should also be applicable to Noril'sk – type geological environments, but its use will require a different interpretive approach. Due to the higher silicate melt – sulphide – melt partition coefficient of Pd (>10,000) relative to Cu (ca. 1,000; Peach et al., 1990) sulphides are strongly enriched in PGE over Cu and the Pd in the remaining silicate melt subsequent to sulphide immis-

cibility event fall sharply. Average mantle Cu/Pd values are generally believed to be about 7000 (Barnes et al., 1988). Some of the low – titanium volcanics and intrusive bodies, as well as Ponta Grossa Arch dykes (PGA – D), have compositions compatible with this value but most are higher. This ratio in conjunction with variations in the Ti/Y, Th/Ta, Nb/La, Gd/Yb, Th/Yb, and La/Sm (the interpretation of these ratios has been mentioned in previous discussions) have been investigated (**Figures 17F-H** and **18A-C**). In all cases (although some are better defined than others) there appears to be a bi – modal population with a compositional break at $\text{Cu}/\text{Pd} \approx 10^{4.6}$. Although the ratios defined by the ordinate can be highly variable there is a relatively clear distinction of the populations based on Cu/Pd. This relationship could imply a decoupling of lithophile and chalcophile elements during the magmatic evolution of these magmas. It is believed that diagrams with Cu/Pd ratios $< 10^{4.6}$ represent bodies that have experienced only limited segregation of immiscible melts, whereas those with ratios above this (up to 10^6) have experienced relatively high degrees of sulphide immiscibility. This Pd – depleted population and its intrusive members should (some PA, PGA and PRR sills) be considered as candidates with the highest potential to host Noril'sk – type Cu – Ni – PGE deposits.

A plot of Cu/Y (**Figure 18D**) is in principle similar to that of $(\text{Pd}/\text{Y})^*1000$ (**Figure 17E**). Primitive mantle Cu/Y is 7.18 (Brügmann, 1993) and is similar to that associated with many Ponta Grossa Arch dykes and some of the Paraná volcanics. Values range from these mantle signatures down to approximately 0.5 and represent samples that have experienced increasing amounts of sulphide melt segregation.

A $(\text{Pd}/\text{Y})^*1000 \times \text{Mg}\#$ plot representing all samples from this study is illustrated in **Figure 19A** along with average values of $(\text{Pd}/\text{Y})^* 1000$ for volcanic suites from the Noril'sk area of Russia and primitive mantle PM = 1.13. Average $(\text{Pd}/\text{Y})^*1000$ values are: Tuklonsky picrites (TK – Pic) = 0.79, Tuklonsky basalts (TK – Bas) = 0.77, Gudchichinsky picrite(Gd – Pic) = 0.39, Mokulaevsky (Mk) = 0.27, Moron-

govsky (Mr) = 0.17, Ivakinsky (Iv) = < 0.07, Nadezhdinsky (Nd) = < 0.09 and Syverminsky (Sv) = < 0.08 (Brügmann et al., 1993). Research on these Siberian Trap volcanic suites and the coeval mineralized intrusions in the Noril'sk – Talnakh mining camp suggests that the Mr, Mk, and Tk suites did not experienced significant sulphide immiscibility; however, the Nd, Iv and Sv volcanics did, and in fact the Nd suite is believed to be comagmatic with the mineralized intrusions. The coincidence in the Pd – depleted (with respect to $(Pd/Y)^{*}1000$)

Paraná samples (<0.05), represented by some samples from the PA, PGA and PRR intrusive groups, with that found in the Nd, Iv and Sv volcanic suites from Noril'sk is encouraging and corroborates previous suggestions concerning the exploration potential of this intrusive Paraná suite. Similarly, a plot of Cu/Y vs. La/Yb also depicts the close correspondence between the Cu – depleted Paraná field and that associated with the Nd, Sv and Iv volcanic suites from the Noril'sk region.

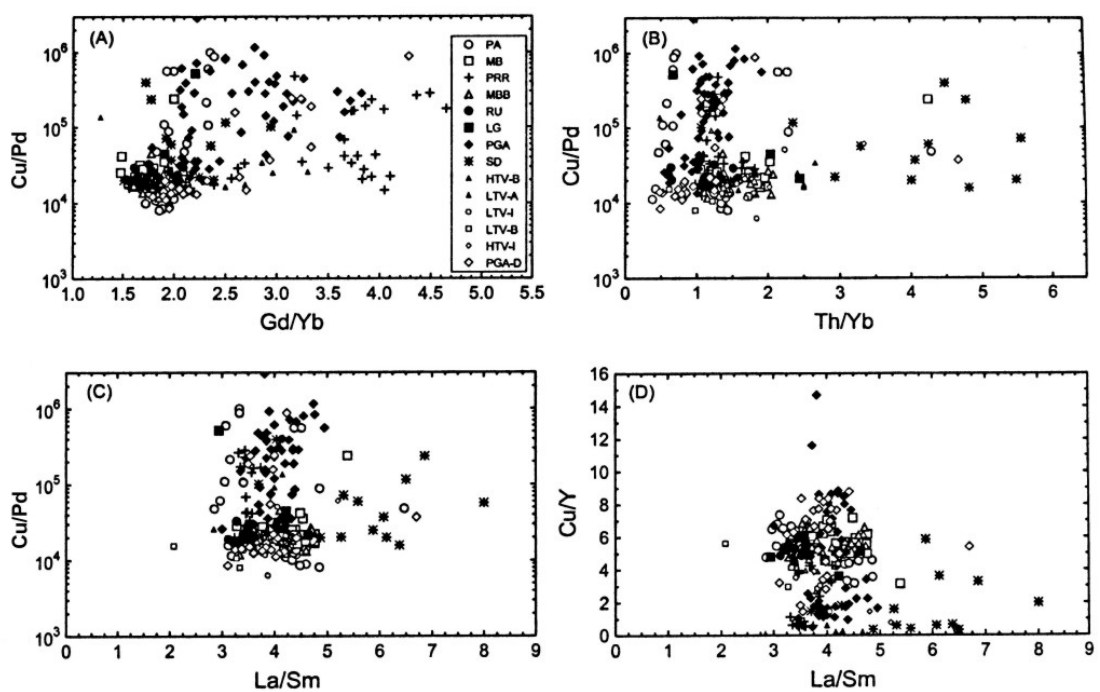


Figure 18 – Cu/Pd, Cu/Y x selected element ratios plots for mafic bodies and sills, dykes (PGA – D), volcanic suites (HYV, LTV), and sedimentary rock (SD), Paraná basin and surrounds.

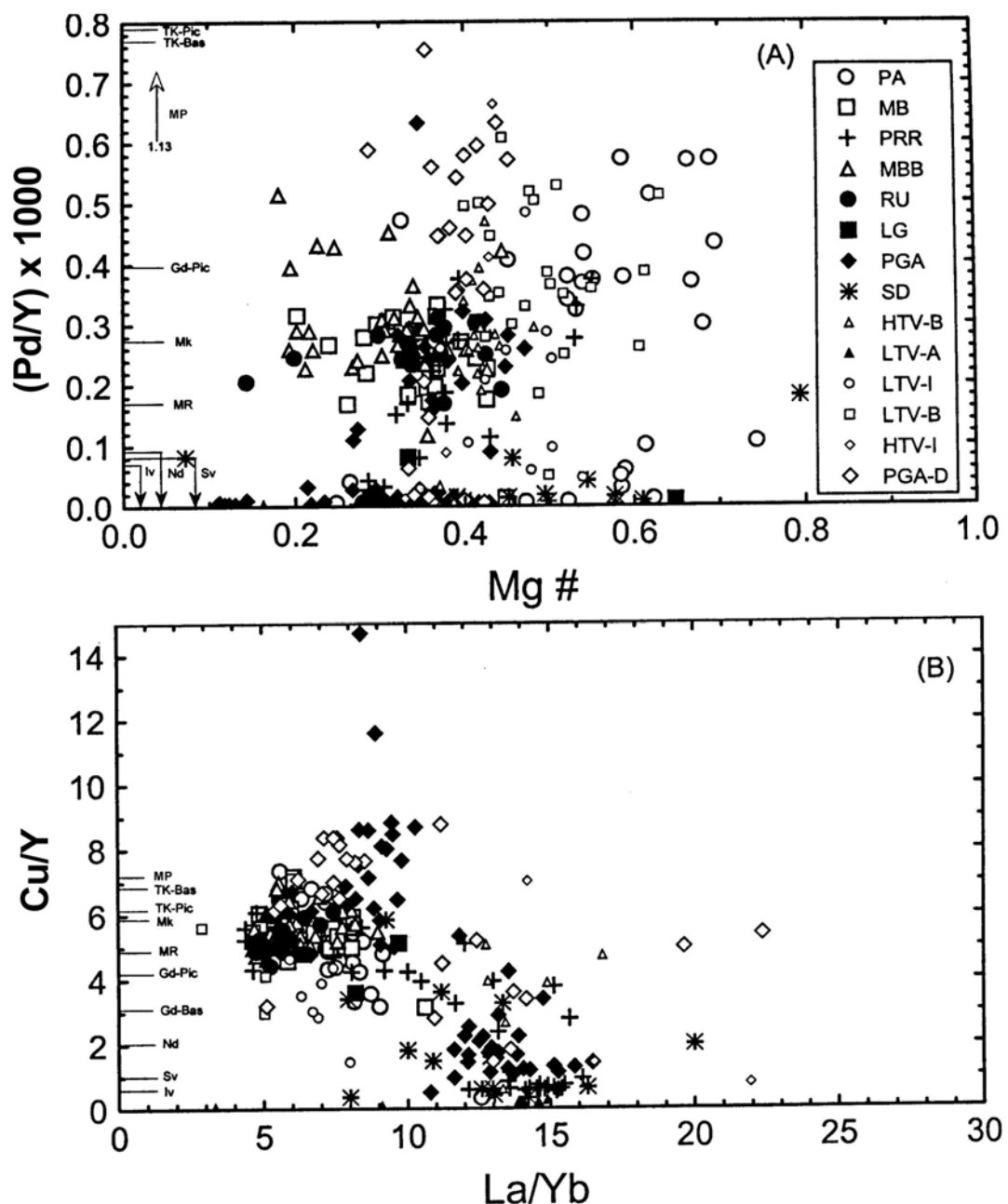


Figure 19 – $(\text{Pd}/\text{Y}) \times 1000 \times \text{Mg}\#$ (A) and $\text{Cu}/\text{Y} \times \text{La}/\text{Yb}$ (B) diagrams for mafic bodies and sills, dykes (PGA – D), volcanic suites (HTV, LTV), and sedimentary rock (SD), Paraná basin and Noril'sk volcanics.

6 - Discussion

The potential for sulphides of the Paraná Basin magmatism was evaluated by Mincato (1994) through the comparison of this kind of mineralization at Noril'sk-Talnakh and Insizwa provinces of Siberia and Karoo trapps. He puts on that sulphide deposits of these two provinces are related to regional and local geological controls. Mainly regarding to the first ones: to the initial phases of magmatism; to the primitive stages of continental rifting structures and to reactivated ancient faults of the basement.

Concerning local aspects, Mincato (op. Cit.) emphasizes the low-Ti toleitic basalt association; to the lowest part of stratiform differentiated bodies; to magmas calcophyle elements Cu-Ni-PGE-poor and to sulphides segregation process with crustal assimilation and multiple injections. Taking these controls into account, he defines as a favorable environment the eastern border of the province whose development was more closely associated to the South- Atlantic Rifting evolution. Otherwise, the widespread and characteristics variation

of the magmatism that leads Piccirilo et al (1988) to separate the Province into three zones, South, Central and North, allowed Mincato (1944) to give a high, medium and low potential to those zones, respectively, mainly taking into account Ti grades and Mg# indexes.

Jefferson et al (1994), focusing more generic characteristics, studied the so called Noril'sk-Talnakh model in comparison with Ni-Cu-PGE deposits in the northwest of Canada gabbroic rocks. **Table B** evaluate the Paraná Basin magmatic deposits potential regarding those generic characteristics.

This table shows a number of coincidences between Siberian and Paraná Traps as well as the important differences, mainly directly concerning the mineral deposits formation. Regarding Paraná Basin magmatism, it is important to emphasize the low importance of differentiation into intrusions and its S depletion (there are only a few samples of S content above 5%).

CHARACTERISTICS	NORIL'SK-TALNAKH REGION (Jefferson et al., 1994)	PARANÁ BASIN
SCALE: Both are catastrophic magmatic events including thick basaltic lava flows and a number of dykes and gabbroic sills.	Na enormous volume ($106,000 \text{ km}^3$) of basaltic flows of until 3,500 m of thickness, known as Siberian Traps. Associated sills are also known but regional extent is unknown because they are overlapped by traps.	Great volume of basaltic lava flows widespread in $1,200,000 \text{ km}^2$; volume of $790,000 \text{ km}^3$ and thickness between 350 and 1,500 m in the basin center. Sills and dykes are intruded in the Palaeozoic sediments and basement. Dykes and sills regional extension is not very well known.
DURATION: The same age; fast magmatism and of a low duration	Upper Permian and Low Triassic rapid eruptions (temporarily) associated to Permo-Triassic extinction (Renne and Basu, 1991 in Jefferson et al, 1994).	Jurassic-Cretaceous with ages between 155 and 100 Ma and a medium age of 161Ma for basaltic lava flows. Sills are 106 to 161 Ma old and dykes 119 to 142 Ma (K/Ar and Rb/Sr ages).
STRATIGRAPHY & VOLCANO PETROLOGY: Rocks show some petrologic similarities.	Lightfoot et al (1990) and Naldrett et al (1992) in Jefferson et al (1994) made descriptions of four volcanism phases in a 2,200 thick column: 1) alkalic to sub-alkalic, tolelitic to picritic 2) thick tuffs 3) tolelitites to picrites 4) tolelitites. Olivine-basalts abound in the Noril'sk region. Isopach Maps show that regional faults control basalt thickness mainly the Noril'sk-Karaelakh Fault (Naldrett et al, 1992). The forth phase is widespread in the Siberian Platform.	According to Piccirillo et al (1998), volcanism is mainly tolelitic (90% vol.), overlapped by rhyodacites and tolelitic andesites (32 flows max.). There are traces of olivine. Alkalitic basalts and picrites were not identified yet. Regional most important tectonic aspects are tectonic or magnetic lineations (Mincato, 1994). Paraná Basin is divided into three main sectors: South tolelitic basalts with low TiO_2 (<2%) and low incompatible trace elements (Pb, Ba, Sr, La, Ce, Zr and Y) in regard to the Northern sector with high TiO_2 content (>2%) and high incompatible trace elements content; the central sector basalts are sometimes low and sometimes high TiO_2 content.
TECTONIC ENVIRONMENT: Both are of cratonic margins.	Northwestern region of the Siberian Platform.	Center-Eastern region of the South-American Platform.
COUNTRY ROCKS STRATIGRAPHY: Sills country rocks include continental sedimentary sequences, non-deformed, non-metamorphic, under-basalt country rocks.	Up to 450 m of coal and gas layers of Tunguska Series of Upper Carboniferous Permian; they are overlapping carbonate-sulfate lake evaporites (Cambrian to Ordovician); fossiliferous limestones and marine mudstones (Silurian to Low Devonian); conglomeratic layers with evaporitic sulphides (Medium Devonian); evaporites (Upper Devonian) and shallow water marine limestone (Carboniferous).	More than 5,000 m thick sedimentary package consisting of Devonian sandstones, Permo-carboniferous varvites and conglomerates; coal beds, sandstones, carbonaceous and bituminous shales and Permian fossiliferous limestones; Triassic sandstones and siltstones.

Table B: Comparative characteristics between Siberian Traps Province and Paraná Igneous Province.

CHARACTERISTICS	NORIL'SK-TALNAKH REGION (Jefferson et al., 1994)	PARANÁ BASIN
GREAT FAULTING ASSOCIATIONS: Closeness to magmatic focuses.	A number of mineralized intrusive centers on the Noril'sk-Talnakh mining camp is associated to the Noril'sk-Kharayelakh fault. This fault is considered a deep one, being a conduit to magma arise in the Lower Triassic and reactivated during the rift period, afterwards. Associated economic intrusions are restricted to the places where this fault affects the borders of the deposition of trough of pre-Permian rocks. These troughs are also coincident to the basalt lava thickening places (Genkin et al., 1981, in Jefferson et al., 1994). At Noril'sk, sulphide economic intrusions were inferred to as representatives of the volcanic conduits irradiating outside and up to the top of the main magmatic deep cameras.	In the literature, there is no reference to mineralized intrusions anywhere. Arches and lineations, thanks to the great number of associated dykes and sills, shall have been acting as magmatism feeder channels, as far as basement reactivated faults at eastern border (rift), where intrusions related to ancient phases of the Atlântico Sul Rift development occur (Mincato, 1994). He refers, as an example, to the Lomba Grande Complex with a 160Ma age; nevertheless, this opening is being widely considered as situated between 135 and 115 Ma (Asmus and Porto, 1972). The biggest intrusion concentration occurs at the North of Piquiri Lineament, at Ponta Grossa Arch and in the coastal region of São Paulo and Rio de Janeiro states (both characterized as dyke swarms)
GABBRO-DOLERITES MORPHOLOGY: Both regions have treelike sills, sills-cutting dykes and a number of tabular sills and dykes with different thicknesses.	i. Blanket shaped bodies varies from thin sills to enormous masses of a number of hundred cubic kilometers. ii. Thin dykes, shorter than some tens of meters in extension. iii. Chonoliths (Genkin, et al., 1981, in Jefferson et al., 1994) defined as gabbro-dolerite intrusions with various shapes: in this region, "chonoliths" assimilate country rocks.	i. Most of them are sills with thicknesses between a few meters to more than one hundred meters. Their area can reach more than one hundred square kilometers. ii. Dykes vary from tens to few hundred meters thick and from 1 to 20 kilometers wide, and iii. Great gabbroic rock masses without a definite shape; an example is the Lomba Grande Complex.
CONTACT METAMORPHISM:	i. and iii. above show wide contact metamorphism aureoles(> 100m). A high number of little skarns with PGE very high grades are characterized in the mineralized fields.	i. and iii. above can present contact metamorphism aureoles very well developed.
S, Se AND As FOUNTAINS:	A number of coal deposits, oil layers and sulphide evaporites are under sills-cut trapps.	A big amount of coal deposits with disseminated pyrite, mostly at the Province's southern sector (Rio Bonito Formation), carbonaceous and dark shales, both with disseminated pyrite (Iraty and Serra Alta formations) were cut by the basic sills.
SULFUR CONTENTS:	The most part of non-economic intrusions has <0.10% of S. Non-economic mineralized intrusions show 0.17 to 0.34% of S. In economic-bearing sulphide mineralized intrusions S contents varies from 0.95 to 2.2%.	Literature analytical data regarding S contents are scarce. Available ones are, as a rule, very low (ever below to 0.9%), except in case they are related to pyrite-bearing rocks. In this present work, grades of more than 1% were found in the Maracajá-Barro Branco Basic Body drilling samples(Table 03, appendix).
CUMULATES:	All magmatic phases show olivine and plagioclase cumulates	Only some intrusions show olivine cumulates, mostly the ancient ones.
DIFFERENTIATION:	A part of the strongly differentiate picritic to granitic suite.	Tolelitic basalts (picrites?) to rhyolitic differentiate suite.
SELENIUM AND ARSENICUM:	Se and As are locally very rich in the gabbro-dolerite sills and contact skarns.	As and Se data are unknown.

Table B: Comparative characteristics between Siberian Traps Province and Paraná Igneous Province. (continued)

7 - Conclusions

1. Intrusions investigated during this study generally have chemical characteristics that are compatible with their geographic location and the established high- and low- titanium geochemical associations for these areas.
2. Al_2O_3 and CaO vs. $\text{Mg}\#$ plots demonstrate that cumulus olivine fractionation was an important process during the early to middle stages of the crystallization history of intrusions from the southernmost portion of the study area (PA group) and gave rise to lithological associations similar to those encountered in mineralized intrusions from the Noril'sk camp.
3. The thicker olivine-rich sills from the Porto Alegre Metropolitan Region to Irui-Leão area are petrogenetically related to the picritic Lomba Grande intrusion. These olivine-rich bodies belong to the low-titanium suite of magmas and represent the most primitive intrusions in the Paraná basin and would be the closest analogues to the host lithologies associated with mineralized intrusions in the Noril'sk-Talnakh camp, Russia. Nevertheless, as a group, they generally do not display favorable chalcophile element depletion signatures, unlike their more fractionated counterparts from the Ponta Grossa Arch, nor association with major fracture zones.
4. Nickel and Cr behave in an identical manner during differentiation and the application of Ni as an exploration tool appears limited particularly when compared to the Pt, Pd and Cu.
5. Statistically significant concentrations of elevated S occur within borehole material from the Maracajá-Barro Branco (MB) when compared with surface material from this same body as well as all others investigated during this study. Samples and portions of the host intrusion with anomalous S warrant further investigation.
6. Sulphur contents associated with the volcanic suites generally fall below the lowest values associated with the S-poor intrusions and thus leaves little doubt that the intrusive bodies have experienced relatively greater degrees of crustal contamination with respect to S.
7. With the exception of the Pt and Pd depleted samples encountered during this study, intrusive and extrusive samples related to Paraná continental flood basalt magmatism have high background concentrations of these noble metals with the highest values occurring in the volcanic suites. Such high values are typical of magmas derived from the continental flood basalt terranes.
8. Palladium increases in the Serra Geral Formation magmas with differentiation and correlates well with Cu. Platinum and Au show no such correlation with differentiation or Cu content.
9. Copper, Pt and Pd concentrations and their various ratios suggest that restricted samples from the olivine-enriched rocks from the Porto Alegre Metropolitan Region to Irui-Leão areas (PA), and nearly all sill material from the Ponta Grossa Arch (PGA) experienced significant chalcophile elements depletion which can only be accounted for by relatively enhanced levels of sulphide segregation from the magmas that generated these samples. Distinct compositional gaps with respect to these elements separate the depleted from non-depleted fields.
10. Dykes from the Ponta Grossa Arch, which are believed to have fed the overlying sills and flows, generally have non-depleted Cu, Pt and Pd signatures; however, nearly all samples of sill material from this same area are depleted in Pd. This depletion would imply that relatively high degrees of sulphide segregation must have occurred in the magmas that gave rise to these bodies relative to those of the dykes and investigated volcanics.

11. As with other continental flood basalt terranes, characteristic elemental ratios from the high- and low-titanium Paraná basalt suites (extrusive and intrusive) are consistent with variable degrees of partial melting of source regions with similar compositions with the former being derived from smaller and the latter from higher degrees of partial melting.
12. Petrochemical interpretations should be bracketed by a number of geochemical discriminators in order to avoid erroneous conclusions.
13. Primitive low-titanium basalt samples are compatible with being parental magmas to the olivine-enriched and picritic cumulates from the Porto Alegre Metropolitan Region to Irui-Leão areas and the Lomba Grande intrusion.
14. Ratios of the chalcophile elements Cu/Pd, Cu/Y, (Pd/Y)*1000, in conjunction with the lithophile elements Ti/Y, Th/Ta, Nb/La, Gd/Yb, Th/Yb and La/Sm demonstrate that many samples from the Ponta Grossa Arch sills and some samples from the Porto Alegre Metropolitan Region to Irui-Leão area and Pouso Redondo-Rio do Campo basic body have experienced significantly higher degrees of metal depletion and crustal contamination relative to the other investigated bodies. In addition, these same depleted bodies have chemical indices similar to Siberian Trap volcanics associated with coeval mineralized intrusions.
15. The coincidence of many chalcophile element depleted intrusions in an area of the Paraná basin containing the most intense fissure-related magmatic activity suggests that sills from the Ponta Grossa Arch are the most favorable geological targets for Noril'sk type ore deposits. These fissures, like the Noril'sk-Karayelakh fault in Russia, may represent the focal point through which the greatest volume of Serra Geral Formation magma passed *en route* to surface from their lower crustal magma chambers. These conduits provide excellent proximal environments for magmas to segregate Ni-Cu-PGE sulphides.

8 - Recommendations

Geochemical characteristics of investigated intrusions of Paraná Basin magmatism suggest that rock samples, restricted to olivine enrichment of Porto Alegre Metropolitan Region/Irui-Leão (PA) and almost all Ponta Grossa Arch sills material have experienced a chalcophile elements intense depletion that is only compatible with relatively high volume of sulphide levels of magmas that generate these rocks. In addition, those same depleted bodies show chemical indexes similar to the Siberian volcanic traps associated to contemporary mineralized intrusions. There are also associated, mainly the Ponta Grossa Arch sills, to fissures of a major intensity event related to magmatic activity, which represents conduits to the *en route* great magma volumes of the Serra Geral Formation and are excellent proximal environments to the Ni-Cu-PGE sulphides segregation. In this context, the above named regions, with remarks to the Ponta Grossa Arch, represent the most promising targets to the deposit occurrences of these metals.

The general non-outcropping character of these intrusions is a handicap to the investigation of their potential because they are underlying thick sedimentary and/or volcanic rocks coverage. Taking into account that, in these conditions, surface prospecting methods such as stream sediments, soil and pan concentrate explorations shall not deliver conclusive results as stated by Chieregati (1995), we recommend the following activities for Ni-Cu-PGE potential evaluation of these regions:

- Satellite images use and interpretation mostly through their composition (e.g.: 7/4/1, 7/4/3 channels) and the use of different bands (e.g.: between 3 and 1 band), images multiplying and division, filter use or main component analysis, aiming to get the data necessary to the magnification of preferred aspects;
- Airbornemagnetometric survey on both regions, aiming to a better definition of the already known bodies and to the discovery of new ones. In the Ponta Grossa Arch the survey must cover all the sills and dykes region;
- Detailed structural studies of the areas with dykes, faults, and so on;
- Systematic transects through the wider outcropping bodies, even those with non apparent textural or compositional differentiations; sample collecting and chemical analyses of their rocks;
- Detailed examination and sampling of the drilling cores from the Porto Alegre Metropolitan/Irui-Leão regions, to search for any possible underground zoning of intrusive bodies with primitive composition and consequent more potential for Ni-Cu-PGE deposits;
- Exploratory drilling aiming to reach the possible mineralized horizons defined by airbornegeophysics surveys.

9 - Bibliographic References

- ABOARRAGE, A.M. & LOPES, R. da C. *Projeto A Borda Leste da Bacia do Paraná: integração geológica e avaliação econômica*. Porto Alegre : DNPM/CPRM , 1986. 18v. (Inédito).
- ALEGRI, V. & VASCONCELOS, C.S. *Comentários sucintos sobre a amostragem de rochas nos domínios do Arco de Ponta Grossa da Bacia do Paraná ; estados do Paraná e São Paulo*. São Paulo : CPRM , 1997. (Inédito).
- ALMEIDA, F.F.M. de. Síntese sobre a Tectônica da Bacia do Paraná. In: SIMPÓSIO REGIONAL DE GEOLOGIA, 3, Curitiba, 1981. *Atas...* Curitiba : SBG, 1981. v.1, p.1-20.
- ASMUS, H.E.; PORTO, R. Classificação das Bacias Sedimentares Brasileiras segundo a Tectônica de Placas. In: CONGRESSO BRASILEIRO DE GEOLOGIA, 16, Belém, 1972. *Anais...* Belém: SBG, 1972. p. 67-90.
- BARNES, S.J.; BOYD, R.; KORNELIUSSEN, A.; NILSSON, L.P.; OFTEN, M.; PEDERSEN, R.B. and ROBINS, B. The use of mantle-normalization and metal ratios in discriminating between the effects of partial melting, crystal fractionation and sulphide segregation on platinum-group elements, gold, nickel and copper : examples from Norway, In: PRICHARD, H.M., POTTS, P.J., BOWLES, J.F.W. ; CRIBB, S.; eds. *Geo-Platinum 87*. Barking : Elsevier, 1988. p.113-143.
- BELLIENI, G.; COMIN CHIARAMONTI, P.; MARQUES, L.S.; MARTINEZ, L.A.; MELFI, E.M.; NARDY, A.J.; PICCIRILLO, E.M. ; STOLFA, D. Continental flood basalts from the central-western regions of the Paraná plateau (Paraguay and Argentina): petrology and petrogenetic aspects. *Neues Jahrbuch Miner. Abh.* v.154 , p.111-139 ,1986.
- BELLIENI, G.; COMIN CHIARAMONTI, P.; MARQUES, L.S.; MELFI, A.J.; PICCIRILLO, E.M.; NARDY, A.J.R. ; ROISENBERG, A. High – and low – TiO₂ flood basalts from the Paraná plateau (Brazil): petrology and geochemical aspects on their mantle origin. *Neues Jahrbuch Miner. Abh.* v.150 , p.273-306 , 1984.
- BRÜGMANN, G.E.; NALDRETT, A.J.; ASIF, M.; LIGHTFOOT, P.C.; GORBACHEV, N.S. ; FEDORENKO, V.A Siderophile and chalcophile metals as tracers of the evolution of the Siberian Trap in the Nioril'sk region, Russia. *Geochimica et Cosmochimica Acta*, v. 57, p.2001-2018 , 1993.
- CHIEREGATI, L.A. *Projeto Platina SP/PR : relatório final das atividades*. São Paulo : CPRM , 1995. 1v. (Inédito).
- CHIEREGATI, L.A. *Projeto Platina SP/PR : relatório técnico anual – 1993*. São Paulo : CPRM , 1993. 1v. (Inédito).
- CORDANI, U.G. & VANDOROS, P. Basaltic rocks of the Paraná bacia. In: BIGARELLA,J. J. ; BECKER, I. D. & PINTO, I. D. ; eds. *Problems in Brazilian Gondwana Geology*. Curitiba : Max Roesner , 1967. p. 207-223.
- COX, K.G. The Karoo Province. In: MACDOUGALL, J.D. ; ed. *Continental Flood Basalts*. Dordrecht : Kluwer , 1988. p. 239-271.
- DIAS, A. *Projeto Platina RS/SC - Soleiras Básicas da Bacia do Paraná : resultados obtidos em 1992*. Porto Alegre : CPRM , 1992. 1v. (Inédito).

- DIAS, A. *Projeto Platina RS/SC - Soleiras Básicas da Bacia do Paraná – Áreas Maracajá – Barro Branco e Rio Uruçanga*. Porto Alegre : CPRM , 1993. 1v. (Inédito).
- FARINA, M. Metais do Grupo da Platina: ambiências geológicas e ensaio sobre a gitologia quantitativa com aplicações para descobrimento de depósitos. In: CONGRESSO BRASILEIRO DE GEOLOGIA, 35, Belém, 1988. *Anais...* Belém: SBG, 1988. v. 1. p. 130-143.
- FERREIRA, F.J.F.M. Alinhamentos Estruturais Magnéticos da Região Oriental da Bacia do Paraná e seu Significativo Tectônico. In: PAULIPETRO ; ed. *Geologia da Bacia do Paraná : reavaliação da potencialidade*. São Paulo : Consórcio IPT/ESP, 1982. p. 143-166.
- FULFARO, V.J.; SANTOS, M.V. & VIANA, R.B. 1982. Compartimentação e evolução tectônica da Bacia do Paraná. *Ver. Bras. GOG*, v. 12, p.590-611.
- GAMA JR., E.; BANDEIRA JR., A. N. & FRANÇA, A.B. Distribuição Espacial e Temporal das Unidades Litoestratigráficos Paleozóicos na Parte Central da Bacia do Paraná. In: PAULIPETRO ; ed. *Geologia da Bacia do Paraná: reavaliação da potencialidade*. São Paulo : Consórcio IPT/CESP, 1982. p. 19-40.
- GRÉGORIE, D.C. Determination of platinum, palladium, ruthenium and iridium in geological material by inductively coupled plasma mass spectrometry with sample introduction by electrothermal vaporisation. *Analytical Chemistry*, v.58, p.616-620 , 1988.
- HULBERT, L. & GRÉGORIE, D.C. *Geochemical Examination of Paraná Magmatism in Southern and Southern-Central Brasil with respect to potencial for Noril'sk – Type Ni – Cu – PGE Deposits*. Ottawa : Geological Survey of Canada , 1999. Canada-Brasil Cooperation Project for Sustainable Development in the Mineral Sector. (Inédito).
- JEFFERSON, C.W.; HULBERT, L.J.; RAINBIRD, R.H.; HALL, G.E.M.; GRÉGORIE, D.C.; GRINENKO, L.I. Mineral Resource Assessment of Neoproterozoic Franklin Igneous Events of Arctic Canada: comparison with the Permo-Triassic Noril'sk – Talmakh Ni – Cu – PGE Deposits of Russia. *Geological Survey of Canada, Open File 2789*, 1994. 48 f.
- LEINZ, V. Contribuição à geologia dos derrames basálticos do sul do Brasil. *Bol. FFC/USP*, v. 5, p.1-61 , 1949.
- LIGHTFOOT, P.C.; HAWKESWORTH, C.J.; HERGT, J.; NALDRETT, A.J.; GORBACHEV, N.; FEDORENKO, V.A. ; DOHERTY, W., Remobilization of the continental lithosphere by a mantle plume: major and trace element, and Sr-, Nd-, and Pb- isotope evidence from picritic and tholeitic lavas of the Noril'sk, Siberian Trap, Russia. *Contributions to Mineralogy and Petrology*, v.114, p. 171-188 , 1993.
- LIGHTFOOT, P.C.; NALDRETT, A.J.; GORBACHEV, N.; FEDORENKO, V.A.; HAWKESWORTH, C.J.; HERGT, J. ; DOHERTY, W., Chemostratigraphy of Siberian Trap lavas, Noril'sk District: Implications for the source of flood basalt magmas and their associated Ni-Cu mineralization, In: LIGHTFOOT, P.C. & NALDRETT, A.J. ; eds. SUDBURY – NORIL'SK SYMPOSIUM , 1994. *Proceedings...* p. 283-312.
- MAIER, W.D.; BARNES, S.J.; DE KLERK, W.J.; TEIGLER, B. ; MITCHELL, A.A., Cu/Pd and Cu/Pt of Silicate Rocks in the Bushveld Complex: Implications for Platinum-Group Element Exploration. *Economic Geology*, V. 91, p.1151-1158 , 1996.
- MANIESI, V. *Petrologia das Soleiras de Diabásio de Reserva e Salto do Itararé, PR*. Rio Claro, 1991. Dissertação (Mestrado) UNIESP, 117 p.

- MARINI, O.J.; FUCK, R.A. & TREIN, E. Intrusivas Básicas Jurássico – Cretáceas do primeiro planalto do Paraná. *Boletim Paranaense de Geologia*, n. 23-25, p. 307-324, 1967.
- MANTOVANI, M.S.V.; MARQUES, L. S.; DE SOUSA, M.A.; CIVETTA, L.; ATALLA, L. ; INNOCENTI, F. Trace element and strontium isotope constrains on the origin and evolution of Paraná continental flood basalts of Santa Catarina state. *Journal of Petrology*, v.26, p.187-209, 1985.
- MELFI, A.J.; PICCIRILLO, E.M. & NARDY, A.J.R. Geological and Magmatic Aspects of the Paraná Basin : an Introduction. In: PICCIRILLO, E.M. & MELFI, A.J. ; eds. *The Mesozoic flood volcanism of the Paraná basin: petrogenetic and geophysical aspects*. São Paulo : IAG-USP, 1988. 600 p.
- MINCATO, R.L. *Avaliação do Potencial da Província Ígnea Continental do Paraná para Mineralizações de Ni-Cu-EGP, a partir, dos modelos Noril'sk e Insizwa*. São Paulo, 1994. 113 p. Dissertação (Mestrado) – Instituto de Geociências, UNICAMP.
- NALDRETT, A.J. *Programa Nacional de Prospecção de Metais do Grupo da Platina*. (Apostila do Curso Ministrado na CPRM, sobre Geologia Econômica e Prospecção de Metais do Grupo da Platina). Rio de Janeiro : CPRM , 1991. 1v. (Inédito).
- NALDRETT, A. J. Ores associated with flood basalts. In: J.A. WHITNEY & A.J. NALDRETT ; eds. Ore deposition associated with magmas. *Reviews in Economic Geology*, v.4, p.103-118, 1989.
- NALDRETT, A.J. & DUKE, M.J. Platinum metals in magmatic sulfide ores. *Science* , v.208 , p. 1417-1428 ,1980.
- PEACH, C.I.; MANTHEZ, E.A. ; KEAYS, R.R. Sulphide melt-silicate melt distribution coefficientes for the noble metals and other chalcophile elements as deduced from MORB: Implications for partial melting: *Geochimica et Cosmochimica Acta*, v.54, p.3379-3389 , 1990.
- PEATE, D.W. & HAWKESWORTH, C.J. Lithospheric to asthenospheric transition in Low-Ti flood basalts from southern Paraná, Brazil. *Chemical Geology*, v.127, p.1-24 , 1986.
- PEATE, D.W. ; HAWKESWORTH, C.J. ; MANTOVANI, M.S.M., Chemical stratigraphy of the Paraná lavas (South America): Classification of magma types and their spatial distribution. *Bulletin of Volcanology*, v. 55 , p.119-139 , 1982.
- PETRI, S. & FÚLFARO, J.V. *Geologia do Brasil*. São Paulo : T.A. QUEIROZ, 1983. 631 p.
- PETRINI, L.; CIVETTA, L.; PICCIRILLO, E.M.; BELLINI, G.; COMIN-CHIARAMONTI, P.; MARQUES, L.S. ; MELFI, A.J. Mantle heterogeneity and crustal contamination in the genesis of Low-Ti continental flood basalts from the Paraná plateau (Brazil): Sr-Nd isotope and geochemical evidence. *Journal of Petrology*, v.28, Part 4, p.701-726 , 1987.
- PICCIRILLO, E.M.; COMIN-CHIARAMONTI, P.; BELLINI, G.; CIVETTA, L.; MARQUES, L. S.; MELFI, A.J., PETRINI, R.; RAPOSO, M.I.B. & STOLFA, D. Petrogenetic Aspects of Continental Flood Basalt-Rhyolite from the Paraná Basin (Brazil). In: PICCIRILLO, E.M. & MELFI, A.J. ; eds. *The Mesozoic flood volcanism of the Paraná basin : petrogenetic and geophysical aspects*. São Paulo : IAG-USP, 1988. 600 p.

- PICCIRILLO, E.M.; COMIN-CHIARAMONTI, P.; MELFI, A.J., STOLFA, D.; BELLINI, G.; MARQUES, L. S.; GIARETTA, A.; NARDY, A.J.R.; PINESI, J.P.P.; RAPOSO, M.I.B.; ROISENBERG, A.; STOLFA, D. Petrochemistry Aspects of Continental Flood Basalt-Rhyolite suites and relatives intrusives from the Paraná basin (Brazil). In: PICCIRILLO, E.M. & MELFI, A.J. ; eds. *The Mesozoic flood volcanism of the Paraná basin* : petrogenetic and geophysical aspects. São Paulo : IAG-USP, 1988. p. 107-156.
- ROMANINI, S.J. & ALBUQUERQUE, L.F. *Geological aspects of the basic intrusions characterized by CPRM's national program for prospection of the PGE in the Paraná Basin*. Porto Alegre : CPRM , 1996. 18 p. (CPRM Internal Report, Porto Alegre Superintendecy) (Inédito).
- SANDER, A. *Projeto Platina RS/SC - Estudo dos Testemunhos de Sondagem das Regiões de Irui-Leão e Rio Pardo*. Porto Alegre : CPRM , 1994b. 1v. (Inédito).
- SANDER, A. *Projeto Platina RS/SC - Soleiras Básicas das Regiões de Irui-Leão e Rio Pardo*. Porto Alegre : CPRM , 1993. 1v.(Inédito).
- SANDER, A. *Projeto Platina RS/SC - Soleiras Básicas do Bacia do Paraná* : resultados obtidos em 1993. Porto Alegre : CPRM, 1994a. 1v. (Inédito).
- SANDER, A. *Projeto Platina RS/SC. Soleiras Básicas do Bacia do Paraná* – resultados obtidos em 1994. Porto Alegre : CPRM , 1995. 1v. (Inédito).
- SCHNEIDER, R.L.; MUHLMAN, H.; TOMAZI, E.Z.; MEDEIROS, R.A.; DAEMON, R.F. & NOGUEIRA, A. A. Revisão Estratigráfica da Bacia do Paraná. In: CONGRESSO BRASILEIRO DE GEOLOGIA, 28 , Porto Alegre, 1974. *Anais...* Porto Alegre : SBG , 1974. v. 1, p.41-65.
- SEN GRUPTA, J.G. & GRÉGORIE, D.C. Determination of ruthenium, palladium, and iridium in 27 international reference silicate and iron-formation rocks, ores and related materials by inductively-coupled plasma mass spectrometry. *Geostandards Newsletter*, v.13, p.197-204 , 1989.
- SOARES, P. C. Estratigrafia das Formações Jurássico – Cretáceas na Bacia do Paraná, Brasil. In: *Sedimentares del Jurásico y Cretáceo de America del Sur*. Buenos Aires : Com. Sudam. del Jur. x Cret., 1981. p. 271-304.
- VIERO, A.P. *Petrologia e Geoquímica do Complexo Básico de Lomba Grande, RS*. Porto Alegre, 1991. Dissertação (Mestrado) UFRGS. 176 p.
- ZALÁN, P.V.; CONCEIÇÃO, J.C.; WOLFF, S.; ASTOLFI, M.A.; VIEIRA, I.S.; APPI, V.T.; NETO, E.V.S.; CERQUEIRA, J.R.; ZANOTTO, O.A.; PAUMER, M.L. ; MARQUES, A. *Análise da Bacia do Paraná*. Rio de Janeiro : PETROBRAS , 1986. p. 195. (Internal Report Gt-Os-009/85, PETROBRAS (Dupex-Cenpes)

**ANALYTICAL RESULTS
AND/OR STATISTICAL
SUMMARY**

Sample	UTM-N m	UTM-E m	SiO ₂ %	TiO ₂ %	Al ₂ O ₃ %	Fe ₂ O ₃ T %	Fe ₂ O ₃ %	FeO %	MnO %	MgO %	CaO %	Na ₂ O %	K ₂ O %	H ₂ OT %	CO ₂ T %	P ₂ O ₅ %	ST %	TOTAL %	Mg#	Ba ppm	Co ppm	Cr ppm	Cu ppm	Ni ppm	Sc ppm	Sr ppm	V ppm	Zn ppm	Zr ppm	Ce ppm	Dy ppm
JBO622	6.676.800	530.310	55,4	2,01	12,90	15,60	2,10	12,1	0,19	2,54	6,09	2,60	2,27	1,1	0,2	0,31	0,04	100,0	--	510	43	30	150	22	30	140	430	110	230	68	7,2
JBO623	6.676.800	530.310	45,9	1,53	16,20	11,80	3,40	7,6	0,16	7,70	10,15	2,10	0,43	3,8	0,3	0,19	0,06	99,5	--	310	49	270	160	140	26	260	230	65	130	33	4,7
JBO624	6.676.800	530.310	42,6	1,31	10,80	13,00	2,50	9,5	0,18	17,05	7,95	1,20	0,30	3,2	2,8	0,12	0,04	99,9	--	130	77	2000	110	630	25	170	220	70	110	21	3,1
JBO625	6.673.982	530.074	56,8	1,94	12,60	14,30	3,00	10,2	0,17	2,51	6,10	2,60	2,38	0,6	0,1	0,28	0,05	99,5	--	470	42	23	140	17	30	150	420	110	240	71	7,7
JBO626	6.675.040	530.030	56,5	2,21	12,50	15,10	3,40	10,5	0,19	2,26	6,15	2,70	2,35	1,0	0,1	0,33	0,03	100,4	--	490	43	13	140	13	31	150	480	120	250	75	8,1
JBO627	6.696.484	510.328	41,1	1,57	14,90	10,80	--	--	0,19	6,90	14,84	1,80	0,36	--	4,0	0,15	1,06	97,8	--	160	46	380	120	100	35	310	270	34	120	25	3,9
JBO628	6.696.484	510.328	47,0	1,65	16,40	11,70	2,50	8,3	0,17	7,50	11,88	2,20	0,37	1,6	0,2	0,16	0,06	100,1	--	160	48	440	150	120	33	250	280	69	110	28	4,0
JBO629	6.698.848	513.639	47,8	1,33	14,90	11,10	2,10	8,1	0,18	8,00	12,55	1,80	0,47	1,5	0,1	0,11	0,04	99,1	--	180	46	410	100	120	43	220	320	59	100	24	4,0
JBO630	6.698.848	513.639	47,6	1,92	14,60	12,80	4,00	7,9	0,19	6,37	12,01	2,40	0,60	1,5	0,3	0,25	0,06	99,7	--	240	51	76	220	67	40	270	350	68	170	45	6,1
JBO631	6.697.500	505.920	51,3	1,31	16,30	10,60	3,30	6,5	0,14	5,49	9,73	2,50	1,13	1,5	0,2	0,23	0,06	99,8	--	320	40	270	120	99	28	260	220	68	150	44	4,4
JBO632	6.697.500	505.920	50,7	0,98	13,80	10,60	2,40	7,4	0,16	10,28	9,01	1,80	0,75	1,8	0,2	0,15	0,05	99,7	--	250	52	920	85	290	30	190	210	63	110	32	3,4
JBO633	6.698.000	516.000	47,2	2,35	15,10	13,60	4,30	8,3	0,19	5,54	11,44	2,50	0,68	1,7	0,1	0,31	0,06	100,0	--	250	51	52	250	56	35	270	380	74	210	53	6,6
JBO634	6.698.000	516.000	47,5	1,24	17,10	10,30	2,10	7,4	0,15	7,72	12,47	2,00	0,52	1,4	0,1	0,15	0,02	100,0	--	180	45	500	150	140	32	250	240	53	100	28	3,9
JBO635	6.701.440	507.000	49,7	0,91	13,60	10,80	2,40	7,6	0,16	10,86	8,87	1,60	0,60	2,2	0,6	0,14	0,04	99,5	--	200	55	980	88	320	27	210	190	61	100	28	3,0
JBO636	6.701.440	507.000	50,1	0,86	13,80	10,60	2,20	7,5	0,16	10,96	8,90	1,60	0,68	2,0	0,3	0,14	0,05	99,5	--	330	54	1000	78	320	28	200	190	60	110	28	3,2
JBO637	6.701.370	501.470	52,0	1,45	15,10	10,40	2,60	7,0	0,15	6,74	9,47	2,10	1,19	1,6	0,2	0,22	0,04	100,0	--	310	40	310	140	110	31	210	240	70	170	45	4,9
JBO638	6.701.370	501.470	50,7	1,02	13,80	10,70	2,60	7,3	0,15	9,77	8,82	1,90	0,79	2,2	0,1	0,16	0,04	99,4	--	220	53	880	88	300	30	190	210	66	120	32	3,6
JBO639	6.679.000	406.999	50,8	1,02	16,50	10,90	2,60	7,4	0,16	5,82	10,70	2,00	0,77	2,1	-0,1	0,14	0,02	100,1	--	340	44	150	110	110	34	250	240	67	100	32	4,0
JBO640	6.682.000	402.000	50,8	1,09	16,20	11,20	3,30	7,1	0,16	6,02	10,30	2,20	0,91	1,4	0,1	0,16	0,08	99,9	--	320	44	150	120	110	31	230	240	66	120	35	4,0
JBO641	6.682.000	402.000	51,1	0,97	17,20	10,10	3,20	6,2	0,14	5,39	10,47	2,20	0,86	1,5	0,1	0,15	-0,02	99,7	--	270	39	130	110	91	28	250	210	57	120	33	3,9
JBO642	6.682.000	402.000	51,4	1,09	16,90	11,00	3,60	6,6	0,16	5,47	10,17	2,20	0,95	1,5	0,1	0,16	0,02	100,4	--	290	43	110	130	94	28	230	220	65	130	37	4,1
JBO643	6.682.000	402.000	50,7	1,08	15,50	11,20	3,00	7,4	0,18	6,28	10,09	2,10	0,92	2,4	0,1	0,14	0,02	100,1	--	250	44	140	120	110	33	250	240	66	110	35	4,1
JBO644	6.680.000	403.000	63,5	0,68	13,40	5,90	5,50	0,3	0,21	2,21	1,53	1,80	4,29	4,9	0,4	0,22	0,02	99,2	--	660	15	58	12	23	13	230	61	120	240	83	5,8
JBO645	6.680.000	403.000	51,4	0,99	17,40	10,30	3,40	6,2	0,14	5,12	10,40	2,20	0,97	1,4	-0,1	0,16	-0,02	100,0	--	380	40	120	120	85	27	290	210	64	120	36	4,0
JBO646	6.670.810	358.000	53,6	1,40</																											

Sample	Er ppm	Eu ppm	Gd ppm	Ho ppm	La ppm	Lu ppm	Nd ppm	Pr ppm	Sm ppm	Tb ppm	Tm ppm	Y ppm	Yb ppm	Ag ppm	Bi ppm	Cs ppm	Ga ppm	Hf ppm	Mo ppm	Nb ppm	Pb ppm	Rb ppm	Ta ppm	Th ppm	Tl ppm	U ppm	Cl ppm	F ppm	Au ppb	Pt ppb	Pd ppb
JBO622	4,2	1,8	7,6	1,40	34	0,60	34	8,9	7,0	1,30	0,59	42	3,9	0,4	-0,5	3,80	22	5,9	1,7	19,0	15	90	1,2	8,90	0,53	2,50	248	716	3,20	1,40	1,70
JBO623	2,6	1,5	4,9	0,90	15	0,33	20	4,4	4,4	0,78	0,34	25	2,1	0,2	0,9	3,20	19	4,0	0,5	11,0	-2	13	0,7	1,40	0,39	0,36	271	391	2,10	0,70	1,50
JBO624	1,7	1,0	3,4	0,61	8	0,24	12	2,8	3,0	0,53	0,25	17	1,6	0,4	0,9	3,70	13	3,0	0,2	8,1	-2	15	0,6	0,90	0,95	0,24	207	268	1,20	0,60	1,80
JBO625	4,5	2,0	8,3	1,60	35	0,66	35	9,1	8,0	1,30	0,63	42	4,3	0,9	0,9	4,00	22	6,9	0,8	19,0	16	95	0,9	9,20	0,55	2,70	196	721	0,70	0,25	0,25
JBO626	4,4	1,9	8,2	1,60	37	0,68	38	9,6	8,2	1,40	0,65	44	4,1	0,5	-0,5	4,50	23	6,7	1,2	21,0	16	93	1,1	9,30	0,53	2,70	178	771	0,25	0,25	0,25
JBO627	2,2	1,3	4,0	0,79	11	0,30	15	3,4	3,6	0,72	0,32	22	2,1	0,3	1,0	0,69	18	3,5	0,4	10,0	-2	8	0,6	1,10	0,27	0,30	1144	634	0,25	0,25	1,10
JBO628	2,2	1,4	4,4	0,80	12	0,31	17	3,8	3,8	0,69	0,30	23	1,9	0,4	0,7	0,84	20	3,5	0,4	11,0	-2	8	0,6	1,10	0,14	0,30	266	252	0,50	1,10	0,70
JBO629	2,2	1,4	4,2	0,79	10	0,32	15	3,3	3,5	0,65	0,29	21	2,0	0,1	-0,5	0,82	18	2,7	-0,2	7,2	-2	12	0,5	0,93	0,18	0,21	235	297	4,90	1,60	2,10
JBO630	3,3	1,7	6,7	1,20	20	0,42	26	6,0	6,0	1,00	0,44	33	2,8	0,5	0,8	0,38	20	5,2	0,4	14,0	2	14	0,8	1,90	0,08	0,48	213	411	2,30	0,25	0,25
JBO631	2,4	1,5	4,6	0,89	21	0,37	22	5,4	4,7	0,75	0,35	25	2,3	0,5	1,3	0,86	20	4,3	0,8	13,0	6	31	0,7	3,10	0,55	0,65	-100	391	4,20	7,10	8,10
JBO632	1,9	1,0	3,8	0,72	15	0,29	16	4,0	3,6	0,61	0,29	20	1,8	0,4	0,8	1,10	16	3,7	0,5	9,1	3	22	0,4	2,60	0,42	0,41	161	341	3,00	5,40	6,00
JBO633	3,5	1,9	7,3	1,30	23	0,47	31	7,0	6,9	1,20	0,48	38	3,1	0,8	-0,5	0,46	22	5,2	0,6	16,0	-2	16	1,0	2,20	0,09	0,56	275	500	2,80	0,25	0,25
JBO634	2,2	1,3	4,2	0,79	12	0,29	17	3,9	3,9	0,67	0,29	22	1,8	0,2	-0,5	0,62	19	3,3	0,4	8,3	2	13	0,5	1,20	0,07	0,36	165	295	7,20	0,25	0,25
JBO635	1,8	1,0	3,4	0,61	13	0,25	14	3,6	2,9	0,52	0,26	18	1,8	0,3	-0,5	1,20	16	3,0	-0,2	8,1	4	18	0,5	2,40	0,42	0,37	120	333	3,60	9,60	10,30
JBO636	1,9	1,0	3,1	0,62	13	0,28	15	3,5	3,0	0,53	0,28	18	1,8	0,3	-0,5	0,86	16	3,0	-0,2	7,9	3	20	0,5	2,40	0,49	0,40	168	317	3,10	7,30	7,80
JBO637	2,8	1,4	5,2	0,96	22	0,41	23	5,6	5,1	0,82	0,38	27	2,6	0,2	0,7	0,70	20	4,9	0,5	15,0	6	36	0,8	3,80	0,26	0,62	172	375	3,70	8,70	10,20
JBO638	2,0	1,2	3,8	0,72	15	0,33	17	4,0	3,4	0,60	0,30	20	2,0	-0,1	-0,5	1,20	16	3,4	-0,2	9,2	4	23	0,5	2,80	0,47	0,45	184	431	0,25	7,70	7,40
JBO639	2,2	1,1	3,7	0,74	15	0,34	17	4,1	3,4	0,64	0,31	22	2,1	0,6	-0,5	2,60	20	3,2	0,3	6,9	5	26	0,4	2,60	0,26	0,58	136	370	2,50	6,80	8,10
JBO640	2,2	1,1	4,1	0,80	17	0,36	19	4,5	3,9	0,67	0,34	23	2,2	0,4	-0,5	0,92	20	3,7	0,2	8,1	5	30	0,5	2,90	0,16	0,65	205	297	2,10	10,10	9,60
JBO641	2,3	1,3	4,0	0,76	16	0,32	18	4,3	3,8	0,68	0,32	21	2,2	0,8	-0,5	0,86	19	3,3	0,3	7,20	4	27	0,4	3,00	0,14	0,63	-100	329	6,30	8,30	10,10
JBO642	2,4	1,3	4,1	0,83	17	0,33	20	4,6	3,9	0,70	0,33	24	2,3	0,3	1,2	0,87	20	4,4	0,4	8,3	5	31	0,5	3,10	0,19	0,73	137	311	2,40	7,50	9,10
JBO643	2,3	1,2	4,0	0,80	17	0,31	18	4,4	3,7	0,66	0,33	23	2,3	1,7	0,8	0,99	19	3,8	0,2	7,9	5	30	0,5	2,90	0,28	0,64	173	374	2,00	8,00	8,60
JBO644	3,4	1,3	6,4	1,20	44	0,52	39	10,0	6,8	1,00	0,51	36	3,5	0,6	1,0	7,80	15	6,2	-0,2	16,0	66	230	1,0	15,00	1,90	4,60	336	606	0,25	0,80	0,25
JBO645	2,2	1,4	4,2	0,77	17	0,31	19	4,3	3,9	0,68	0,32	22	2,1	0,5	0,9	0,78	20	3,9	0,3	7,7	6	30	0,4	2,90	0,29	0,72	104	373	1,90	6,10	7,50
JBO646	3,2	1,3	5,5	1,10	21	0,49	23	5,6	5,0	0,93	0,48	30	2,9	0,5	1,3	3,50	19	4,7	0,3	10,0	7	58	0,6	5,00	0,29	1,20	255	501	3,30	11,50	12,20
JBO647	5,5	3,1	11,0	1,90	29	0,74	41	8,9	9,3	1,70	0,74	53	5,2	0,5	-0,5	0,76	24	7,5	0,8	21,0	5	29	1,2	2,20	0,18	0,60	271</				

Sample	UTM-N m	UTM-E m	SiO ₂ %	TiO ₂ %	Al ₂ O ₃ %	Fe ₂ O ₃ T %	Fe ₂ O ₃ %	FeO %	MnO %	MgO %	CaO %	Na ₂ O %	K ₂ O %	H ₂ OT %	CO ₂ T %	P ₂ O ₅ %	ST %	TOTAL %	Mg#	Ba ppm	Co ppm	Cr ppm	Cu ppm	Ni ppm	Sc ppm	Sr ppm	V ppm	Zn ppm	Zr ppm	Ce ppm	Dy ppm
JBO651	6.840.235	656.835	52,4	1,94	13,70	15,50	4,00	10,3	0,23	3,57	7,93	2,80	1,20	1,6	-0,1	0,22	0,10	100,1	--	300	45	23	200	29	33	160	470	110	160	41	6,7
JBO652	6.840.150	655.565	52,8	1,70	12,90	15,40	2,70	11,4	0,26	4,02	8,04	2,60	1,19	1,5	0,1	0,22	0,69	100,2	--	320	46	23	220	29	36	140	430	110	150	41	7,1
JBO653	6.850.000	657.000	52,7	2,63	12,20	17,70	6,40	10,2	0,23	2,04	6,55	2,70	1,61	2,0	-0,1	0,47	0,05	99,9	--	330	46	12	400	-10	29	150	300	140	310	71	11,0
JBO654	6.850.000	657.000	53,2	1,66	14,20	14,40	3,50	9,8	0,20	3,78	8,24	2,80	1,24	1,0	-0,1	0,27	0,02	99,9	--	250	44	24	230	32	33	150	410	96	160	44	6,5
JBO655	6.850.000	657.000	47,5	1,77	12,60	14,30	--	--	0,27	4,26	9,33	2,20	1,05	--	2,2	0,21	1,35	97,2	--	280	44	19	230	26	35	150	440	110	150	39	6,5
JBO656	6.846.000	655.000	51,6	1,83	12,80	15,20	2,70	11,2	0,20	3,52	7,60	2,70	1,28	1,0	-0,1	0,24	0,02	96,7	--	300	46	23	230	30	35	130	430	100	180	47	7,4
JBO657	6.846.000	655.000	50,1	1,76	13,30	16,10	--	--	0,40	4,20	6,91	2,60	1,15	--	0,1	0,21	2,74	99,6	--	260	51	23	260	30	36	130	450	120	160	48	7,1
JBO659	6.848.000	655.000	52,5	1,86	13,70	15,30	--	--	0,25	3,71	8,09	2,60	1,21	--	0,1	0,22	1,02	100,8	--	300	50	25	240	30	36	180	450	120	160	43	7,0
JBO660	6.848.000	655.000	52,3	2,07	12,90	16,60	4,10	11,2	0,23	3,76	7,76	2,70	1,32	1,3	-0,1	0,25	0,08	100,1	--	320	49	26	230	30	36	160	470	110	180	45	7,5
JBO661	6.832.010	651.500	53,6	2,15	13,40	15,30	5,60	8,7	0,19	2,46	6,81	2,70	1,95	1,6	-0,1	0,36	0,03	99,7	--	430	45	17	280	16	31	160	460	120	270	72	7,9
JBO662	6.832.010	651.500	54,0	1,54	13,20	14,20	3,70	9,4	0,22	3,60	7,67	2,70	1,68	1,5	0,1	0,26	0,37	100,1	--	520	45	23	220	24	36	160	370	99	200	53	6,5
JBO663	6.832.010	651.500	54,2	1,99	13,50	14,90	4,90	9,0	0,19	2,68	6,93	2,70	1,90	1,3	-0,1	0,28	0,10	99,8	--	420	46	17	230	19	32	160	470	110	220	61	6,9
JBO665	6.828.000	650.000	51,0	1,85	13,60	15,30	--	--	0,25	4,04	3,28	3,10	1,15	--	1,0	0,27	1,30	96,3	--	280	55	17	240	25	43	94	500	120	210	61	7,2
JBO666	6.828.000	650.000	51,0	1,87	13,60	15,40	--	--	0,25	4,07	3,30	3,10	1,16	--	0,1	0,27	3,08	97,3	--	310	54	45	240	43	44	100	500	120	220	45	5,7
JBO668	6.834.000	653.000	59,9	1,28	14,40	9,50	2,70	6,1	0,17	3,51	1,47	2,10	2,28	4,8	-0,1	0,17	0,12	99,1	--	380	29	57	120	35	23	100	220	120	220	72	6,0
JBO669	6.834.000	653.000	50,9	1,70	13,50	14,50	--	--	0,34	3,66	4,34	2,50	1,56	--	0,3	0,24	2,66	96,5	--	410	51	17	280	23	46	160	510	130	190	55	6,6
JBO670	6.826.600	651.400	53,2	2,42	12,80	16,50	6,20	9,2	0,20	2,36	6,54	2,60	1,94	1,4	0,1	0,30	0,10	99,6	--	470	49	20	250	17	33	150	640	130	230	66	7,3
JBO671	6.826.600	651.400	53,9	1,64	12,90	14,60	3,70	9,8	0,21	3,22	7,30	2,60	1,76	1,5	-0,1	0,25	0,79	99,7	--	450	46	14	230	20	37	160	430	110	190	59	6,8
JBO672	6.828.000	649.000	52,2	1,79	13,90	13,80	--	--	0,44	4,42	3,66	2,60	1,94	--	-0,1	0,27	1,65	96,8	--	450	49	18	220	25	41	150	480	120	220	65	6,7
JBO673	6.834.000	645.000	54,3	1,91	13,60	14,70	4,70	9,0	0,20	2,81	6,93	2,70	1,80	1,4	-0,1	0,26	0,13	99,9	--	450	44	14	210	18	33	150	470	110	210	61	6,8
JBO674	6.834.000	645.000	54,6	1,62	13,10	14,80	--	--	0,20	3,10	7,36	2,60	1,76	--	0,1	0,26	1,09	100,7	--	360	43	15	230	20	36	150	410	110	200	58	6,7
JBO675	6.834.000	647.000	52,9	1,96	13,20	15,10	--	--	0,20	2,68	6,67	2,50	1,87	--	-0,1	0,26	1,02	98,5	--	420	45	14	260	24	31	140	460	120	220	62	6,9
JBO676	6.834.000	647.000	53,9	1,63	13,10	15,00	3,40	10,4	0,19	3,04	7,28	3,30	1,36	2,7	0,1	0,25	0,10	100,8	--	380	44	14	200	19	33	130	400	100	200	55	6,7
JBO679	6.817.760	657.349	50,2	1,50	13,00	15,30	--	--	0,25	5,19	8,07	2,40	1,08	--	0,3	0,20	1,73	99,2	--	260	52	20	240	44	34	150	380	97	150	43	5,6
JBO680	6.817.760	657.349	52,7	1,41	13,30	14,40	3,80	9,5	0,21	4,86	8,41	2,70	1,31	1,3	0,2	0,23	0,06														

Sample	Er ppm	Eu ppm	Gd ppm	Ho ppm	La ppm	Lu ppm	Nd ppm	Pr ppm	Sm ppm	Tb ppm	Tm ppm	Y ppm	Yb ppm	Ag ppm	Bi ppm	Cs ppm	Ga ppm	Hf ppm	Mo ppm	Nb ppm	Pb ppm	Rb ppm	Ta ppm	Th ppm	Tl ppm	U ppm	Cl ppm	F ppm	Au ppb	Pt ppb	Pd ppb
JBO651	4,0	1,7	5,9	1,30	20	0,60	22	5,4	5,4	1,10	0,56	38	3,8	0,6	0,7	2,70	21	4,8	0,4	11,0	6	45	0,7	4,30	0,26	1,20	188	446	4,40	10,40	10,80
JBO652	4,3	1,7	6,5	1,50	19	0,64	23	5,5	5,4	1,20	0,61	40	4,1	0,3	0,7	3,60	22	4,8	0,3	11,0	7	46	0,7	4,50	0,36	1,30	290	406	2,20	11,00	10,90
JBO653	6,5	2,4	12,0	2,20	35	0,91	40	9,6	8,9	1,80	0,93	60	6,0	1,1	0,7	3,00	23	7,8	0,8	19,0	10	61	1,1	8,10	0,38	2,40	264	728	4,90	2,30	18,90
JBO654	4,1	1,7	6,4	1,40	22	0,56	24	5,9	5,6	1,10	0,56	37	3,7	1,8	-0,5	2,00	22	4,5	0,3	11,0	7	49	0,6	4,50	0,23	1,30	178	488	3,20	16,30	11,60
JBO655	4,0	1,8	6,3	1,40	19	0,63	22	5,1	5,1	1,10	0,59	38	3,9	2,1	0,7	2,00	22	4,5	0,7	10,0	6	40	0,7	4,40	0,60	1,30	290	442	0,60	7,60	10,30
JBO656	4,3	1,8	7,0	1,50	23	0,66	26	6,2	6,1	1,30	0,62	43	4,1	0,5	0,7	2,00	22	5,3	0,8	13,0	7	53	0,8	4,90	0,28	1,40	128	543	3,50	9,60	8,30
JBO657	4,3	1,7	7,0	1,50	24	0,63	25	5,9	5,9	1,20	0,61	41	4,2	1,1	0,9	2,30	23	5,2	0,7	11,0	7	45	0,7	4,70	0,40	1,30	-100	522	3,50	9,60	8,10
JBO659	4,3	2,0	7,3	1,50	20	0,59	23	5,3	5,7	1,10	0,61	42	4,1	0,3	0,8	2,30	23	5,0	1,1	11,0	8	46	0,7	4,70	0,45	1,50	224	441	4,60	10,50	10,50
JBO660	4,4	1,9	7,3	1,60	20	0,65	25	5,9	6,1	1,20	0,64	44	4,3	0,5	-0,5	2,10	22	4,8	0,9	13,0	8	52	0,7	4,50	0,26	1,30	124	443	4,90	9,50	8,10
JBO661	4,7	2,0	8,0	1,70	34	0,63	36	8,7	7,5	1,30	0,69	47	4,2	1,4	0,9	3,10	23	6,5	1,6	22,0	12	72	1,3	8,50	0,40	2,20	180	606	7,00	7,60	7,90
JBO662	3,9	1,6	7,0	1,40	25	0,52	26	6,6	6,0	1,00	0,56	39	3,6	0,5	-0,5	2,40	21	4,9	0,5	15,0	10	62	0,8	6,30	0,39	1,60	284	507	4,90	9,90	8,30
JBO663	4,2	1,9	7,2	1,60	29	0,62	30	7,4	6,6	1,20	0,61	41	4,2	0,3	1,0	3,60	23	6,4	1,1	20,0	11	72	1,1	7,50	0,40	2,00	172	505	6,20	11,60	9,00
JBO665	4,5	1,1	6,5	1,50	29	0,69	29	7,3	6,7	1,10	0,70	42	4,4	0,4	-0,5	2,00	25	5,4	0,8	19,0	12	44	1,1	7,60	0,35	1,90	306	963	8,00	11,20	9,50
JBO666	3,5	1,4	5,5	1,20	20	0,53	23	5,4	5,0	0,92	0,50	34	3,3	0,7	-0,5	1,20	22	4,3	0,6	13,0	7	36	0,8	3,90	0,22	0,92	247	1009	4,30	3,50	11,30
JBO668	3,4	1,1	6,6	1,30	35	0,51	33	8,5	6,5	1,00	0,51	38	3,3	0,9	0,7	4,60	21	5,6	1,6	23,0	21	140	1,5	14,00	0,56	3,70	200	543	0,60	0,70	0,50
JBO669	4,1	1,4	6,4	1,40	26	0,61	28	6,8	5,8	1,10	0,61	39	4,3	0,5	1,0	2,50	23	5,3	0,7	17,0	10	60	1,0	7,20	0,38	1,80	-100	560	7,10	8,80	6,70
JBO670	4,5	2,0	7,5	1,60	32	0,62	31	7,9	7,1	1,20	0,67	44	4,2	0,4	-0,5	3,30	23	5,8	1,1	22,0	12	73	1,2	7,80	0,42	1,90	238	570	9,90	10,70	11,70
JBO671	4,1	1,7	6,9	1,50	27	0,62	28	6,9	6,2	1,10	0,62	42	4,0	0,4	0,5	3,10	22	4,8	0,9	17,0	12	67	0,9	6,70	0,51	1,80	267	520	8,00	11,00	10,60
JBO672	4,1	1,6	7,1	1,50	31	0,62	31	7,6	6,8	1,20	0,62	41	4,1	0,5	0,9	3,10	25	6,0	1,3	18,0	12	75	1,1	8,00	0,46	2,10	281	808	7,10	13,10	10,00
JBO673	4,0	1,8	6,8	1,40	29	0,60	30	7,5	6,1	1,10	0,57	42	3,6	0,5	-0,5	3,90	24	5,2	1,0	19,0	11	70	1,0	7,10	0,31	1,70	147	503	8,00	12,60	12,60
JBO674	4,3	1,7	6,8	1,40	28	0,57	28	7,0	5,9	1,10	0,60	41	3,8	0,2	0,5	4,10	22	4,9	0,8	16,0	15	67	0,9	7,00	0,43	1,80	255	445	9,20	11,70	12,80
JBO675	4,1	1,7	7,1	1,50	30	0,54	30	7,3	6,3	1,10	0,61	42	3,9	1,0	-0,5	3,70	22	5,2	2,7	19,0	14	72	1,1	7,00	0,68	1,80	241	429	8,30	14,30	11,70
JBO676	4,2	1,8	7,1	1,50	27	0,57	28	6,7	6,1	1,10	0,61	40	3,7	0,2	-0,5	2,90	21	4,8	0,5	16,0	6	48	0,9	7,00	0,26	1,70	259	456	8,90	12,80	12,20
JBO679	3,5	1,5	6,3	1,20	20	0,52	22	5,2	4,9	0,95	0,52	36	3,5	0,5	-0,5	1,50	19	4,0	1,1	12,0	7	41	0,7	4,20	0,25	1,10	246	461	4,10	1,60	8,20
JBO680	3,6	1,5	6,1	1,30	21	0,55	23	5,5	5,3	0,99	0,56	37	3,6	0,4	0,7	1,20	19	4,4	0,8	13,0	6	47	0,7	4,60	0,27	1,20	182	404	10,20	1,60	6,50
JBO681	3,5	1,5	6,0	1,30	20	0,52	22	5,5	4,8	0,99	0,51	37	3,3	0,2	1,1	1,60	19	3,7	1,2	13,0	6	40									

Sample	UTM-N m	UTM-E m	SiO ₂ %	TiO ₂ %	Al ₂ O ₃ %	Fe ₂ O ₃ T	Fe ₂ O ₃	FeO	MnO	MgO	CaO	Na ₂ O	K ₂ O	H ₂ OT	CO ₂ T	P ₂ O ₅	ST	TOTAL	Mg#	Ba ppm	Co ppm	Cr ppm	Cu ppm	Ni ppm	Sc ppm	Sr ppm	V ppm	Zn ppm	Zr ppm	Ce ppm	Dy ppm
JB0722	6.850.150	654.950	53,2	2,11	12,90	16,30	5,00	10,2	0,20	3,21	7,34	2,70	1,48	1,6	-0,1	0,28	0,03	100,3	--	320	47	18	280	26	34	130	460	110	240	54	8,3
JB0723	6.850.150	654.950	53,3	1,92	13,30	16,10	4,30	10,6	0,21	3,73	7,92	2,70	1,27	1,1	-0,1	0,28	0,03	100,8	--	270	45	19	220	29	36	150	450	110	170	49	7,7
JB0724	6.841.200	656.400	53,4	1,79	13,40	15,70	3,90	10,6	0,21	3,60	7,76	2,70	1,36	1,2	-0,1	0,26	0,02	100,3	--	320	45	20	240	27	34	150	390	100	190	50	7,5
JB0725	6.843.950	654.600	53,4	2,69	12,30	18,10	6,90	10,1	0,21	1,82	6,01	2,80	1,77	1,6	-0,1	0,46	0,03	100,2	--	390	42	10	470	10	27	130	300	140	330	80	11,0
JB0726	6.845.400	652.100	53,7	2,15	13,40	15,90	5,20	9,6	0,18	2,72	7,16	2,70	1,53	1,6	0,1	0,34	0,02	100,6	--	340	44	13	320	19	30	140	400	100	250	62	8,9
JB0727	6.845.400	652.100	52,2	2,90	12,50	17,80	6,60	10,1	0,21	2,24	6,45	2,80	1,51	1,9	-0,1	0,39	0,03	99,9	--	310	47	13	380	12	31	140	360	140	290	66	9,2
JB0728	6.845.400	652.100	53,4	1,79	13,70	15,00	3,60	10,2	0,20	3,72	8,03	2,80	1,25	1,0	-0,1	0,25	0,02	100,1	--	300	43	21	220	31	34	140	430	94	170	46	7,0
JB0729	6.845.500	656.900	54,1	2,46	12,10	16,90	7,00	8,9	0,18	1,86	6,21	2,80	1,75	2,0	0,1	0,59	0,05	100,3	--	390	42	11	510	-10	28	130	240	130	340	95	13,0
JB0730	6.845.500	656.900	53,5	1,72	13,80	14,90	3,90	9,9	0,18	3,59	7,86	2,80	1,35	1,3	-0,1	0,32	0,03	100,3	--	320	42	21	250	30	32	140	460	87	180	52	6,9
JB0731	6.846.300	654.225	52,9	1,86	12,60	16,10	4,20	10,7	0,21	3,76	7,34	2,70	1,44	1,4	-0,1	0,27	0,18	99,7	--	280	46	19	240	28	36	150	410	110	190	49	7,9
JB0732	6.846.300	654.225	51,7	2,87	12,70	18,10	6,60	10,3	0,20	2,41	6,88	2,70	1,43	1,6	-0,1	0,37	0,04	99,8	--	320	48	12	390	15	30	140	460	130	260	64	9,4
JB0733	6.848.720	655.600	54,1	1,72	13,30	15,20	3,80	10,2	0,20	3,47	7,42	2,90	1,44	1,3	-0,1	0,28	0,02	100,3	--	320	42	20	270	27	33	140	390	100	210	52	8,1
JB0735	6.849.750	655.950	53,4	1,95	13,40	15,80	4,20	10,4	0,20	3,56	7,63	2,80	1,34	1,4	-0,1	0,23	0,02	100,6	--	270	46	21	220	28	34	150	430	110	170	44	7,1
JB0736	6.850.000	654.375	52,7	1,90	14,10	14,60	4,70	8,9	0,18	3,60	8,05	2,80	1,23	1,2	-0,1	0,37	0,05	100,0	--	260	45	27	270	35	32	150	520	110	170	53	6,9
JB0737	6.848.600	653.720	52,6	2,26	13,80	16,20	5,80	9,4	0,19	3,48	7,88	2,70	1,15	1,2	-0,1	0,22	0,02	100,7	--	310	47	20	210	28	34	150	570	130	160	41	7,0
JB0738	6.839.100	656.000	53,2	1,96	13,40	16,00	4,20	10,6	0,20	3,37	7,41	2,80	1,44	1,4	-0,1	0,29	0,04	100,4	--	330	48	20	280	26	33	140	440	110	210	52	8,0
JB0739	6.831.550	652.550	53,3	2,34	12,70	15,70	6,70	8,1	0,18	1,92	6,15	2,60	2,15	2,0	-0,1	0,58	0,03	98,9	--	520	47	16	340	10	30	140	440	120	340	110	10,0
JB0740	6.831.900	647.840	53,5	2,37	12,80	16,60	6,40	9,2	0,20	2,14	6,35	2,80	1,88	1,6	-0,1	0,38	0,07	99,8	--	490	45	16	350	10	30	220	420	130	310	82	9,1
JB0741	6.831.000	651.450	54,0	2,18	13,20	15,30	5,90	8,5	0,18	2,54	6,61	2,60	1,94	1,7	-0,1	0,37	0,03	99,9	--	450	46	16	290	17	32	140	500	120	270	78	8,1
JB0742	6.831.000	648.200	53,9	2,23	12,90	16,20	6,70	8,5	0,19	2,41	6,34	2,50	1,97	2,0	-0,1	0,30	0,04	100,1	--	470	47	15	260	16	33	130	540	130	270	70	7,5
JB0743	6.831.000	648.200	54,1	1,24	12,90	13,70	4,30	8,5	0,18	4,19	7,92	2,80	1,54	1,8	-0,1	0,37	0,03	100,0	--	360	45	26	270	31	39	140	320	98	220	70	7,5
JB0744	6.831.550	644.200	53,2	1,46	13,60	14,10	5,10	8,1	0,18	3,92	8,02	2,50	1,54	2,0	0,1	0,38	0,02	100,2	--	370	46	28	250	31	37	130	360	82	210	72	8,0
JB0745	6.831.550	642.820	51,5	1,88	13,10	15,60	5,70	8,9	0,20	3,91	8,18	2,40	1,42	1,7	0,1	0,39	0,03	99,6	--	330	56	25	280	33	39	140	550	94	210	73	8,8
JB0746	6.836.760	647.200	53,5	1,98	13,50	14,90	5,90	8,1	0,18	3,05	7,00	2,50	1,86	1,7	-0,1	0,35	-0,02	99,7	--	420	44	19	270	24	33	140	460	100	230	70	8,1
JB0747	6.836.950	644.500	51,4	1,52	15,80	12,80	4,20																								

Sample	Er ppm	Eu ppm	Gd ppm	Ho ppm	La ppm	Lu ppm	Nd ppm	Pr ppm	Sm ppm	Tb ppm	Tm ppm	Y ppm	Yb ppm	Ag ppm	Bi ppm	Cs ppm	Ga ppm	Hf ppm	Mo ppm	Nb ppm	Pb ppm	Rb ppm	Ta ppm	Th ppm	Tl ppm	U ppm	Cl ppm	F ppm	Au ppb	Pt ppb	Pd ppb
JB0722	4,9	1,8	7,8	1,80	23	0,75	28	6,6	6,8	1,30	0,75	50	4,9	1,3	-0,5	2,00	22	5,9	1,0	14,0	9	56	0,7	6,10	0,29	1,70	117	567	3,70	5,70	15,40
JB0723	4,4	1,9	7,0	1,60	21	0,63	26	6,4	6,4	1,10	0,65	46	4,3	0,6	0,5	2,00	22	5,2	0,8	14,0	8	50	0,8	4,80	0,24	1,30	177	532	4,40	13,20	12,50
JB0724	4,2	1,8	6,8	1,50	22	0,64	25	6,3	6,2	1,20	0,64	44	4,2	0,2	0,5	2,20	23	5,2	0,6	14,0	8	54	0,8	5,30	0,24	1,40	188	555	4,70	12,90	14,60
JB0725	6,6	2,4	11,0	2,30	36	0,93	42	10,0	10,0	1,90	0,95	67	6,5	0,5	-0,5	3,60	24	8,3	1,3	23,0	12	68	1,4	9,00	0,36	2,60	194	788	10,90	5,20	34,50
JB0726	4,9	2,1	8,7	1,80	27	0,75	31	7,8	7,5	1,40	0,74	52	4,8	0,3	-0,5	2,20	23	6,3	1,0	16,0	9	60	1,0	6,60	0,30	1,90	170	638	5,20	3,90	12,50
JB0727	5,4	2,1	9,1	1,90	30	0,83	35	8,2	8,2	1,50	0,84	56	5,4	0,3	-0,5	2,60	24	7,2	1,1	20,0	10	57	1,2	7,50	0,28	2,00	122	663	6,60	0,25	16,20
JB0728	4,1	1,7	6,6	1,50	21	0,59	24	5,8	6,0	1,10	0,60	41	3,9	-0,1	-0,5	1,80	22	4,7	0,9	12,0	7	50	0,8	4,70	0,22	1,30	184	531	3,10	13,70	9,60
JB0729	7,6	2,5	13,0	2,70	43	1,10	51	12,0	12,0	2,20	1,10	79	7,3	0,5	0,5	3,20	24	8,8	1,0	21,0	12	71	1,1	10,00	0,29	2,70	200	942	10,80	0,70	31,20
JB0730	3,9	1,7	7,1	1,40	24	0,58	27	6,5	6,3	1,10	0,62	43	3,9	0,4	0,5	1,80	21	4,8	0,6	12,0	6	50	0,6	4,90	0,24	1,30	194	534	3,90	10,60	12,30
JB0731	4,6	1,9	7,9	1,60	22	0,66	27	6,2	6,6	1,30	0,71	49	4,5	0,3	0,8	1,60	20	5,3	0,8	13,0	7	57	0,6	5,20	0,29	1,40	207	544	3,90	14,20	12,70
JB0732	5,5	2,2	9,5	2,10	29	0,82	33	7,9	8,2	1,60	0,84	57	5,3	0,3	0,6	2,30	22	6,7	1,0	17,0	8	53	0,5	6,90	0,28	1,90	118	651	9,30	2,20	24,60
JB0733	4,7	1,9	7,9	1,80	24	0,69	28	6,6	6,7	1,30	0,70	48	4,4	0,7	0,8	2,00	22	5,8	0,7	13,0	8	59	0,5	6,00	0,28	1,60	151	543	5,40	11,50	14,10
JB0734	3,2	1,5	7,4	1,20	40	0,48	40	11,0	7,6	1,10	0,50	38	3,1	0,8	-0,5	11,00	20	5,5	1,1	17,0	23	190	0,6	17,00	1,00	3,20	409	1490	4,50	2,20	3,00
JB0735	4,3	1,9	6,9	1,50	20	0,66	24	5,4	5,8	1,20	0,66	44	4,3	0,3	1,0	2,00	20	5,3	0,7	13,0	6	52	0,5	5,00	0,26	1,30	128	486	2,30	13,60	12,80
JB0736	4,0	1,7	7,4	1,50	25	0,54	29	6,5	6,8	1,10	0,58	41	3,6	0,3	0,5	2,00	21	4,4	0,7	12,0	6	47	0,5	4,80	0,23	1,20	167	567	4,50	23,10	12,00
JB0737	4,1	1,9	6,7	1,50	20	0,64	22	5,1	5,9	1,10	0,69	44	4,2	0,3	0,5	2,00	22	4,3	0,7	13,0	6	43	0,4	4,60	0,25	1,20	162	480	3,70	11,30	11,70
JB0738	4,5	2,0	8,1	1,60	23	0,71	27	6,4	6,9	1,30	0,73	46	4,5	0,5	0,5	2,00	21	5,6	0,8	14,0	8	54	0,7	5,80	0,31	1,60	212	541	4,10	10,40	14,30
JB0739	5,9	2,2	11,0	2,30	52	0,86	53	13,0	11,0	1,70	0,89	62	5,8	0,6	0,6	3,50	22	7,8	1,3	27,0	14	83	1,0	12,00	0,43	2,80	121	869	7,70	4,40	14,10
JB0740	5,0	2,2	9,3	2,00	40	0,75	41	9,5	8,5	1,50	0,79	53	5,2	0,5	0,8	3,40	22	7,7	1,2	24,0	11	71	0,8	9,40	0,45	2,10	134	699	7,60	1,10	13,70
JB0741	4,5	1,9	8,3	1,60	37	0,71	38	9,3	7,9	1,40	0,70	47	4,6	1,0	0,8	2,80	21	6,8	1,1	23,0	12	71	1,0	9,20	0,37	2,10	165	603	7,10	7,40	10,80
JB0742	4,3	1,9	7,9	1,60	34	0,69	35	8,4	7,4	1,20	0,70	46	4,4	0,3	0,5	3,30	21	6,3	1,1	22,0	12	73	0,8	9,00	0,45	2,10	192	561	10,60	14,60	19,70
JB0743	4,4	1,7	8,1	1,60	33	0,63	35	8,7	7,4	1,30	0,68	48	4,1	0,5	-0,5	1,50	20	5,3	0,7	15,0	8	60	0,8	6,90	0,26	1,50	109	571	4,40	9,90	12,40
JB0744	4,5	1,7	8,2	1,60	34	0,71	36	8,9	7,8	1,30	0,71	48	4,5	0,7	-0,5	1,70	20	5,3	0,8	17,0	9	55	0,8	7,00	0,26	1,70	160	507	6,80	19,10	12,40
JB0745	4,9	1,8	8,9	1,90	34	0,78	36	8,9	8,3	1,50	0,79	52	5,0	0,6	0,8	1,60	21	5,9	0,9	17,0	8	52	0,8	6,80	0,28	1,60	-100	578	3,30	3,50	6,10
JB0746	4,5	1,8	8,1	1,60	34	0,68	34	8,3	7,4	1,30	0,70	44	4,4	0,4	-0,5	4,10	20	5,8	1,0	21,0	11	67	1,0	8,00	0,38	1,80	126	597	6,70	13,20	19,90
JB0747	2,7	1,5	5,0	1,00	15	0,43	17	4,0	4,5	0,79	0,42	28	2,7	0,3	-0,5	0,83</															

Sample	UTM-N m	UTM-E m	SiO ₂ %	TiO ₂ %	Al ₂ O ₃ %	Fe ₂ O ₃ T %	Fe ₂ O ₃ %	FeO %	MnO %	MgO %	CaO %	Na ₂ O %	K ₂ O %	H ₂ OT %	CO ₂ T %	P ₂ O ₅ %	ST %	TOTAL %	Mg#	Ba ppm	Co ppm	Cr ppm	Cu ppm	Ni ppm	Sc ppm	Sr ppm	V ppm	Zn ppm	Zr ppm	Ce ppm	Dy ppm
JBO756	6844200	669400	53,0	1,75	14,20	14,40	3,40	9,9	0,20	3,93	8,19	2,70	1,23	0,8	-0,1	0,29	0,02	99,7	--	310	44	27	200	34	34	150	470	92	150	46	6,6
JBO757	6838750	674400	53,5	1,59	13,80	14,60	3,50	10,0	0,19	3,87	8,07	2,80	1,21	1,1	-0,1	0,26	-0,02	99,9	--	300	43	22	210	31	35	140	420	95	160	44	7,2
JBO758	6838750	674400	53,4	2,39	12,70	17,10	6,50	9,6	0,20	1,93	6,41	2,80	1,63	1,6	0,1	0,40	0,12	99,8	--	360	43	13	320	13	27	150	380	130	340	72	11,0
JBO759	6839750	673550	53,7	1,89	13,30	15,90	4,00	10,7	0,22	3,68	7,82	2,70	1,30	0,9	-0,1	0,25	0,03	100,6	--	300	46	18	220	29	35	130	440	110	180	45	7,3
JBO760	6840800	674125	53,6	2,02	13,10	15,60	4,00	10,4	0,19	3,00	7,25	2,80	1,53	1,2	-0,1	0,33	0,03	99,5	--	310	44	13	300	22	32	140	420	100	230	56	8,2
JBO761	6840800	674125	57,2	1,81	12,10	15,50	5,40	9,1	0,19	1,18	5,27	3,00	2,18	1,7	-0,1	0,55	0,06	99,8	--	400	34	-10	570	-10	22	120	60	160	510	110	16,0
JBO762	6843550	673000	52,9	1,78	14,00	14,60	3,50	10,0	0,19	3,92	8,23	2,80	1,15	0,9	-0,1	0,30	0,02	99,7	--	290	44	23	210	35	34	140	470	95	150	46	6,9
JBO763	6845450	673300	53,1	1,74	14,10	14,50	3,40	10,0	0,20	3,97	8,36	2,80	1,14	0,9	-0,1	0,25	-0,02	100,0	--	270	43	24	190	33	34	150	460	91	150	42	6,4
JBO764	6845575	674700	52,8	2,03	13,00	16,20	3,80	11,2	0,22	3,74	7,83	2,60	1,27	0,9	-0,1	0,25	-0,02	99,8	--	290	43	21	200	28	35	140	480	120	160	47	7,3
JBO765	6842200	675630	52,9	2,13	13,40	15,70	4,30	10,3	0,21	3,60	7,91	2,70	1,18	1,1	-0,1	0,24	0,02	100,1	--	310	44	22	200	28	34	140	470	110	170	43	7,2
JBO766	6843325	671350	52,1	2,07	13,30	16,20	4,30	10,7	0,23	3,55	7,75	2,60	1,18	1,4	0,5	0,22	0,04	100,0	--	270	43	20	200	27	32	140	470	110	170	43	7,1
JBO767	6845450	677950	53,0	1,88	13,90	15,10	4,10	9,9	0,20	3,98	8,28	2,70	1,13	0,9	-0,1	0,26	0,02	100,3	--	260	43	28	190	34	33	140	490	96	150	44	6,5
JBO768	6849250	670600	53,3	1,98	13,40	16,00	4,50	10,3	0,22	3,61	7,94	2,70	1,19	1,1	-0,1	0,22	-0,02	100,6	--	270	42	22	200	27	33	140	470	110	160	41	6,8
JBO770	6844150	664850	50,8	1,71	15,10	13,40	2,80	9,5	0,19	4,86	10,20	2,50	0,68	1,2	0,1	0,31	0,06	100,1	--	230	40	78	200	49	31	240	230	87	160	51	6,2
JBO771	6844900	664450	50,5	1,99	15,40	13,90	3,00	9,8	0,19	4,67	9,73	2,50	0,63	1,2	-0,1	0,21	0,10	99,9	--	230	47	49	190	46	31	230	300	98	140	39	5,4
JBO772	6842700	665250	50,1	1,97	15,10	14,40	3,50	9,8	0,20	4,61	9,68	2,50	0,67	1,7	0,2	0,31	0,16	100,6	--	280	46	25	220	47	32	230	290	99	160	51	6,2
STATISTICAL SUMMARY	Median		53,7	1,95	13,8	--	1,56	12,6	0,20	3,86	8,1	2,73	1,20	--	--	0,26	0,03	--	0,35	290	43	22	200	30	33,0	140	450	99	160	45,5	7,0
	Min.		50,9	1,61	13,4	--	1,36	11,0	0,19	1,21	5,4	2,54	0,64	--	--	0,21	0,02	--	0,14	230	34	5	190	5	22,0	120	60	87	140	39,0	5,4
	Max.		58,6	2,45	15,6	--	1,75	14,2	0,24	4,93	10,3	3,07	2,23	--	--	0,56	0,16	--	0,44	400	47	78	570	49	35,0	240	490	160	510	110,0	16,0
	S.D.		1,7	0,20	0,9	--	0,10	0,8	0,01	0,95	1,2	1,2	0,39	--	--	0,09	0,04	--	0,08	43	3	18	96	11	3,4	38	119	18	97	17,5	2,5

Table 05 – Analytical data of rock samples from the Urussanga body (RU) - Serra Geral Magmatism
(Fe₂O₃T of the samples and Fe₂O₃ e FeO of the statistical summary were respectively calculated in ferric and ferrous oxides contents).

(Cont.)

Sample	Er ppm	Eu ppm	Gd ppm	Ho ppm	La ppm	Lu ppm	Nd ppm	Pr ppm	Sm ppm	Tb ppm	Tm ppm	Y ppm	Yb ppm	Ag ppm	Bi ppm	Cs ppm	Ga ppm	Hf ppm	Mo ppm	Nb ppm	Pb ppm	Rb ppm	Ta ppm	Th ppm	Tl ppm	U ppm	Cl ppm	F ppm	Au ppb	Pt ppb	Pd ppb
JBO756	3,8	1,7	6,5	1,40	21	0,54	24	5,6	6,4	1,10	0,59	36	3,7	0,3	0,7	2,50	21	4,4	0,6	11,0	8	46	0,6	4,60	0,26	1,20	178	478	1,20	17,40	6,10
JBO757	4,2	1,8	7,1	1,50	20	0,60	24	5,7	6,2	1,20	0,67	40	4,1	0,5	-0,5	1,60	22	4,4	0,5	10,0	7	46	0,5	5,00	0,27	1,30	139	472	3,50	16,20	12,40
JBO758	6,4	2,4	10,0	2,40	34	0,93	38	9,1	10,0	1,80	0,98	60	6,1	1,2	0,9	10,00	21	8,5	1,2	19,0	11	64	1,1	9,60	0,37	2,60	245	625	6,70	1,80	14,70
JBO759	4,4	1,9	6,9	1,50	21	0,65	24	5,6	5,9	1,20	0,69	43	4,5	0,4	1,2	2,50	20	4,8	0,7	13,0	7	50	0,7	5,00	0,30	1,30	344	496	3,60	10,40	10,60
JBO760	4,6	1,9	7,8	1,60	25	0,70	29	6,9	7,0	1,30	0,73	49	4,5	0,5	0,7	2,50	21	5,7	0,7	14,0	8	59	0,7	6,00	0,29	1,60	296	563	5,70	5,10	13,80
JBO761	9,0	2,9	15,0	3,30	49	1,40	56	13,0	14,0	2,50	1,40	95	9,3	0,3	0,9	8,20	23	12,0	1,5	26,0	13	90	1,4	14,00	0,49	3,50	312	908	9,80	3,50	19,50
JBO762	3,9	1,7	6,9	1,30	22	0,57	24	5,6	6,1	1,10	0,58	40	3,7	0,5	1,2	2,20	21	4,0	0,7	12,0	6	50	0,6	4,50	0,27	1,20	143	515	2,80	15,70	10,10
JBO763	3,7	1,7	6,2	1,30	20	0,56	22	5,1	5,6	1,00	0,58	38	3,7	0,9	0,5	2,20	21	4,4	0,6	11,0	5	46	0,6	4,10	0,25	1,10	238	411	3,40	17,70	11,20
JBO764	4,2	1,8	7,0	1,50	22	0,65	24	6,0	6,5	1,20	0,66	45	4,2	0,7	1,0	2,50	22	5,1	1,0	14,0	13	55	0,7	4,90	0,28	1,30	262	457	3,60	11,20	10,50
JBO765	4,2	1,9	7,2	1,50	20	0,65	21	5,3	6,4	1,10	0,67	41	4,2	0,8	-0,5	2,40	20	4,3	1,0	13,0	7	44	0,7	4,90	0,29	1,30	219	499	4,10	10,90	10,60
JBO766	4,2	1,8	6,7	1,50	21	0,64	22	5,2	5,8	1,10	0,64	41	4,2	0,2	-0,5	3,30	21	4,5	0,8	13,0	9	46	0,7	4,70	0,27	1,30	243	451	3,90	12,70	9,90
JBO767	3,8	1,7	6,7	1,30	21	0,57	23	5,5	5,8	1,10	0,57	39	3,7	0,2	0,7	2,20	22	4,2	0,8	12,0	6	46	0,6	4,40	0,25	1,20	199	441	4,50	17,00	11,00
JBO768	4,1	1,8	6,6	1,40	19	0,60	21	5,2	5,4	1,10	0,58	41	4,0	0,2	0,7	4,60	21	4,4	0,8	12,0	6	45	0,5	4,50	0,24	1,20	200	454	3,70	10,70	11,00
JBO769	4,3	1,4	6,8	1,40	36	0,69	34	9,1	7,4	1,10	0,69	44	4,5	0,5	0,7	30,00	21	8,9	0,2	17,0	18	230	1,3	18,00	1,20	3,60	165	538	0,25	1,20	0,80
JBO770	3,4	2,0	6,9	1,30	23	0,50	27	6,1	6,4	1,10	0,51	35	3,3	0,6	-0,5	3,90	19	4,4	0,8	14,0	2	15	0,6	2,10	0,07	0,45	194	416	2,30	7,30	6,70
JBO771	3,1	1,9	5,7	1,10	18	0,45	21	5,0	5,2	0,92	0,46	32	2,8	0,2	0,8	3,50	21	4,0	0,7	14,0	-2	17	0,5	1,70	0,10	0,37	132	374	3,70	9,30	8,00
JBO772	3,5	1,9	7,1	1,30	23	0,47	28	6,4	6,6	1,10	0,51	36	3,1	0,3	0,7	2,40	21	4,3	0,8	15,0	-2	17	0,7	2,00	0,08	0,39	404	436	1,80	10,70	10,90
Median	4,1	1,8	6,9	1,4	2,10	0,60	24,0	5,6	6,3	1,10	0,62	40,5	4,0	0,4	0,70	2,5	21,0	4,4	0,8	13,0	7	46	0,6	4,65	0,27	1,25	228	464	3,60	10,80	10,70
Min.	3,1	1,7	5,7	1,1	18,0	0,45	21,0	5,0	5,2	0,92	0,46	32,0	2,8	0,2	0,25	1,6	19,0	4,0	0,5	10,0	1	15	0,5	1,70	0,07	0,37	132	374	1,20	1,80	6,10
Max.	16,0	2,9	15,0	3,3	49,0	1,40	56,0	14,0	14,0	2,50	1,40	95,0	9,3	1,20	1,20	10,0	23,0	12,0	1,5	26,0	13	90	1,4	14,00	0,49	3,50	404	908	9,80	17,70	19,50
S.D.	2,5	0,3	2,2	1,4	17,5	0,23	8,9	2,2	2,2	0,39	0,23	14,9	1,5	0,3	0,32	2,3	0,9	2,1	0,3	3,8	4	19	0,2	2,98	0,10	0,78	76	124	2,10	4,90	3,20

Table 05 – Continued

Sample	UTM-N m	UTM-E m	SiO ₂ %	TiO ₂ %	Al ₂ O ₃ %	Fe ₂ O ₃ T %	Fe ₂ O ₃ %	FeO %	MnO %	MgO %	CaO %	Na ₂ O %	K ₂ O %	H ₂ OT %	CO ₂ T %	P ₂ O ₅ %	ST %	TOTAL %	Mg#	Ba ppm	Co ppm	Cr ppm	Cu ppm	Ni ppm	Sc ppm	Sr ppm	V ppm	Zn ppm	Zr ppm	Ce ppm	Dy ppm
JBO682	6996150	639700	49,4	3,81	11,60	17,00	5,20	10,6	0,26	3,09	6,79	2,60	1,98	2,0	0,5	1,75	0,16	100,0	--	690	44	13	35	-10	21	420	71	150	350	140	13,0
JBO683	6999500	636500	49,3	4,02	12,40	16,00	4,10	10,7	0,23	2,90	8,08	2,90	1,92	1,0	0,1	2,32	0,10	100,2	--	640	44	13	44	-10	20	500	110	140	320	140	14,0
JBO684	6996100	641920	48,6	3,95	11,90	16,50	5,40	10,0	0,23	2,90	7,84	2,70	1,97	1,4	0,1	2,44	0,12	99,7	--	700	44	14	43	-10	20	460	100	150	330	150	14,0
JBO685	7001150	640800	52,2	2,93	12,70	14,70	3,30	10,3	0,22	3,59	7,35	2,90	1,87	0,9	0,1	1,29	0,07	99,9	--	610	41	-10	46	-10	24	480	110	130	300	110	10,0
JBO686	6979000	601700	51,3	2,04	13,30	16,00	4,50	10,4	0,23	4,70	8,41	2,60	1,18	1,2	0,2	0,24	-0,02	100,4	--	440	49	44	190	43	37	180	470	110	180	54	6,3
JBO687	6981850	600750	51,3	2,00	13,40	15,90	4,60	10,2	0,23	4,69	8,45	2,50	1,17	1,2	-0,1	0,22	-0,02	100,1	--	480	48	38	170	42	35	180	460	110	170	50	6,0
JBO688	6992650	658650	50,5	3,38	12,50	15,30	3,30	10,8	0,22	3,37	7,73	2,80	1,85	0,9	0,1	1,69	0,07	99,5	--	670	43	10	66	-10	22	490	150	140	300	120	12,0
JBO689	6889450	656850	50,7	3,64	12,00	16,20	4,90	10,2	0,24	2,94	6,67	2,80	2,11	2,1	0,3	1,66	0,16	100,5	--	700	42	-10	37	-10	22	400	68	160	350	130	12,0
JBO690	6998350	601050	49,5	3,52	12,10	15,40	5,10	9,3	0,21	2,75	8,01	2,70	2,04	1,6	0,1	2,53	0,11	99,8	--	670	42	-10	71	-10	20	470	85	160	360	170	15,0
JBO691	6993950	603740	51,2	2,68	13,80	14,00	3,40	9,5	0,18	3,16	7,53	2,90	1,91	2,1	0,2	1,28	0,08	100,1	--	630	50	25	220	28	27	410	270	130	270	130	11,0
JBO692	6995250	603350	51,1	3,19	13,50	14,30	4,30	9,0	0,18	3,95	6,91	2,90	1,91	2,2	0,1	0,98	0,05	100,3	--	520	60	65	210	59	26	310	360	130	280	110	10,0
JBO693	6990900	589000	52,3	1,11	14,80	12,00	3,00	8,1	0,17	6,23	10,45	2,40	0,87	0,8	-0,1	0,14	-0,02	100,4	--	220	44	94	150	64	39	160	310	70	120	27	4,5
JBO694	7011200	592950	49,5	3,47	12,10	15,40	5,10	9,3	0,21	2,82	8,12	2,70	2,06	1,6	-0,1	2,61	0,14	99,8	--	640	44	10	47	-10	20	470	75	150	360	170	15,0
JBO695	7008500	594200	53,9	2,33	13,50	12,60	3,50	8,2	0,17	4,32	5,96	3,10	2,16	1,9	-0,1	0,78	0,09	100,0	--	510	45	61	170	58	26	270	330	120	260	110	9,3
JBO696	7012300	599350	49,1	3,64	11,90	15,70	5,20	9,4	0,21	2,80	7,96	2,70	1,98	1,7	0,1	2,48	0,12	99,5	--	640	46	10	42	-10	20	450	90	150	350	160	14,0
JBO697	7007500	599050	49,5	3,96	12,10	15,40	5,00	9,3	0,20	2,80	7,65	2,70	2,01	1,6	0,1	2,16	0,11	99,4	--	660	48	10	41	-10	21	470	85	150	360	160	14,0
JBO698	7005900	595600	52,0	1,99	13,20	16,70	4,70	10,8	0,23	3,95	8,15	2,70	1,12	1,2	-0,1	0,22	0,02	100,3	--	320	48	20	220	31	36	130	500	120	150	40	7,1
JBO699	7005400	593000	49,4	3,53	12,00	15,50	4,80	9,6	0,21	3,01	8,23	2,70	2,01	1,5	-0,1	2,58	0,12	99,8	--	610	41	10	39	-10	20	470	77	140	330	160	14,0
JBOT00	7002600	586050	51,8	1,04	15,40	11,20	2,60	7,7	0,16	6,26	10,76	2,40	0,78	0,8	-0,1	0,13	-0,02	99,8	--	200	39	78	140	63	34	180	270	59	96	24	4,0
JBOT01	6997600	591300	49,1	3,79	12,00	15,90	5,40	9,4	0,22	2,71	8,11	2,70	2,00	1,5	0,1	2,59	0,13	99,9	--	650	45	10	58	-10	20	470	86	160	330	170	14,0
JBOT02	7006900	584100	51,4	1,21	14,40	12,50	2,60	8,9	0,18	6,43	10,21	2,40	0,75	1,1	-0,1	0,13	-0,02	99,8	--	230	43	66	140	61	35	140	320	70	110	25	4,3
JBOT03	6995600	590600	52,6	2,17	13,20	16,80	4,50	11,1	0,23	3,66	7,47	2,70	1,23	1,2	0,1	0,22	0,03	100,5	--	370	46	20	190	27	34	180	520	120	160	45	7,3
JBOT04	6996300	593900	50,5	3,80	12,10	15,60	5,20	9,4	0,21	2,89	7,53	2,70	2,08	1,5	-0,1	2,14	0,15	100,3	--	620	43	12	44	-10	21	440	74	150	370	160	15,0
JBOT05	7039250	654130	51,4	2,79	13,50	14,80	4,10	9,6	0,20	4,13	7,83	2,60	1,72	1,6	-0,1	0,51	0,07	100,3	--	500	44	19	170	32	27	360	400	110	240	79	7,3
JBOT06	7039250	654130	50,4	2,50	14,00	14,90	4,10	9,7	0,19	4,12	7,30	2,50	1																		

Sample	Er ppm	Eu ppm	Gd ppm	Ho ppm	La ppm	Lu ppm	Nd ppm	Pr ppm	Sm ppm	Tb ppm	Tm ppm	Y ppm	Yb ppm	Ag ppm	Bi ppm	Cs ppm	Ga ppm	Hf ppm	Mo ppm	Nb ppm	Pb ppm	Rb ppm	Ta ppm	Th ppm	Tl ppm	U ppm	Cl ppm	F ppm	Au ppb	Pt ppb	Pd ppb
JBO682	5,9	5,0	18,0	2,40	61	0,68	85	19,0	17,0	2,40	0,77	63	4,7	1,0	-0,5	1,30	25	8,1	2,2	43,0	7	53	2,1	5,70	0,19	1,40	253	1801	0,25	0,25	1,70
JBO683	6,0	5,7	20,0	2,50	65	0,65	95	21,0	19,0	2,60	0,77	67	4,3	-0,1	0,5	1,20	25	7,9	2,2	39,0	6	49	2,1	5,10	0,15	1,30	181	2307	1,50	0,25	0,25
JBO684	6,4	5,7	19,0	2,60	67	0,65	99	22,0	20,0	2,70	0,83	69	4,7	0,8	-0,5	1,00	25	8,1	2,1	39,0	6	51	2,1	5,50	0,19	1,40	233	2079	1,50	0,25	0,25
JBO685	4,7	4,2	14,0	2,00	50	0,58	69	15,0	14,0	1,90	0,68	54	3,7	0,5	1,0	1,30	25	7,1	1,4	30,0	6	50	1,7	4,80	0,17	1,20	227	1733	0,50	0,25	1,10
JBO686	3,8	1,7	6,7	1,30	25	0,53	29	6,6	6,0	1,00	0,52	38	3,3	0,2	1,1	0,99	21	4,3	0,6	14,0	6	37	0,7	3,60	0,19	0,79	161	498	4,20	3,50	10,40
JBO687	3,4	1,6	6,1	1,30	23	0,46	25	6,0	5,4	0,98	0,51	36	3,1	0,5	0,7	0,89	20	4,5	0,8	13,0	5	37	0,7	3,30	0,16	0,71	140	543	3,20	7,10	13,50
JBO688	5,3	4,6	17,0	2,20	53	0,58	77	17,0	16,0	2,10	0,71	58	3,9	-0,1	1,0	1,20	24	7,3	1,5	32,0	6	47	1,8	4,80	0,15	1,20	116	1571	6,40	0,25	0,25
JBO689	5,5	4,7	17,0	2,30	57	0,60	81	17,0	17,0	2,20	0,77	59	4,2	0,5	0,9	1,70	24	8,2	1,7	40,0	7	59	1,9	5,70	0,25	1,50	256	1917	3,80	0,25	2,50
JBO690	6,8	5,5	22,0	2,80	79	0,71	110	24,0	23,0	2,90	0,87	75	4,9	-0,1	-0,5	1,90	24	8,5	1,7	39,0	8	56	2,3	6,10	0,25	1,50	202	2277	0,60	0,25	0,25
JBO691	5,4	3,8	16,0	2,20	59	0,61	83	18,0	17,0	2,10	0,70	58	3,9	0,2	-0,5	2,10	26	6,5	1,2	26,0	6	57	1,5	5,40	0,24	1,60	604	1505	3,60	5,40	9,80
JBO692	5,0	3,0	14,0	2,00	52	0,60	67	16,0	15,0	1,90	0,66	53	4,0	0,4	0,8	2,50	24	7,6	1,3	26,0	10	72	1,4	6,50	0,30	2,00	324	1138	3,60	6,30	7,20
JBO693	2,6	1,1	4,5	0,94	12	0,36	15	3,4	3,6	0,67	0,38	30	2,4	0,7	1,2	1,60	18	3,1	0,7	6,4	4	37	0,5	2,70	0,15	0,76	177	475	3,40	8,50	9,90
JBO694	6,5	5,5	20,0	2,80	80	0,76	110	25,0	23,0	2,90	0,85	75	5,2	0,2	-0,5	1,30	25	8,5	1,9	40,0	7	54	2,1	6,00	0,18	1,40	186	2088	0,25	0,60	1,70
JBO695	4,6	2,5	11,0	1,80	49	0,62	59	14,0	12,0	1,60	0,67	52	4,2	0,2	-0,5	3,20	23	6,8	0,8	21,0	11	81	1,2	7,60	0,30	2,10	197	1122	3,00	6,50	5,90
JBO696	6,2	5,6	19,0	2,70	76	0,74	100	24,0	22,0	2,70	0,83	73	5,2	0,1	-0,5	1,20	25	8,2	1,9	41,0	7	52	2,4	5,70	0,20	1,30	238	2200	0,80	0,25	1,00
JBO697	6,1	5,2	19,0	2,50	72	0,71	97	23,0	20,0	2,60	0,81	71	5,1	0,5	-0,5	1,40	26	8,3	2,4	45,0	7	53	2,7	5,50	0,18	1,30	222	2276	0,25	0,25	0,25
JBO698	4,1	1,7	6,4	1,40	18	0,61	21	5,2	5,7	1,10	0,58	42	4,1	0,2	-0,5	1,90	22	4,1	0,3	11,0	6	43	0,7	4,00	0,22	1,00	127	420	4,70	12,10	12,10
JBO699	6,3	5,4	19,0	2,60	73	0,70	100	23,0	21,0	2,60	0,87	73	4,8	0,2	-0,5	1,10	24	7,8	1,9	40,0	6	53	2,3	5,20	0,18	1,30	174	2202	0,25	0,25	0,90
JBOT00	2,2	1,1	3,6	0,81	11	0,30	13	3,1	3,1	0,63	0,32	23	2,3	0,2	0,5	1,50	18	2,8	0,4	6,3	4	31	0,4	2,50	0,14	0,71	118	461	2,00	9,80	8,60
JBOT01	6,4	5,6	20,0	2,70	79	0,71	110	25,0	23,0	2,80	0,86	77	5,1	0,1	-0,5	1,20	25	8,0	2,1	43,0	8	55	2,6	5,50	0,15	1,30	130	2150	0,25	0,25	0,25
JBOT02	2,4	1,1	3,8	0,90	11	0,36	14	3,2	3,4	0,67	0,36	25	2,5	0,5	0,6	2,50	18	3,0	0,4	6,8	6	32	0,4	2,70	0,13	0,78	748	398	2,20	7,40	6,90
JBOT03	4,4	1,9	6,7	1,50	20	0,61	24	5,5	5,9	1,10	0,64	44	4,3	0,7	1,0	2,10	23	4,9	0,9	13,0	7	49	0,7	4,60	0,22	1,30	188	470	2,80	10,50	12,00
JBOT04	6,5	5,6	19,0	2,60	74	0,76	98	23,0	21,0	2,70	0,85	71	5,1	0,1	-0,5	1,20	25	8,7	2,2	45,0	8	58	2,6	6,00	0,19	1,40	182	1805	1,30	0,25	1,30
JBOT05	3,8	2,8	8,6	1,50	36	0,49	43	10,0	9,7	1,30	0,52	40	3,6	0,3	-0,5	1,50	23	6,5	1,0	25,0	7	49	1,3	4,60	0,25	1,10	258	1039	3,10	9,20	9,70
JBOT06	4,0	2,8	8,0	1,50	34	0,55	37	9,0	8,3	1,30	0,57	42	3,7	0,1	-0,5	2,00	26	5,7	0,9	20,0	8	45	1,1	4,30	0,19	1,00	211	565	7,20	10,70	11,30
JBOT07	4,6	2,8	10,0	1,80	37	0,64	46	11,0	11,0	1,50	0,70	48	4,4	0,4	-0,5	1,70	24	7,2</td													

Informe de Recursos Minerais

Sample	UTM-N m	UTM-E m	SiO ₂ %	TiO ₂ %	Al ₂ O ₃ %	Fe ₂ O ₃ T %	Fe ₂ O ₃ %	FeO %	MnO %	MgO %	CaO	Na ₂ O %	K ₂ O %	H ₂ OT %	CO ₂ T %	P ₂ O ₅ %	ST %	TOTAL	Mg#	Ba ppm	Co ppm	Cr ppm	Cu ppm	Ni ppm	Sc ppm	Sr ppm	V ppm	Zn ppm	Zr ppm	Ce ppm	Dy ppm
CL-1-B	7.278.877	509.368	51,8	3,62	12,90	15,00	2,10	11,6	0,23	3,85	7,68	3,00	1,51	0,8	0,1	0,72	0,22	100,1	--	550	63	12	26	-10	28	400	330	110	290	88	8,6
CL-1-C	7.278.877	509.368	49,5	3,46	12,10	16,20	4,50	10,5	0,24	3,45	7,09	2,90	1,58	2,8	0,2	1,04	0,16	99,6	--	520	66	15	70	-10	25	320	350	130	350	130	10,0
CL-1-D	7.279.141	509.248	50,4	3,19	13,10	14,80	6,00	7,9	0,21	2,82	6,98	3,00	1,82	2,9	0,2	0,92	0,20	99,6	--	570	64	22	100	11	22	370	370	130	390	110	9,7
CL-1-E	7.279.581	509.202	55,1	1,52	11,90	15,00	--	--	0,19	1,02	4,25	2,70	3,29	--	0,7	0,64	1,88	98,3	--	840	29	21	200	-10	14	340	18	160	740	190	15,0
CL-2-A	7.279.607	509.331	51,2	2,09	11,50	16,10	--	--	0,20	3,01	6,25	2,50	2,05	--	0,3	0,92	1,24	97,4	--	630	49	19	60	-10	23	330	230	160	410	120	10,0
CL-2-B	7.279.607	509.331	46,5	2,88	12,20	16,80	--	--	0,24	3,70	7,79	2,80	1,55	--	0,7	0,90	1,07	97,2	--	470	67	24	120	-10	26	350	470	160	290	110	9,4
CL-2-C	7.279.607	509.331	54,5	1,89	12,50	15,20	6,20	8,1	0,21	0,97	5,23	2,90	2,78	2,9	0,2	1,08	0,27	99,7	--	870	35	18	290	-10	14	460	20	190	650	180	14,0
CL-2-D	7.279.607	509.331	59,1	1,21	12,40	11,90	6,00	5,3	0,17	0,72	3,51	3,20	3,83	3,0	0,1	0,47	0,18	99,2	--	920	23	19	140	-10	11	370	11	150	800	190	14,0
CL-2-E	7.279.607	509.331	57,4	1,50	12,00	13,60	6,60	6,3	0,20	0,86	4,29	3,00	3,27	3,1	0,3	0,72	0,11	99,6	--	910	29	19	210	-10	13	420	13	170	830	200	16,0
CL-2-F	7.279.607	509.331	56,5	1,65	12,00	14,30	6,30	7,2	0,21	1,09	4,59	2,90	3,19	2,9	0,1	0,81	0,12	99,5	--	920	34	21	240	-10	13	410	25	160	710	190	15,0
CL-2-H	7.279.607	509.331	56,7	1,40	12,00	14,20	7,20	6,3	0,21	0,79	3,99	3,00	3,33	3,4	0,1	0,62	0,27	99,3	--	970	28	16	170	-10	12	400	11	180	810	210	16,0
CL-2-I	7.279.607	509.331	47,7	2,91	12,60	17,40	7,60	8,8	0,23	3,12	7,03	2,50	1,65	4,5	0,2	0,84	0,10	99,8	--	540	66	13	120	-10	23	360	390	140	320	110	9,1
CL-3	7.275.549	516.198	48,7	3,39	13,20	16,00	5,30	9,6	0,20	4,43	8,44	2,50	1,34	1,8	0,2	0,59	0,35	100,0	--	400	77	57	230	40	30	370	580	100	240	88	7,4
CL-4	7.281.457	515.224	50,3	3,42	13,00	14,60	5,00	8,7	0,19	3,39	7,52	2,80	1,79	2,0	0,2	1,07	0,13	99,5	--	560	73	18	110	16	25	380	360	120	370	130	11,0
CL-5	7.281.726	517.788	49,4	2,92	13,10	16,20	5,20	9,9	0,20	4,29	8,49	2,30	1,19	2,0	0,3	0,52	0,17	100,0	--	400	71	43	170	63	28	200	380	100	270	94	7,3
CL-6-B	7.285.755	510.561	52,6	1,95	13,50	14,70	6,30	7,6	0,19	1,82	6,39	2,40	1,88	3,7	0,2	0,73	0,06	99,2	--	480	42	10	450	-10	22	260	110	130	530	130	16,0
CL-7	7.288.627	518.367	49,7	2,11	14,50	14,30	4,70	8,6	0,17	4,81	8,95	2,40	1,22	2,1	0,1	0,44	0,05	99,9	--	400	64	99	380	67	30	300	400	90	210	75	7,2
CL-8-A	7.275.550	513.867	48,9	3,69	13,60	15,70	6,00	8,7	0,21	3,14	7,30	3,00	1,56	2,4	0,2	0,95	0,15	99,8	--	460	71	-10	140	-10	23	380	380	120	350	120	9,7
CL-8-B	7.275.550	513.867	58,6	1,38	12,30	12,60	5,70	6,2	0,19	0,72	4,10	3,10	3,52	2,8	0,1	0,62	0,16	99,5	--	980	23	-10	170	-10	12	380	12	160	820	220	17,0
CL-8-C	7.275.550	513.867	48,5	2,87	13,00	16,30	7,20	8,1	0,23	3,20	7,21	2,80	1,52	3,9	0,2	0,90	0,06	99,7	--	430	56	12	71	-10	23	370	340	130	290	100	8,6
CL-10-A	7.264.311	510.485	50,1	3,27	12,70	15,30	5,00	9,2	0,22	3,67	7,52	2,80	1,77	2,3	0,1	0,89	0,13	99,6	--	570	63	15	99	13	27	370	350	120	330	110	9,4
CL-10-B	7.264.311	510.485	51,1	2,68	12,40	15,70	7,60	7,3	0,24	1,99	6,42	2,80	2,27	3,5	0,1	1,44	0,26	100,1	--	640	49	12	94	-10	17	380	160	160	510	170	14,0
CL-12-A	7.383.212	616.666	46,5	3,20	12,60	18,40	10,30	7,3	0,18	4,40	8,53	2,10	1,19	2,5	0,1	0,48	0,08	99,5	--	370	80	13	370	61	35	240	850	89	220	72	7,1
CL-12-B	7.383.212	616.666	49,2	2,04	15,20	13,20	4,80	7,5	0,16	4,95	9,19	2,40	1,13	2,4	0,3	0,45	0,13	99,9	--	400	66	120	300	99	28	310	350	85	200	67	6,2
CL-12-C	7.383.212	616.666	49,6	2,25	14,90	13,60	3,60	9,0</td																							

Sample	Er ppm	Eu ppm	Gd ppm	Ho ppm	La ppm	Lu ppm	Nd ppm	Pr ppm	Sm ppm	Tb ppm	Tm ppm	Y ppm	Yb ppm	Ag ppm	Bi ppm	Cs ppm	Ga ppm	Hf ppm	Mo ppm	Nb ppm	Pb ppm	Rb ppm	Ta ppm	Th ppm	Tl ppm	U ppm	Cl ppm	F ppm	Au ppb	Pt ppb	Pd ppb
CL-1-B	4,4	3,6	11,0	1,70	41	0,55	50	12,0	11,0	1,60	0,63	52	3,8	0,5	-0,5	1,60	25	6,9	1,3	41,0	9	39	4,9	3,90	0,25	0,82	392	881	1,00	0,25	0,60
CL-1-C	5,5	3,3	13,0	2,10	58	0,69	71	17,0	14,0	1,90	0,71	62	4,5	1,4	-0,5	0,57	25	8,2	1,6	30,0	7	37	1,6	5,20	0,09	1,00	157	1103	0,25	0,25	0,25
CL-1-D	5,1	3,1	12,0	1,90	54	0,65	63	15,0	13,0	1,70	0,64	57	4,1	1,5	0,6	1,20	27	9,1	1,8	27,0	13	43	1,5	5,90	0,17	1,20	182	1050	1,00	0,25	0,25
CL-1-E	8,6	4,7	18,0	3,10	91	1,20	110	25,0	20,0	2,60	1,10	89	7,2	1,3	0,8	3,10	30	17,0	2,5	51,0	10	80	2,8	11,00	0,35	2,20	407	1085	0,25	0,25	0,25
CL-2-A	5,8	3,7	13,0	2,10	57	0,78	68	16,0	13,0	1,90	0,76	62	4,9	0,9	1,0	1,40	25	10,0	1,5	30,0	40	50	1,6	6,30	0,18	1,40	212	1594	0,25	0,25	0,70
CL-2-B	5,0	3,1	12,0	1,90	50	0,63	62	15,0	13,0	1,70	0,66	57	4,0	0,6	2,2	1,50	26	7,3	1,5	22,0	8	37	1,3	4,50	0,23	0,90	219	1799	0,60	0,60	0,25
CL-2-C	7,4	4,6	17,0	2,70	90	0,93	100	25,0	19,0	2,50	1,00	85	6,1	0,3	0,5	2,50	29	13,0	2,5	48,0	14	68	2,2	9,40	0,21	1,90	320	1562	0,25	0,25	0,25
CL-2-D	7,8	4,0	16,0	2,80	94	1,00	98	25,0	19,0	2,40	1,00	84	6,8	1,3	0,5	2,70	30	17,0	2,3	47,0	23	98	2,1	13,00	0,26	2,40	167	1628	0,25	0,25	0,25
CL-2-E	8,6	4,5	18,0	3,10	100	1,10	110	27,0	21,0	2,70	1,10	93	7,2	0,7	0,7	3,20	30	18,0	2,5	53,0	10	82	2,7	12,00	0,22	2,40	273	1682	0,50	0,25	0,25
CL-2-F	7,5	4,6	18,0	2,90	87	0,95	100	24,0	20,0	2,90	1,10	83	6,6	0,8	0,8	2,60	29	16,0	2,5	48,0	11	75	2,1	9,50	0,24	2,10	240	1367	0,25	0,25	0,80
CL-2-H	8,2	4,5	20,0	3,20	97	1,10	110	26,0	22,0	3,10	1,20	89	7,5	1,7	0,8	3,40	29	18,0	2,8	54,0	12	81	2,4	11,00	0,23	2,50	380	1820	0,25	0,25	0,25
CL-2-I	4,4	3,4	12,0	1,80	48	0,58	62	14,0	13,0	1,80	0,63	53	4,0	0,5	0,9	1,50	27	8,0	1,5	27,0	7	40	1,4	4,70	0,19	1,10	229	1005	0,25	0,25	0,25
CL-3	3,6	2,6	9,5	1,40	39	0,49	50	11,0	10,0	1,40	0,51	43	3,3	1,3	1,4	0,47	24	7,3	1,1	24,0	4	30	1,6	3,40	0,09	0,77	180	829	1,60	0,25	0,25
CL-4	5,4	3,6	15,0	2,20	60	0,67	76	17,0	16,0	2,20	0,74	62	4,6	1,7	0,8	0,76	25	9,1	1,3	30,0	5	41	1,7	4,90	0,17	1,10	211	1270	0,25	0,25	0,25
CL-5	3,4	2,7	9,5	1,40	42	0,45	51	12,0	10,0	1,40	0,48	40	3,1	1,7	0,7	1,30	21	7,0	1,0	23,0	8	32	1,2	3,90	0,10	0,90	206	834	3,20	0,25	0,90
CL-6-B	8,4	3,7	18,0	3,20	57	1,30	74	17,0	2,90	1,30	0,94	8,6	0,7	1,3	1,40	26	13,0	1,8	34,0	14	49	1,8	6,70	0,15	1,60	238	998	3,40	1,30	3,00	
CL-7	3,8	2,2	8,2	1,50	35	0,56	40	9,7	8,3	1,40	0,57	43	3,7	0,6	1,0	0,96	22	6,1	0,9	19,0	5	33	1,0	3,80	0,17	0,87	150	638	5,30	12,10	13,2
CL-8-A	4,7	3,3	13,0	1,90	51	0,60	68	16,0	14,0	1,90	0,68	55	4,2	0,6	1,0	1,00	26	9,2	1,3	28,0	5	35	1,7	5,10	0,12	1,20	231	1156	2,30	0,25	0,50
CL-8-B	8,5	4,7	20,0	3,40	100	1,10	120	29,0	23,0	3,20	1,20	98	7,8	1,4	0,9	1,90	30	19,0	2,7	56,0	12	85	2,4	11,00	0,20	2,40	222	1549	1,60	0,25	0,60
CL-8-C	4,1	3,7	11,0	1,70	46	0,55	59	14,0	12,0	1,70	0,60	49	3,8	0,7	1,0	1,30	25	7,2	1,4	28,0	4	33	1,7	4,30	0,11	0,93	178	1062	2,70	0,25	0,50
CL-10-A	4,6	3,3	12,0	1,80	50	0,61	63	15,0	13,0	1,80	0,65	54	4,3	0,4	1,0	0,84	23	8,6	1,4	28,0	4	42	1,7	4,50	0,10	1,00	205	1070	2,00	0,25	0,25
CL-10-B	6,4	4,7	17,0	2,60	77	0,83	95	23,0	20,0	2,60	0,92	75	5,7	0,5	1,0	1,20	26	12,0	2,2	38,0	7	50	2,3	7,20	0,21	1,60	239	1559	1,40	0,25	0,25
CL-12-A	3,8	2,0	8,1	1,50	32	0,53	39	9,3	8,3	1,30	0,56	43	3,7	0,9	0,8	3,10	23	6,1	1,0	18,0	3	32	1,2	3,70	0,10	0,83	175	642	6,60	12,80	27,20
CL-12-B	3,4	2,0	7,5	1,30	31	0,48	37	8,8	7,7	1,20	0,51	37	3,4	0,5	1,0	0,53	20	6,2	1,2	16,0	3	28	1,1	3,40	0,11	0,82	203	654	4,90	10,20	10,40
CL-12-C	3,1	1,9	6,8	1,20	28	0,44	33	7,8	7,0	1,10	0,45	34	2,9	0,6	0,6	0,79	21	4,7	0,7	16,0	5	27	0,9	2,90	0,11	0,66	191	608	4,50	5,80	7,80
CL-12-D	4,4	2,5	9,8	1,70	37	0,65	46	11,0	9,7	1,50	0,68	49	4,4																		

Sample	UTM-N m	UTM-E m	SiO ₂ %	TiO ₂ %	Al ₂ O ₃ %	Fe ₂ O ₃ T %	Fe ₂ O ₃ %	FeO %	MnO %	MgO %	CaO %	Na ₂ O %	K ₂ O %	H ₂ OT %	CO ₂ T %	P ₂ O ₅ %	ST %	TOTAL %	Mg#	Ba ppm	Co ppm	Cr ppm	Cu ppm	Ni ppm	Sc ppm	Sr ppm	V ppm	Zn ppm	Zr ppm	Ce ppm	Dy ppm
CL-6-A	7.285.755	510.561	49,4	2,64	12,30	15,40	4,80	9,5	0,21	6,25	8,17	2,20	1,44	2,2	0,2	0,63	0,04	100,0	--	460	65	43	410	39	37	330	470	120	260	78	10,0
CL-9	7.251.476	514.116	49,5	3,60	13,00	15,40	4,30	10,0	0,19	3,88	7,98	2,60	1,58	1,7	0,1	0,84	0,05	99,4	--	500	73	28	170	29	27	370	500	110	280	100	8,6
CL-11	7.283.950	547.793	50,8	2,34	14,00	14,70	4,00	9,6	0,19	4,50	8,66	2,40	1,44	1,6	0,1	0,39	0,04	100,1	--	520	63	84	360	55	31	310	430	98	240	80	6,7
CL-17-B	7.388.509	611.565	50,2	2,91	13,50	15,10	4,10	9,9	0,21	4,54	9,24	2,40	0,66	2,1	0,1	0,31	0,04	100,2	--	220	58	85	260	45	36	340	440	96	210	52	7,2
CL-22-A	7.403.558	668.784	50,4	2,10	13,40	14,90	5,40	8,5	0,20	5,09	8,81	2,80	1,14	1,5	0,2	0,35	0,02	100,0	--	360	54	86	280	60	34	260	410	79	200	59	6,9
CL-22-B	7.403.558	668.784	50,8	2,19	14,40	14,60	5,50	8,2	0,18	3,64	8,50	2,60	1,18	2,4	0,2	0,36	0,07	100,2	--	360	52	40	360	38	29	270	380	87	220	64	6,9
CL-22-C	7.403.558	668.784	49,7	2,01	13,40	15,10	5,00	9,1	0,21	5,67	9,65	2,40	0,81	1,4	0,2	0,22	0,02	99,9	--	290	55	77	220	61	36	260	430	83	140	39	5,2
CL-22-D	7.403.558	668.784	50,8	3,26	12,90	14,70	5,50	8,3	0,19	4,27	7,59	2,80	2,01	1,4	0,2	0,59	0,02	99,9	--	460	56	35	250	54	25	350	500	84	360	110	8,8
CL-23-A	7.404.327	668.026	50,1	2,02	14,00	14,50	5,00	8,6	0,19	4,69	8,93	2,60	1,06	1,8	0,1	0,33	0,03	99,4	--	380	53	68	310	53	31	250	390	79	200	56	6,5
CL-23-C	7.404.327	668.026	49,0	2,09	13,40	15,50	6,00	8,6	0,22	5,50	9,48	2,40	0,85	2,2	0,3	0,24	0,02	100,2	--	260	58	66	240	60	35	240	440	84	150	43	5,3
CL-24	7.410.276	664.362	51,3	2,63	13,50	15,30	4,70	9,6	0,20	4,06	8,71	2,50	0,98	1,4	0,1	0,40	0,05	100,1	--	270	60	61	360	48	35	200	470	97	220	63	9,2
CL-25-A	7.419.450	656.706	49,2	4,15	13,10	15,90	5,10	9,7	0,20	3,71	7,82	2,70	1,08	2,5	0,2	0,46	0,06	99,9	--	510	65	20	110	22	25	430	510	98	260	78	7,1
CL-26-A	7.418.621	655.921	50,5	2,51	13,20	15,80	5,20	9,5	0,22	4,22	8,79	2,50	1,03	1,5	0,2	0,36	0,03	99,8	--	280	55	66	320	43	35	210	450	92	220	59	8,7
CL-26-B	7.418.621	655.921	49,6	2,45	13,60	15,40	9,00	5,7	0,16	4,72	8,52	2,50	1,03	2,4	0,1	0,29	0,01	100,1	--	420	49	64	160	42	35	210	440	90	200	48	8,2
CL-28-A	7.414.113	653.909	50,3	3,61	13,20	14,90	5,20	8,7	0,20	3,38	7,45	2,70	1,84	2,2	0,1	0,95	0,04	99,9	--	680	55	26	170	30	21	440	350	110	340	110	9,0
CL-28-B	7.414.113	653.909	50,3	2,38	13,80	14,30	4,90	8,5	0,20	4,77	8,97	2,40	1,13	2,1	0,2	0,31	0,10	100,0	--	400	55	77	280	57	34	270	430	85	200	56	6,3
CL-30	7.412.676	648.080	50,6	2,50	13,20	15,40	5,60	8,8	0,19	3,96	8,38	2,40	1,22	2,4	0,1	0,43	0,02	99,8	--	420	57	69	410	44	33	230	420	99	230	67	8,0
CL-35	7.424.370	644.928	50,3	3,98	13,20	14,30	4,30	9,0	0,18	3,67	7,54	2,60	1,48	2,5	0,2	0,53	0,05	99,5	--	580	61	34	60	33	23	470	480	100	320	85	7,6
CL-36	7.423.867	644.625	50,6	3,46	12,60	14,20	6,20	7,2	0,18	4,29	6,85	2,40	2,15	3,0	0,2	0,69	0,09	99,9	--	670	62	68	94	48	23	330	430	96	360	110	8,8
CL-37	7.422.550	645.199	50,7	2,26	14,40	14,60	6,00	7,8	0,17	4,12	8,52	2,60	1,31	2,1	0,2	0,36	0,05	100,6	--	440	56	56	340	46	29	260	440	87	210	65	6,8
CL-38	7.420.506	648.132	50,3	2,13	14,40	14,30	5,30	8,1	0,18	4,34	8,82	2,50	1,06	2,1	0,1	0,33	0,04	99,7	--	390	57	71	320	54	30	270	400	87	190	58	6,6
CL-41	7.419.824	656.240	51,8	2,38	13,80	11,60	6,80	4,3	0,11	3,86	7,76	2,70	2,09	3,4	0,1	0,84	0,00	100,1	--	720	51	-10	220	21	18	1000	280	98	280	120	8,8
CL-45-B	7.416.201	646.445	50,3	2,54	13,40	15,30	4,30	9,9	0,21	4,48	8,83	2,50	0,67	2,1	0,3	0,34	0,04	100,0	--	430	58	68	280	49	36	220	440	98	230	63	7,4
CL-46	7.417.740	645.467	51,3	2,69	12,60	16,30	6,30	9,0	0,21	2,98	7,46	2,40	1,52	2,6	0,2	0,62	0,03	100,0	--	580	56	32	490	26	30	210	370	110	300	96	11,0
CL-48-A	7.414.281	650.115	51,3	2,26	13,80																										

Sample	Er ppm	Eu ppm	Gd ppm	Ho ppm	La ppm	Lu ppm	Nd ppm	Pr ppm	Sm ppm	Tb ppm	Tm ppm	Y ppm	Yb ppm	Ag ppm	Bi ppm	Cs ppm	Ga ppm	Hf ppm	Mo ppm	Nb ppm	Pb ppm	Rb ppm	Ta ppm	Th ppm	Tl ppm	U ppm	Cl ppm	F ppm	Au ppb	Pt ppb	Pd ppb
CL-6-A	5,6	2,6	12,0	2,10	33	0,81	47	10,0	11,0	1,90	0,83	61	5,5	1,4	1,0	0,41	22	7,2	1,3	21,0	3	29	1,2	3,00	0,09	0,64	186	654	6,20	6,00	15,80
CL-9	4,1	3,2	11,0	1,70	48	0,52	59	14,0	12,0	1,70	0,58	47	3,5	0,9	1,2	0,61	24	7,0	1,3	26,0	4	34	1,8	3,70	0,10	0,84	222	1048	2,50	0,25	0,70
CL-11	3,5	2,3	7,9	1,40	38	0,49	42	10,0	8,6	1,30	0,53	41	3,4	2,4	1,2	1,10	22	6,1	1,0	22,0	5	40	1,3	4,30	0,28	0,92	714	679	7,80	13,40	18,30
CL-17-B	3,9	2,2	7,8	1,50	23	0,59	31	6,7	6,7	1,10	0,61	43	3,9	0,1	-0,5	22,00	21	5,4	1,6	18,0	33	27	0,9	2,40	0,04	0,50	220	449	4,10	9,40	13,80
CL-22-A	3,7	1,8	7,3	1,40	26	0,56	32	7,5	6,9	1,10	0,56	42	3,7	1,2	-0,5	0,44	20	5,0	0,8	16,0	4	27	0,9	2,90	0,08	0,56	200	440	8,10	14,80	20,90
CL-22-B	3,7	2,0	7,5	1,40	29	0,58	35	8,1	7,2	1,10	0,57	43	3,9	0,7	-0,5	0,53	22	5,5	1,2	19,0	5	28	1,4	3,10	0,10	0,63	124	639	3,70	12,50	32,40
CL-22-C	2,8	1,6	5,5	1,10	18	0,45	22	4,9	5,0	0,81	0,44	31	2,9	1,8	-0,5	0,51	19	4,0	1,0	13,0	3	18	0,8	2,00	0,06	0,41	116	406			
CL-22-D	4,1	2,6	10,0	1,70	46	0,54	59	13,0	12,0	1,50	0,61	48	3,7	2,0	-0,5	0,80	23	8,2	1,5	27,0	5	46	1,5	4,60	0,12	0,94	-100	547			
CL-23-A	3,4	1,8	6,8	1,30	26	0,51	30	7,1	6,6	1,00	0,52	38	3,4	1,5	-0,5	0,38	20	5,2	0,9	100,0	4	25	33,0	2,90	0,08	0,61	119	506	6,60	13,50	22,60
CL-23-C	2,8	1,6	5,2	1,10	20	0,41	23	5,4	4,9	0,84	0,43	31	2,9	0,7	-0,5	0,39	20	4,0	0,9	14,0	3	20	0,9	2,20	0,07	0,42	125	395	6,20	13,00	19,60
CL-24	5,0	2,5	9,5	1,80	28	0,72	38	8,3	8,3	1,50	0,75	57	5,0	1,9	-0,5	0,18	22	5,6	1,3	17,0	3	21	0,9	2,40	0,08	0,51	143	596	5,30	9,50	25,40
CL-25-A	3,4	2,8	8,3	1,30	35	0,46	44	10,0	8,8	1,20	0,48	39	3,2	0,9	-0,5	0,56	23	6,4	1,2	27,0	5	32	1,5	3,40	0,13	0,68	153	698	0,25	0,25	0,70
CL-26-A	4,8	2,4	9,2	1,80	26	0,74	36	7,8	8,0	1,40	0,70	52	4,8	1,0	-0,5	0,30	21	5,9	1,0	17,0	4	22	0,9	2,50	0,05	0,55	129	614	7,50	8,20	23,20
CL-26-B	4,5	2,5	8,8	1,70	23	0,67	32	6,9	7,4	1,30	0,68	50	4,5	0,7	-0,5	1,80	21	5,2	1,0	15,0	3	26	0,8	2,20	0,08	0,47	142	407	4,90	6,20	18,70
CL-28-A	4,3	3,8	12,0	1,70	51	0,54	65	15,0	13,0	1,60	0,61	50	3,6	0,5	-0,5	0,97	25	8,2	1,9	34,0	6	42	1,4	4,50	0,13	0,88	171	1196	1,80	5,30	3,10
CL-28-B	3,8	1,9	6,7	1,30	26	0,52	29	7,0	6,4	1,10	0,53	40	3,5	0,5	-0,5	0,51	21	5,0	1,2	19,0	4	26	1,0	2,90	0,09	0,56	192	633	3,30	8,90	14,30
CL-30	4,9	2,2	8,8	1,60	31	0,66	37	9,0	8,8	1,40	0,65	49	4,1	0,5	-0,5	0,37	22	5,6	0,9	20,0	20	28	1,0	3,40	0,11	0,61	129	558	8,70	8,60	27,40
CL-35	4,0	3,2	9,7	1,40	39	0,46	50	12,0	11,0	1,50	0,52	41	3,0	0,7	-0,5	3,10	26	7,9	1,8	34,0	5	51	1,7	4,10	0,12	0,82	171	885	0,25	0,25	0,25
CL-36	4,4	3,2	12,0	1,60	49	0,53	65	15,0	14,0	1,70	0,59	51	3,6	1,0	-0,5	0,83	26	8,1	1,8	33,0	8	51	1,8	4,80	0,17	0,98	164	1101	0,25	0,25	0,50
CL-37	4,00	1,90	7,50	1,40	30,0	0,56	35,0	8,60	7,80	1,20	0,58	44,00	3,80	0,7	0,8	0,41	24	5,5	1,3	20,0	4	30	1,1	3,60	0,11	0,71	247	487	9,80	8,80	20,20
CL-38	3,80	1,90	6,90	1,30	27,0	0,54	32,0	7,60	7,20	1,10	0,55	42,00	3,30	0,6	0,7	0,60	23	5,0	1,1	17,0	4	25	1,0	2,80	0,09	0,58	249	526	6,30	14,90	24,30
CL-41	3,80	3,90	12,00	1,60	55,0	0,45	68,0	16,00	13,00	1,70	0,50	44,00	2,80	0,6	-0,5	0,67	29	7,2	1,1	23,0	7	51	1,6	5,10	0,18	1,20	208	1107	1,80	2,00	0,25
CL-45-B	4,10	2,00	7,30	1,50	29,0	0,60	34,0	7,80	7,20	1,20	0,57	43,00	3,80	1,3	-0,5	0,58	22	5,7	1,0	20,0	4	25	1,1	3,10	0,07	0,64	280	604	4,50	6,90	15,30
CL-46	6,10	2,50	12,00	2,20	46,0	0,84	53,0	13,00	11,00	1,80	0,85	64,00	5,40	3,0	0,6	0,51	25	7,8	1,0	25,0	5	40	1,3	4,50	0,10	0,90	341	1095	8,70	9,10	37,60
CL-48-A	4,40	1,90	7,80	1,50	27,0	0,62	31,0	7,40	7,00	1,20	0,59	43,00	3,80	1,1	-0,5	0,25	22	5,3	0,9	17,0	4	25	0,9	2,80	0,08	0,58	180	399	6,50	5,90	23,30
Median	4,0	2,4	8,7	1,4	30,0	0,54	37,0	8,6	8,3	1,2	0,53	43,0																			

		SiO ₂ %	TiO ₂ %	Al ₂ O ₃ %	Fe ₂ O ₃ T %	Fe ₂ O ₃ %	FeO %	MnO %	MgO %	CaO %	Na ₂ O %	K ₂ O %	H ₂ OT %	CO ₂ T %	P ₂ O ₅ %	ST %	TOTAL %	Mg#	Ba ppm	Co ppm	Cr ppm	Cu ppm	Ni ppm	Sc ppm	Sr ppm	V ppm	Zn ppm	Zr ppm	Ce ppm	Dy ppm
STATISTICAL SUMMARY	Median	54,57	2,55	14,83	--	1,22	9,91	0,18	3,80	7,45	2,96	2,31	--	--	0,65	0,01	--	0,40	688	34	46	72	42	24	631	257	120	358	108	--
	Min.	51,02	2,03	13,01	--	0,93	7,51	0,14	2,07	4,14	2,44	1,00	--	--	0,30	0,01	--	0,33	473	17	8	39	4	14	336	119	108	157	39	--
	Max.	60,27	3,80	14,35	--	1,51	12,20	0,22	5,27	9,59	3,87	4,15	--	--	0,71	0,04	--	0,44	1137	44	83	267	65	40	777	343	134	490	173	--
	S.D.	3,90	0,84	0,61	--	0,24	1,95	0,03	1,40	2,38	0,66	1,38	--	--	0,19	0,02	--	0,05	288	12	34	123	29	11	193	113	14	141	56	--

Table 10 – Statistical summary of the analytical results of rock samples from the high-Ti intermediate volcanic suites (HTV-I) - Serra Geral Magmatism (Fe₂O₃T of the samples and Fe₂O₃ e FeO of the statistical summary were respectively calculated in ferric and ferrous oxides contents).

(Cont.)

		SiO ₂ %	TiO ₂ %	Al ₂ O ₃ %	Fe ₂ O ₃ T %	Fe ₂ O ₃ %	FeO %	MnO %	MgO %	CaO %	Na ₂ O %	K ₂ O %	H ₂ OT %	CO ₂ T %	P ₂ O ₅ %	ST %	TOTAL %	Mg#	Ba ppm	Co ppm	Cr ppm	Cu ppm	Ni ppm	Sc ppm	Sr ppm	V ppm	Zn ppm	Zr ppm	Ce ppm	Dy ppm
STATISTICAL SUMMARY	Median	50,85	1,54	15,31	--	1,36	11,01	0,19	5,75	10,75	2,49	0,68	--	--	0,21	--	--	0,48	294	46	147	128	80	40	226	307	93	114	30,8	--
	Min.	49,20	0,96	13,88	--	1,04	8,45	0,15	3,70	9,07	1,85	0,15	--	--	0,14	--	--	0,40	148	38	43	99	42	32	154	221	75	73	13,0	--
	Max.	52,20	2,01	17,15	--	1,50	12,11	0,25	8,07	11,72	3,20	1,24	--	--	0,39	0,01	--	0,63	491	52	433	180	174	44	369	369	113	167	45,0	--
	S.D.	0,90	0,28	0,67	--	0,11	0,92	0,03	1,13	0,74	0,28	0,31	--	--	0,07	--	--	0,07	95	3	116	41	30	3,6	62	74	19	26	8,8	--

Table 11 – Statistical summary of the analytical results of rock samples from the low-Ti basic volcanic suites (LTV-B) - Serra Geral Magmatism (Fe₂O₃T of the samples and Fe₂O₃ e FeO of the statistical summary were respectively calculated in ferric and ferrous oxides contents).

(Cont.)

		SiO ₂ %	TiO ₂ %	Al ₂ O ₃ %	Fe ₂ O ₃ T %	Fe ₂ O ₃ %	FeO %	MnO %	MgO %	CaO %	Na ₂ O %	K ₂ O %	H ₂ OT %	CO ₂ T %	P ₂ O ₅ %	ST %	TOTAL %	Mg#	Ba ppm	Co ppm	Cr ppm	Cu ppm	Ni ppm	Sc ppm	Sr ppm	V ppm	Zn ppm	Zr ppm	Ce ppm	Dy ppm
STATISTICAL SUMMARY	Median	53,62	1,36	14,50	--	1,26	10,17	0,19	4,95	9,23	2,61	1,46	--	--	0,23	--	--	0,47	358	43	39	117	40	35	240	298	108	153	45,9	--
	Min.	53,17	1,05	12,84	--	1,08	8,72	0,16	3,30	6,47	2,12	1,15	--	--	0,12	--	--	0,35	289	40	9	61	19	31	193	216	89	111	32,0	--
	Max.	56,83	2,19	15,94	--	1,55	12,56	0,21	5,74	9,66	3,28	2,60	--	--	0,32	0,02	--	0,54	461	46	97	181	106	39	294	396	124	228	66,3	--
	S.D.	1,13	0,32	1,12	--	0,13	1,06	0,02	0,75	0,94	0,30	0,41	--	--	0,05	--	--	0,06	53	2,2	29	47	23	2,7	30	56	12,5	34,7	10,2	--

Table 12 – Statistical summary of the analytical results of rock samples from the low-Ti intermediate volcanic suites (LTV-I) - Serra Geral Magmatism (Fe₂O₃T of the samples and Fe₂O₃ e FeO of the statistical summary were respectively calculated in ferric and ferrous oxides contents).

(Cont.)

	Er ppm	Eu ppm	Gd ppm	Ho ppm	La ppm	Lu ppm	Nd ppm	Pr ppm	Sm ppm	Tb ppm	Tm ppm	Y ppm	Yb ppm	Ag ppm	Bi ppm	Cs ppm	Ga ppm	Hf ppm	Mo ppm	Nb ppm	Pb ppm	Rb ppm	Ta ppm	Th ppm	Tl ppm	U ppm	Cl ppm	F ppm	Au ppb	Pt ppb	Pd ppb
Median	--	3,78	--	--	51,5	0,50	63	--	12,1	1,6	--	44	3,3	--	0,03	0,47	26	8,6	--	38	11,8	51	2,2	5,8	--	1,7	152	833	0,27	5,70	10,00
Min.	--	1,80	--	--	20,3	0,43	54	--	5,3	0,8	--	27	3,0	--	0,01	0,19	26	3,8	--	27	9,5	29	0,9	2,6	--	0,6	50	449	0,11	1,30	0,64
Max.	--	4,42	--	--	79,6	0,56	82	--	15,3	1,8	--	50	3,6	--	0,04	1,80	27	12,4	--	45	14,2	116	3,3	12,1	--	3,0	175	1112	0,44	8,50	17,90
S.D.	--	1,16	--	--	25,3	25,3	14	--	4,2	0,4	--	11	0,4	--	0,01	1,02	0,6	3,6	--	0,6	3,3	41	1,0	4,2	--	1,0	56	280	0,13	3,56	8,41

Table 10 – Continued

	Er ppm	Eu ppm	Gd ppm	Ho ppm	La ppm	Lu ppm	Nd ppm	Pr ppm	Sm ppm	Tb ppm	Tm ppm	Y ppm	Yb ppm	Ag ppm	Bi ppm	Cs ppm	Ga ppm	Hf ppm	Mo ppm	Nb ppm	Pb ppm	Rb ppm	Ta ppm	Th ppm	Tl ppm	U ppm	Cl ppm	F ppm	Au ppb	Pt ppb	Pd ppb
Median	--	1,36	--	--	14,0	0,40	17	--	4,2	0,73	--	27	2,3	--	--	0,21	--	2,9	--	--	--	15	0,55	2,0	--	0,3	82	302	0,33	11,20	11,60
Min.	--	1,00	--	--	4,4	0,27	10	--	3,1	0,55	--	20	1,7	--	--	0,05	17	1,8	--	6	--	8	0,22	0,7	--	0,2	50	173	0,08	3,90	1,50
Max.	--	2,01	--	--	22,0	0,62	27	--	6,0	1,21	--	56	3,9	--	--	1,34	20	4,5	--	12	--	29	0,92	4,7	--	1,5	150	475	1,00	26,70	57,00
S.D.	--	0,27	--	--	4,6	0,08	5	--	0,7	0,15	--	8	0,6	--	--	0,36	--	0,7	--	--	--	6	0,18	0,9	--	0,3	74	81	0,28	6,99	10,31

Table 11 – Continued

	Er ppm	Eu ppm	Gd ppm	Ho ppm	La ppm	Lu ppm	Nd ppm	Pr ppm	Sm ppm	Tb ppm	Tm ppm	Y ppm	Yb ppm	Ag ppm	Bi ppm	Cs ppm	Ga ppm	Hf ppm	Mo ppm	Nb ppm	Pb ppm	Rb ppm	Ta ppm	Th ppm	Tl ppm	U ppm	Cl ppm	F ppm	Au ppb	Pt ppb	Pd ppb
Median	--	1,48	--	--	21,2	0,46	25,3	--	5,2	0,91	--	30	2,9	--	0,04	0,89	21	3,7	--	13	8,1	48	0,8	5,1	--	0,89	108	460	0,22	5,60	6,30
Min.	--	1,00	--	--	15,7	0,30	19,7	--	4,1	0,68	--	23	2,3	--	0,01	0,45	16	2,9	--	8	5,8	30	0,5	3,8	--	0,45	50	292	0,11	1,60	1,20
Max.	--	2,26	--	--	32,2	0,65	35,9	--	7,9	1,34	--	46	46	--	0,05	2,65	22	5,8	--	16	11,9	91	1,1	9,0	--	2,65	138	621	0,51	16,20	15,00
S.D.	--	0,39	--	--	4,8	0,13	4,9	--	1,2	0,24	--	7,5	7,5	--	0,02	0,74	2,1	0,9	--	2,8	2,2	19	0,2	1,5	--	0,74	38	105	0,10	5,46	4,79

Table 12 – Continued

		SiO ₂ %	TiO ₂ %	Al ₂ O ₃ %	Fe ₂ O ₃ T %	Fe ₂ O ₃ %	FeO %	MnO %	MgO %	CaO %	Na ₂ O %	K ₂ O %	H ₂ OT %	CO ₂ T %	P ₂ O ₅ %	ST %	TOTAL	Mg#	Ba ppm	Co ppm	Cr ppm	Cu ppm	Ni ppm	Sc ppm	Sr ppm	V ppm	Zn ppm	Zr ppm	Ce ppm	Dy ppm
STATISTICAL SUMMARY	Median	65,84	1,14	13,89	--	0,72	5,80	0,13	1,30	2,66	3,25	4,90	--	--	0,37	0,01	--	0,28	1350	14	7	16	5	13	275	22	110	590	155	12
	Min.	64,85	1,08	13,63	--	0,63	5,10	0,11	0,56	1,56	2,38	4,71	--	--	0,33	0,00	--	0,16	1300	13	5	13	5	12	210	21	100	560	140	10
	Max.	66,38	1,21	15,42	--	0,76	6,12	0,44	1,41	3,02	3,40	5,19	--	--	0,41	1,21	--	0,30	2500	69	13	34	5	14	350	33	240	630	240	36
	S.D.	0,53	0,05	0,67	--	0,04	0,34	0,15	0,32	0,51	0,37	0,20	--	--	0,03	0,49	--	0,05	481	22	3,6	7,8	--	0,7	46	5	55	23	36	11

Table 13 – Statistical summary of the analytical results of rock samples from the low-Ti acid volcanic suites (LTV-A) - Serra Geral Magmatism
(Fe₂O₃T of the samples and Fe₂O₃ e FeO of the statistical summary were respectively calculated in ferric and ferrous oxides contents).

(Cont.)

Sample	UTM-N m	UTM-E m	SiO ₂ %	TiO ₂ %	Al ₂ O ₃ %	Fe ₂ O ₃ T %	Fe ₂ O ₃ %	FeO %	MnO %	MgO %	CaO %	Na ₂ O %	K ₂ O %	H ₂ OT %	CO ₂ T %	P ₂ O ₅ %	ST %	TOTAL	Mg#	Ba ppm	Co ppm	Cr ppm	Cu ppm	Ni ppm	Sc ppm	Sr ppm	V ppm	Zn ppm	Zr ppm	Ce ppm	Dy ppm
CL-1-A	7.278.877	509.368	66,5	0,58	12,50	4,40	1,70	2,4	0,05	3,13	2,23	3,40	3,45	2,8	0,2	0,20	0,01	99,2	--	720	14	48	18	20	10	270	63	51	190	73	4,8
CL-12-E	7.383.105	617.180	70,1	0,63	12,80	3,40	2,90	0,5	0,02	1,54	0,78	3,20	2,62	4,0	0,2	0,17	0,00	99,5	--	790	12	41	15	19	8	120	56	43	270	90	5,8
CL-13-B	7.388.182	616.611	46,1	3,89	13,70	15,70	7,60	7,3	0,26	4,57	6,22	2,60	1,53	5,8	0,4	0,53	0,05	100,5	--	480	63	13	61	26	31	400	480	100	300	84	8,0
CL-17-C	7.388.509	611.565	64,7	0,60	12,50	3,90	2,00	1,7	0,17	2,42	5,32	3,50	3,52	2,4	0,6	0,13	0,00	99,5	--	570	12	48	26	22	10	200	61	56	210	78	6,4
CL-27-D	7.414.634	654.748	67,7	0,48	12,10	4,30	4,10	0,2	0,04	2,34	0,80	2,70	4,43	4,8	0,1	0,16	0,00	99,9	--	780	13	54	19	20	7	130	50	51	370	61	4,7
CL-48-B	7.414.281	650.115	69,2	0,57	12,30	3,20	2,90	0,2	0,01	1,99	0,50	3,10	3,83	4,7	0,1	0,13	0,00	99,5	--	660	13	42	29	17	8	140	42	48	250	91	13,0
JBO658	6.848.000	655.000	62,2	0,58	13,00	9,50	--	--	0,16	2,85	2,48	4,10	2,41	--	0,3	0,19	1,01	98,8	--	540	28	58	99	34	11	150	110	120	170	53	4,7
JBO664	6.832.010	651.500	51,9	1,66	12,90	14,10	--	--	0,35	3,31	5,21	2,90	1,95	--	0,9	0,26	2,67	98,2	--	390	49	19	240	22	36	130	430	130	210	65	7,0
JBO667	6.834.000	653.000	75,6	0,60	10,10	4,40	--	--	0,06	1,65	0,42	1,30	2,06	2,7	0,1	0,08	0,68	99,7	--	450	13	52	59	30	10	100	63	88	140	50	2,9
JBO677	6.834.000	647.000	25,0	0,24	4,70	3,00	--	--	0,47	16,89	26,16	0,00	0,23	5,4	16,5	0,12	0,99	99,8	--	150	11	15	40	10	3	120	53	-5	90	43	2,7
JBO678	6.834.000	647.000	28,0	0,53	6,60	7,00	2,20	4,4	0,42	12,23	23,41	0,80	0,32	4,2	15,8	0,13	0,97	100,0	--	170	19	28	76	22	13	140	130	28	68	30	3,2
JBOT34	6.848.720	655.600	66,7	0,64	16,10	6,60	0,40	5,6	0,10	2,52	0,90	2,20	3,16	1,4	-0,1	0,25	0,58	100,6	--	340	20	58	61	42	14	100	76	86	210	85	6,2
JBOT50	6.808.150	657.500	60,8	0,72	12,60	8,73	--	--	-0,01	0,31	0,25	4,21	2,84	--	0,2	0,30	5,27	96,4	--	970	14	69	80	11	13	65	86	24	160	87	8,1
STATISTICAL SUMMARY	Median	67,20	0,63	13,12	--	0,46	3,7	0,08	2,53	1,61	2,94	2,87	--	--	0,17	0,30	--	0,50	510	13	48	49	21	10,5	130	63	51	210	75	6,0	
	Min.	32,25	0,31	6,06	--	0,25	2,0	0,01	0,33	0,26	0,00	0,30	--	--	0,04	0,00	--	0,07	150	8	13	15	10	3,9	65	42	42	68	30	2,7	
	Max.	78,34	4,15	17,48	--	1,67	13,56	0,61	21,79	37,74	4,42	4,68	--	--	0,57	5,53	--	0,93	970	63	69	240	42	36,0	400	130	480	370	91	13,0	
	S.D.	14,31	0,98	2,91	--	0,44	3,56	0,20	6,10	10,89	1,25	1,30	--	--	0,13	1,54	--	0,20	241	16	17,5	58,5	9	8,9	86	39	142	91	19	2,7	

Table 14 – Analytical data from Paraná Basin sedimentary rocks (SD) - Serra Geral Magmatism
(Fe₂O₃T of the samples and Fe<sub

	Er ppm	Eu ppm	Gd ppm	Ho ppm	La ppm	Lu ppm	Nd ppm	Pr ppm	Sm ppm	Tb ppm	Tm ppm	Y ppm	Yb ppm	Ag ppm	Bi ppm	Cs ppm	Ga ppm	Hf ppm	Mo ppm	Nb ppm	Pb ppm	Rb ppm	Ta ppm	Th ppm	Tl ppm	U ppm	Cl ppm	F ppm	Au ppb	Pt ppb	Pd ppb
Median	6,0	3,75	15	2,2	74	0,80	84	21	17	2,1	0,84	65	5,3	0,50	0,35	3,2	25	13	2,2	51	5	150	2,3	13	0,51	2,7	189	732	0,75	0,25	0,65
Min.	5,4	3,30	12	1,9	70	0,73	78	20	15	2,0	0,76	60	4,8	0,20	0,25	1,8	24	12	1,9	48	5	140	2,0	12	0,47	2,5	177	554	0,25	0,25	0,25
Max.	35,0	7,40	33	10,0	91	4,50	150	33	32	4,8	4,80	530	25,0	1,90	0,90	5,6	27	15	2,7	52	5	170	2,8	13	0,70	3,2	249	1153	19,90	0,25	0,80
S.D.	11,7	1,53	9,6	3,2	8	1,49	27	5	6	1,4	1,60	187	8,0	0,40	0,27	1,5	1,2	1,2	0,3	1,7	--	10	0,3	0,5	0,09	0,3	27	218	7,94	--	0,21

Table 13 – Continued

Sample	Er ppm	Eu ppm	Gd ppm	Ho ppm	La ppm	Lu ppm	Nd ppm	Pr ppm	Sm ppm	Tb ppm	Tm ppm	Y ppm	Yb ppm	Ag ppm	Bi ppm	Cs ppm	Ga ppm	Hf ppm	Mo ppm	Nb ppm	Pb ppm	Rb ppm	Ta ppm	Th ppm	Tl ppm	U ppm	Cl ppm	F ppm	Au ppb	Pt ppb	Pd ppb
CL-1-A	2,7	0,9	5,2	0,96	34	0,42	32	8,7	6,4	0,83	0,41	30	2,7	1,0	-0,5	4,90	17	4,9	0,7	15,0	12	170	0,8	15,00	0,40	3,20	170	406	1,20	0,25	0,25
CL-12-E	3,2	1,3	6,5	1,10	43	0,49	41	10,0	7,7	1,00	0,50	36	3,3	0,3	-0,5	5,40	15	6,3	0,4	16,0	110	130	1,0	14,00	0,53	3,30	418	812	1,80	0,25	0,25
CL-13-B	3,7	3,4	10,0	1,50	37	0,50	49	11,0	10,0	1,40	0,54	41	3,4	0,2	0,7	2,20	26	7,8	1,2	27,0	10	40	1,3	3,60	0,18	0,76	293	951	2,30	0,25	0,60
CL-17-C	4,1	1,5	7,3	1,30	48	0,55	43	11,0	7,9	1,00	0,53	43	3,7	0,2	-0,5	4,70	14	5,0	0,7	15,0	20	160	0,9	15,00	0,44	2,80	216	336	0,25	0,25	0,70
CL-27-D	2,5	1,0	5,7	0,94	44	0,40	39	10,0	6,9	0,79	0,38	29	2,7	0,4	-0,5	4,30	14	8,5	0,9	13,0	19	160	0,5	13,00	0,53	1,40	207	758	0,50	0,25	1,20
CL-48-B	7,3	3,1	16,0	2,60	91	0,98	79	20,0	14,0	2,10	0,98	87	6,4	0,3	0,5	3,70	14	6,2	-0,2	15,0	18	180	0,9	15,00	0,63	2,40	117	416	1,00	0,25	0,25
JBO658	2,9	0,8	5,0	1,00	23	0,43	27	6,7	5,7	0,80	0,43	29	2,9	0,4	0,5	5,50	15	4,6	18,0	15,0	38	120	0,9	13,00	1,40	10,00	362	1255	4,60	1,50	0,25
JBO664	4,3	1,9	7,2	1,50	37	0,57	30	7,8	6,3	1,10	0,61	41	4,0	0,4	0,7	2,10	23	5,1	1,6	17,0	12	80	1,0	7,20	0,68	2,20	-100	915	4,90	11,40	9,60
JBO667	1,6	0,6	3,2	0,59	24	0,25	20	5,4	3,5	0,44	0,26	18	1,8	0,8	-0,5	1,30	14	3,1	1,3	13,0	13	98	0,8	8,60	0,46	1,90	285	469	5,20	0,25	0,25
JBO677	1,6	0,6	3,3	0,58	28	0,24	21	5,2	3,5	0,44	0,23	20	1,4	0,5	1,0	1,80	6	2,1	8,2	5,5	34	12	0,3	4,60	1,10	5,00	698	840	0,25	1,00	0,70
JBO678	1,9	0,7	3,4	0,64	19	0,24	16	4,0	3,1	0,54	0,26	21	1,7	0,8	0,6	1,90	9	1,5	5,6	4,1	22	14	0,3	2,50	0,69	5,30	694	627	1,20	1,20	3,80
JB0734	3,2	1,5	7,4	1,20	40	0,48	40	11,0	7,6	1,10	0,50	38	3,1	0,8	-0,5	11,00	20	5,5	1,1	17,0	23	190	0,6	17,00	1,00	3,20	409	1490	4,50	2,20	3,00
JB0750	4,0	2,0	9,2	1,60	41	0,62	44	11,0	9,6	1,40	0,64	44	4,1	0,8	1,8	0,63	14	4,8	13,0	19,0	31	75	0,3	12,00	0,80	8,70	-100	330	4,80	0,25	3,60
Median	3,2	1,35	6,6	1,15	37	0,49	36	9,5	7,1	1,00	0,50	37	3,2	0,45	0,50	4,0	14,5	5,0	1,1	15,0	19	125	0,8	13,0	0,66	3,20	250	692	1,50	0,45	0,70
Min.	1,6	0,63	3,2	0,58	19	0,24	16	4,0	3,1	0,44	0,23	18	1,4	0,20	0,25	0,6	6,5	1,5	0,1	4,1	10	12	0,3	2,5	0,18	0,76	0,76	330	0,25	0,25	0,25
Max.	7,3	3,40	16,0	2,60	91	0,98	79	20,0	14,0	2,10	0,98	87	6,4	1,00	1,80	5,5	26,0	8,9	18,0	27,0	110	230	1,3	18,0	1,40	10,00	10,00	1490	11,40	11,40	9,60
S.D.	1,5	0,86	3,3	0,53	17	0,20	16	3,9	2,9	0,44	0,20	17	1,3	0,26	0,43	1,5	5,1	2,18	5,5	5,5	25	68	0,3	5,1	0,34	2,65	349	1,99	1,99	2,93	

Table 14 – Continued